Eur. Phys. J. C (2023) 83:781
https://doi.org/10.1140/epjc/s10052-023-11869-1

THE EUROPEAN PHYSICAL JOURNAL C

Regular Article - Experimental Physics

Searches for exclusive Higgs and Z boson decays into a vector quarkonium state and a photon using 139 fb^{-1} of ATLAS $\sqrt{s} = 13$ TeV proton–proton collision data

ATLAS Collaboration[⋆]

CERN, 1211 Geneva 23, Switzerland

Received: 9 August 2022 / Accepted: 3 November 2022 / Published online: 5 September 2023

Abstract Searches for the exclusive decays of Higgs and Z bosons into a vector quarkonium state and a photon are performed in the $\mu^+\mu^-\gamma$ final state with a proton–proton collision data sample corresponding to an integrated luminosity of 139 fb^{-1} collected at $\sqrt{s} = 13$ TeV with the ATLAS detector at the CERN Large Hadron Collider. The observed data are compatible with the expected backgrounds. The 95% confidence-level upper limits on the branching fractions of the Higgs boson decays into $J/\psi\,\gamma$, $\psi(2S)\,\gamma$, and $\Upsilon(1S, 2S, 3S)\,\gamma$ are found to be 2.0×10^{-4}, 10.5×10^{-4}, and $(2.5, 4.2, 3.4) \times 10^{-4}$, respectively, assuming Standard Model production of the Higgs boson. The corresponding 95% CL upper limits on the branching fractions of the Z boson decays are 1.2×10^{-6}, 2.4×10^{-6}, and $(1.1, 1.3, 2.4) \times 10^{-6}$. An observed 95% CL interval of $(-133, 175)$ is obtained for the κ_c/κ_γ ratio of Higgs boson coupling modifiers, and a 95% CL interval of $(-37, 40)$ is obtained for κ_b/κ_γ.

1 Introduction

The Higgs boson, H, was first observed by the ATLAS [1] and CMS [2] collaborations in 2012 [3,4] with a mass of approximately 125 GeV. Detailed measurements of its properties [5,6] have confirmed its role in the spontaneous breaking of electroweak symmetry and the mass generation of the massive vector bosons [7,8]. In the Standard Model (SM), the mass generation for fermions is implemented through Yukawa interactions. The ATLAS and CMS collaborations have reported observations of Higgs boson decays into a pair of τ-leptons [9,10], a pair of bottom quarks [11,12], and associated production of Higgs bosons with top-quark pairs [13,14]. These measurements represent a complete observation of Higgs boson couplings to third-generation charged fermions, and are in agreement with SM expectations. Recently, evidence has been reported for the Higgs boson coupling to muons in the second generation through the decay $H \to \mu^+\mu^-$ [15,16]. Direct searches for $H \to c\bar{c}$ have been performed by both the ATLAS and CMS collaborations [17–20], as have searches for $H \to e^+e^-$ decays [21,22], but no further experimental evidence currently exists for the Higgs boson couplings to the first and second generations of fermions. Searches for potential beyond-the-SM (BSM) couplings of the Higgs boson have also been performed by the ATLAS and CMS collaborations, including searches for flavour-changing neutral currents via the t-quark decays $t \to cH$ and $t \to uH$ [23–26], and the lepton-flavour-violating decays $H \to e\mu$, $H \to e\tau$ and $H \to \mu\tau$ [21,27,28]. No evidence for these couplings has been found.

A direct method for accessing the couplings of the first- and second-generation quarks is the study of inclusive $H \to q\bar{q}$ decays. While these channels have large branching fractions, their experimental sensitivity is substantially obscured by large multi-jet backgrounds. Searches for the exclusive, radiative decays of the Higgs boson into a vector meson state and a photon offer an alternative way to probe the quark Yukawa couplings [29–31]. Although their branching fractions are comparatively small, these radiative decays have a distinct experimental signature, which helps suppress the large multi-jet backgrounds that affect the $H \to q\bar{q}$ searches. Figure 1 shows Feynman diagrams depicting the $H \to \mathcal{Q}\gamma$ process, where $\mathcal{Q}$ is a vector quarkonium state. There are two primary contributions to the decay amplitude: the direct amplitude $\mathcal{A}_{\text{dir}}$ occurs via the quark Yukawa coupling; the indirect amplitude $\mathcal{A}_{\text{ind}}$ occurs at the one-loop level in the SM through the $H \to \gamma\gamma^*$ decay, where the virtual photon subsequently fragments into a vector quarkonium state. The two processes interfere destructively, and despite being loop-induced, the indirect amplitude is typically the more dominant contribution in decays of the Higgs boson into a vector meson state and a photon.

Higgs boson decays in the charmonium sector, $H \to J/\psi\,\gamma$ and $H \to \psi(2S)\,\gamma$, offer an opportunity to

⋆ e-mail: atlas.publications@cern.ch

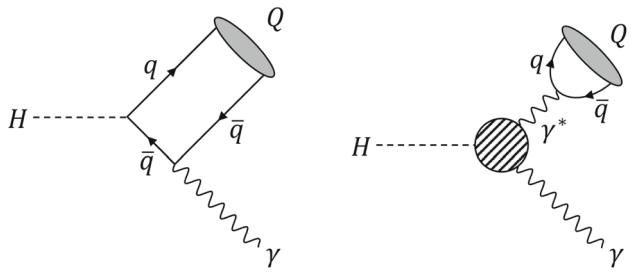

(a) Direct amplitude (b) Indirect amplitude

Fig. 1 Feynman diagrams depicting the **a** direct amplitude and **b** indirect amplitude contributing to the $H \to \mathcal{Q}\gamma$ process, where $\mathcal{Q}$ is a vector quarkonium state. The hatched circle in **b** denotes a set of one-loop diagrams

access both the magnitude and the sign of the charm-quark Yukawa coupling [29,30]; the corresponding decays in the bottomonium sector, $H \to \Upsilon(1S, 2S, 3S)\,\gamma$, can provide information about the real and imaginary parts of the bottom-quark coupling to the Higgs boson [31]. Studies of these decays complement searches for the inclusive $H \to c\bar{c}$ and $H \to b\bar{b}$ decays. The results of recent independent calculations of the branching fractions expected for these decays in the SM are presented in Table 1, and are of the order of 10^{-6} for $H \to J/\psi\,\gamma$ and of order 10^{-9} to 10^{-8} for $H \to \Upsilon(1\,S, 2\,S, 3\,S)\,\gamma$ [31–36]. The branching fraction for $H \to \psi(2S)\,\gamma$ is expected to be $(1.03 \pm 0.06) \times 10^{-6}$. This was obtained via a private communication from the authors of Ref. [34], who used an estimate of the value of the order-v^2 non-relativistic QCD long-distance matrix element, where v is the velocity of the heavy quarks in the $\mathcal{Q}$ rest frame. It is noted that the branching fractions for decays in the bottomonium sector are small compared to those in the charmonium sector: in this case there is an almost perfect cancellation between the direct and indirect decay amplitudes, caused by the mass of the b-quark being large compared to the masses of quarks in the first and second generations.

Deviations of the quark Yukawa couplings from SM expectations can lead to significant enhancements in the branching fractions of these radiative decays, particularly in the bottomonium sector. Such deviations can arise in BSM theories [37]. For instance, the quark masses may not originate entirely from the Higgs mechanism, but could also be induced by other, subdominant, sources of electroweak symmetry breaking [38]. Some further examples are the Froggatt–Nielsen mechanism [39], the Randall–Sundrum family of models [40], the minimal flavour violation framework [41], the Higgs-dependent Yukawa couplings model [42], and the possibility of the Higgs boson being a composite pseudo-Goldstone boson [43].

The Z boson production cross section at the LHC [44] is approximately 1000 times larger than the Higgs boson production cross section [37,45], which allows rare Z boson decays to be probed to much smaller branching fractions than Higgs boson decays to the same final state. Similarly to the Higgs boson decays in Fig. 1, radiative decays of the Z boson into a vector quarkonium state and a photon receive analogous contributions from direct and indirect amplitudes. In $Z \to \mathcal{Q}\gamma$ decays, the power corrections in terms of the ratio of the QCD energy scale to the vector-boson mass are small. As discussed in Ref. [46], this allows the light-cone distribution amplitudes (LCDAs) of the mesons to be probed in a theoretically clean region where power corrections are in control, which is not possible in other applications of the QCD factorisation approach. These decays have not yet been measured, but recent independent calculations of the SM branching fractions for $Z \to J/\psi\,\gamma$ and $Z \to \Upsilon(1S, 2S, 3S)\,\gamma$ are presented in Table 2 and are expected to be of order 10^{-8} to 10^{-7} [46–48]. No value has been calculated for $Z \to \psi(2S)\,\gamma$.

Decays of the Higgs and Z bosons into J/ψ or $\Upsilon(1S, 2S, 3S)$ and a photon were searched for by the ATLAS Collaboration, initially with up to 20.3 fb^{-1} of data collected at $\sqrt{s} = 8$ TeV [49] and subsequently with up to 36.1 fb^{-1} of data collected at $\sqrt{s} = 13$ TeV [50]; the latter search also introduced the study of the $\psi(2S)$ decay channels. The obtained 95% confidence level (CL) upper limits on the branching fractions were 3.5×10^{-4} and 2.0×10^{-3} for $H \to J/\psi\,\gamma$ and $H \to \psi(2S)\,\gamma$, respectively, and $(4.9, 5.9, 5.7) \times 10^{-4}$ for $H \to \Upsilon(1S, 2S, 3S)\,\gamma$. The corresponding 95% CL upper limits for the analogous Z boson decays were 2.3×10^{-6}, 4.5×10^{-6} and $(2.8, 1.7, 4.8)$

Table 1 Recent calculations of the $H \to \mathcal{Q}\gamma$ branching fractions expected in the Standard Model

Vector quarkonium state	SM branching fraction, $\mathcal{B}(H \to \mathcal{Q}\gamma)$		
	Ref. [31] (2015)	Refs. [33,34] (2017)	Ref. [36] (2019)
J/ψ	$2.95^{+0.17}_{-0.17} \times 10^{-6}$	$2.99^{+0.16}_{-0.15} \times 10^{-6}$	$3.01^{+0.15}_{-0.15} \times 10^{-6}$
$\Upsilon(1S)$	$4.61^{+1.76}_{-1.23} \times 10^{-9}$	$5.22^{+2.02}_{-1.70} \times 10^{-9}$	$9.97^{+4.04}_{-3.03} \times 10^{-9}$
$\Upsilon(2S)$	$2.34^{+0.76}_{-1.00} \times 10^{-9}$	$1.42^{+0.72}_{-0.57} \times 10^{-9}$	$2.62^{+1.39}_{-0.91} \times 10^{-9}$
$\Upsilon(3S)$	$2.13^{+0.76}_{-1.13} \times 10^{-9}$	$0.91^{+0.48}_{-0.38} \times 10^{-9}$	$1.87^{+1.05}_{-0.69} \times 10^{-9}$

Table 2 Overview of calculations of the Standard Model $Z \to Q\gamma$ branching fractions

Vector quarkonium state	SM branching fraction, $\mathcal{B}(Z \to Q\gamma)$		
	Ref. [46] (2015)	Ref. [47] (2015)	Ref. [48] (2018)
J/ψ	$8.02^{+0.46}_{-0.44} \times 10^{-8}$	$9.96^{+1.86}_{-1.86} \times 10^{-8}$	$8.96^{+1.51}_{-1.38} \times 10^{-8}$
$\Upsilon(1S)$	$5.39^{+0.17}_{-0.15} \times 10^{-8}$	$4.93^{+0.51}_{-0.51} \times 10^{-8}$	$4.80^{+0.26}_{-0.25} \times 10^{-8}$
$\Upsilon(2S)$	–	–	$2.44^{+0.14}_{-0.13} \times 10^{-8}$
$\Upsilon(3S)$	–	–	$1.88^{+0.11}_{-0.10} \times 10^{-8}$

$\times 10^{-6}$. The $H \to J/\psi\,\gamma$ and $Z \to J/\psi\,\gamma$ decays have also been searched for by the CMS Collaboration [51,52], yielding similar upper limits of 7.6×10^{-4} and 1.4×10^{-6} from 35.9 fb^{-1} of data collected at $\sqrt{s} = 13$ TeV. In addition, the ATLAS Collaboration has searched for the rare Higgs and Z boson decays to light vector mesons $H(Z) \to \phi\,\gamma$ and $H(Z) \to \rho\,\gamma$ [53,54], while the CMS Collaboration has also searched for Higgs boson decays into a Z boson and a ρ or ϕ meson [55], and Higgs and Z boson decays into pairs of J/ψ or $\Upsilon(1S, 2S, 3S)$ mesons [56].

This paper describes searches for Higgs and Z boson decays into the exclusive final states $J/\psi\,\gamma$, $\psi(2S)\,\gamma$, and $\Upsilon(1S, 2S, 3S)\,\gamma$, and then into $\mu^+\mu^-\gamma$, using 139 fb^{-1} of ATLAS proton–proton (pp) collision data collected between 2015 and 2018 at $\sqrt{s} = 13$ TeV. Hereafter, where no distinction is relevant, the J/ψ and $\psi(2S)$ states are collectively denoted by $\psi(nS)$, and the $\Upsilon(1S, 2S, 3S)$ states are denoted by $\Upsilon(nS)$. The results are interpreted in the kappa framework [37,57] in terms of the ratios κ_c/κ_γ and κ_b/κ_γ, where κ_c, κ_b and κ_γ are the modifiers of the coupling between the Higgs boson and the charm quark, bottom quark, and the effective coupling between the Higgs boson and the photon, respectively.

2 ATLAS detector and data sample

ATLAS [1] is a multipurpose particle detector with an approximately forward–backward symmetric cylindrical geometry and near 4π coverage in solid angle.[1] It consists of an inner tracking detector, electromagnetic and hadronic calorimeters, and a muon spectrometer.

The inner tracking detector (ID) covers the pseudorapidity range $|\eta| < 2.5$ and is surrounded by a thin superconducting solenoid providing a 2 T magnetic field. At small radii, a high-granularity silicon pixel detector covers the vertex region and typically provides four measurements per track. The first hit is usually in the insertable B-layer, an additional layer installed in 2015 before 13 TeV data taking began [58,59]. It is followed by a silicon microstrip tracker, which provides up to eight measurement points per track. The silicon detectors are complemented by a gas-filled straw-tube transition radiation tracker, which enables radially extended track reconstruction up to $|\eta| = 2.0$ with typically 35 measurements per track.

Electromagnetic (EM) calorimetry within $|\eta| < 3.2$ is provided by barrel and endcap high-granularity lead/liquid-argon (LAr) EM calorimeters with an additional thin LAr presampler covering $|\eta| < 1.8$ to correct for energy loss in upstream material; for $|\eta| < 2.5$ the EM calorimeter is divided into three layers in depth. A steel/scintillator-tile calorimeter provides hadronic calorimetry for $|\eta| < 1.7$. LAr technology with copper as absorber is used for the hadronic calorimeters in the endcap region, $1.5 < |\eta| < 3.2$. The solid-angle coverage is completed with forward copper/LAr and tungsten/LAr calorimeter modules in $3.1 < |\eta| < 4.9$ optimised for EM and hadronic measurements, respectively.

The muon spectrometer (MS) surrounds the calorimeters and features trigger and high-precision tracking chambers measuring the deflection of muons in a magnetic field provided by three air-core superconducting toroidal magnets. The field integral of the toroids ranges between 2.0 and 6.0 T m across most of the detector. The precision chamber system covers the region $|\eta| < 2.7$ with three layers of monitored drift tubes, complemented by cathode strip chambers in the forward regions. The muon trigger system covers the range $|\eta| < 2.4$, featuring resistive plate chambers in the barrel and thin gap chambers in the endcap regions.

A two-level trigger and data acquisition system is used to record events for offline analysis [60]. The first-level trigger is implemented in hardware and uses a subset of detector information. This is followed by a software-based high-level trigger which outputs events for permanent storage at an average rate of 1 kHz, reduced from the maximum first-level rate of 100 kHz. An extensive software suite [61] is used in the

[1] ATLAS uses a right-handed coordinate system with its origin at the nominal interaction point (IP) in the centre of the detector and the z-axis along the beam pipe. The x-axis points from the IP to the centre of the LHC ring, and the y-axis points upward. Cylindrical coordinates (r, ϕ) are used in the transverse plane, ϕ being the azimuthal angle around the z-axis. The pseudorapidity is defined in terms of the polar angle θ as $\eta = -\ln\tan(\theta/2)$.

reconstruction and analysis of real and simulated data, in detector operations, and in the trigger and data acquisition systems of the experiment.

Data samples considered in this analysis were collected during stable beam conditions with all relevant detector systems functional [62] and were recorded by a combination of triggers requiring a photon and either one or two muons in the event. Due to the increasing instantaneous luminosity, the transverse momentum thresholds and identification requirements were modified during the data-taking periods. Available throughout the data collection period was a trigger requiring a photon fulfilling the 'medium' identification criteria [63] and transverse momentum p_{T}^{γ} greater than 25 GeV, and at least one muon identified at the first-level trigger with p_{T}^{μ} greater than 24 GeV. In the 2015 and 2016 data collection periods, this was complemented with a trigger requiring a photon fulfilling the 'loose' identification criteria [63] and $p_{\mathrm{T}}^{\gamma} > 35$ GeV, and at least one muon identified at the high-level trigger with $p_{\mathrm{T}}^{\mu} > 18$ GeV. During the 2017 and 2018 data collection, a trigger requiring an isolated photon fulfilling the 'tight' identification criteria [63] and $p_{\mathrm{T}}^{\gamma} > 35$ GeV and at least one muon identified at the high-level trigger with $p_{\mathrm{T}}^{\mu} > 18$ GeV, and a trigger requiring a 'loose' photon with $p_{\mathrm{T}}^{\gamma} > 35$ GeV, a muon identified at the first-level trigger with $p_{\mathrm{T}}^{\mu} > 15$ GeV and an additional muon identified at the high-level trigger with $p_{\mathrm{T}}^{\mu} > 2$ GeV were used. For candidate signal events that fulfil the analysis selection, described in Sect. 3, the trigger efficiency exceeds 97% in all cases. The uncertainty in the trigger efficiency is estimated to be 0.8% [64,65]. After applying trigger and data-quality requirements, the integrated luminosity of the data sample used in this search corresponds to 139.0 ± 2.4 fb^{-1}, obtained using the LUCID-2 detector [66] for the primary luminosity measurements and with the uncertainty in the integrated luminosity derived using the method described in Refs. [67,68]. The average number of pp interactions per bunch crossing ranged from about 13 in 2015 to about 39 in 2018.

3 Event selection

In addition to the trigger and data-quality requirements, selection criteria based on geometric acceptance, event kinematics, isolation, and vertex quality are imposed to select candidate $H(Z) \to \mathcal{Q}\gamma \to \mu^+\mu^-\gamma$ events. Reconstructed muon candidates must be either 'segment-tagged', where an ID track matches at least one track segment in the MS, or 'combined', where an ID track matches a full track in the MS [69]. Muons must also have an absolute value of pseudorapidity $|\eta^{\mu}| < 2.5$ and a transverse momentum $p_{\mathrm{T}}^{\mu} > 3$ GeV. Pairs of oppositely charged muons are fitted to a common vertex with the track parameter uncertainties taken into account [70]. Pairs satisfying a loose χ^2 requirement for this fit are combined to reconstruct candidate $\mathcal{Q} \to \mu^+\mu^-$ decays. The higher-p_{T} muon in each pair, called the leading muon, is required to have $p_{\mathrm{T}}^{\mu} > 18$ GeV. Dimuons with a mass $m_{\mu^+\mu^-}$ between 2.4 GeV and 4.3 GeV are selected as $\psi(nS) \to \mu^+\mu^-$ candidates, and those with a mass 8.0 GeV $< m_{\mu^+\mu^-} <$ 12.0 GeV are selected as $\Upsilon(nS) \to \mu^+\mu^-$ candidates. To improve the sensitivity of the $\Upsilon(nS)\gamma$ analysis in resolving the individual $\Upsilon(nS)$ states, events are classified into two exclusive categories based upon muon pseudorapidity to account for differences in resolution across the ATLAS detector. Events where both muons satisfy $|\eta^{\mu}| < 1.05$ are placed in the higher-resolution barrel (B) category, otherwise they are placed in the endcap (EC) category.

Candidate $\mathcal{Q} \to \mu^+\mu^-$ decays are subjected to further isolation and vertex-quality requirements. The sum of the p_{T} of ID tracks within a cone of variable size $\Delta R = \sqrt{(\Delta\phi)^2 + (\Delta\eta)^2} = \min\{10\,\mathrm{GeV}/(p_{\mathrm{T}}^{\mu}\,[\mathrm{GeV}]), 0.3\}$ around the leading muon is required to be less than 6% of the $\mathcal{Q}$ candidate's transverse momentum, $p_{\mathrm{T}}^{\mu^+\mu^-}$ [71]. This sum excludes the ID track associated with the leading muon itself, as well as the ID track associated with the subleading muon if it falls inside the ΔR cone. To mitigate the effects of multiple pp interactions in the same or neighbouring bunch crossings, only ID tracks that originate from the primary vertex are considered, which is defined as the reconstructed vertex with the highest $\Sigma\, {p_{\mathrm{T}}}^2$ of all associated tracks used in the formation of the vertex. To reject contributions from events involving b-hadron decays which result in displaced vertices, the vector leading from the primary vertex to the dimuon vertex is projected onto the direction of the $\mathcal{Q}$ candidate's transverse momentum, and the signed projection L_{xy} is required to be smaller than three times its uncertainty, $\sigma_{L_{xy}}$, such that $|L_{xy}/\sigma_{L_{xy}}| < 3$.

Photons are reconstructed from clusters of energy in the electromagnetic calorimeter. Clusters that match ID tracks consistent with the hypothesis of a photon conversion into e^+e^- are classified as converted photon candidates, whilst clusters that have no matching ID tracks are classified as unconverted candidates [63]. Reconstructed photon candidates are required to satisfy the 'tight' photon identification criteria [63], have absolute pseudorapidity $|\eta^{\gamma}| < 2.37$, excluding the calorimeter barrel/endcap transition region $1.37 < |\eta^{\gamma}| < 1.52$, and have transverse momentum $p_{\mathrm{T}}^{\gamma} > 35$ GeV. Further track- and calorimeter-isolation requirements are imposed to suppress contamination from jets: the sum of the p_{T} of all ID tracks originating from the primary vertex and within $\Delta R = 0.2$ of the photon direction, excluding any associated with the reconstructed photon, is required to be less than 5% of p_{T}^{γ}; the sum of the p_{T} of the calorimeter energy clusters within $\Delta R =$

0.4 of the photon direction, excluding the energy cluster of the reconstructed photon, is required to be less than $\left(2.45\text{ GeV} + 0.022 \times p_{\mathrm{T}}^{\gamma}\text{ [GeV]}\right)$. The calorimeter isolation variable is corrected to account for contributions associated with other pp interactions in the same bunch crossing [63].

Combinations of a $\mathcal{Q} \to \mu^+\mu^-$ candidate and a photon that satisfy $\Delta\phi(\mathcal{Q},\gamma) > \pi/2$ are retained for further analysis: this requirement suppresses contributions from events where the quarkonium and photon candidates have a small angular separation. If multiple combinations are possible, a situation that arises in fewer than 2% of events that pass the trigger requirements, the combination of the highest-p_{T} photon and the $\mathcal{Q}$ candidate with an invariant mass closest to that of the J/ψ meson is retained. To maintain a common event selection for the Higgs and Z boson analyses, while ensuring near-optimal sensitivity for both, a variable $p_{\mathrm{T}}^{\mu^+\mu^-}$ threshold that depends on the invariant mass of the $\mathcal{Q}\gamma$ system, $m_{\mu^+\mu^-\gamma}$, is applied. For the $\psi(nS) \to \mu^+\mu^-$ ($\Upsilon(nS) \to \mu^+\mu^-$) candidates, the $p_{\mathrm{T}}^{\mu^+\mu^-}$ threshold is 40 GeV (34 GeV) for $m_{\mu^+\mu^-\gamma} \leq 91$ GeV, and 54.4 GeV (52.7 GeV) for $m_{\mu^+\mu^-\gamma} \geq 140$ GeV. In the region $91\text{GeV} < m_{\mu^+\mu^-\gamma} < 140$ GeV, the $p_{\mathrm{T}}^{\mu^+\mu^-}$ threshold varies linearly between its fixed values outside this region. The $p_{\mathrm{T}}^{\mu^+\mu^-}$ thresholds are chosen to optimise the significance of potential signals at the Higgs and Z boson masses.

4 Signal modelling

The expected $H(Z) \to \mathcal{Q}\gamma$ signals were modelled using Monte Carlo (MC) simulated events to extract analytical approximations of the final observables. Several Higgs boson production modes were considered in the simulation of the $H \to \mathcal{Q}\gamma$ events. In order of decreasing production cross section, these are gluon–gluon fusion (ggH), vector-boson fusion (VBF), and associated production of a H boson with a Z boson (ZH), a $W^{\pm}$ boson (WH) or a $t\bar{t}$ top-quark pair ($t\bar{t}H$). Explicit simulation of the $t\bar{t}H$ Higgs boson production mechanism is an addition with respect to the analysis strategy of the 36.1 fb^{-1} study [50]. The contribution of Higgs bosons produced in association with a $b\bar{b}$ bottom-quark pair ($b\bar{b}H$) was not directly simulated, but was included by scaling up the production cross section used to normalise the ggH sample. This assumes that the efficiency for $b\bar{b}H$ events is equal to that for ggH; their inclusion increases the signal yield by less than 1%. For the $Z \to \mathcal{Q}\gamma$ signal events, Z boson production was modelled inclusively.

The Powheg Box v2 MC event generator [72–76] was used to model the ggH and VBF Higgs boson production mechanisms, calculated up to next-to-leading order (NLO) in α_s. Powheg Box was interfaced with Pythia 8.212 [77,78], which used the CTEQ6L1 parton distribution functions [79] and a set of tuned parameters called the AZNLO tune [80] to model the parton shower, hadronisation, and underlying event. The Pythia 8.212 event generator was used to model the ZH and WH production mechanisms, with NNPDF2.3lo parton distribution functions [81] and the A14 tune [82] for hadronisation and the underlying event. The MadGraph5_aMC@NLO 2.2.2 [83] event generator, interfaced with Pythia 8.212 for the parton shower, was used to model the $t\bar{t}H$ production mechanism, using the same parton distribution functions and event tune as the ZH and WH samples. Inclusive Z boson production was modelled with the same event generators, parton distribution functions, and event tune as the ggH and VBF Higgs boson production mechanisms. The subsequent decays of the Higgs and Z bosons into $J/\psi\,\gamma$, $\psi(2S)\,\gamma$ and $\Upsilon(1S, 2S, 3S)\,\gamma$ were simulated as a cascade of two-body decays, where the explicit simulation of $\psi(2S)\,\gamma$ decays is an addition to the analysis strategy compared to the 36.1 fb^{-1} study [50], which modelled these events by using $J/\psi\,\gamma$ samples. Interference effects between $J/\psi\,\gamma$ produced in Z boson decays and non-resonant QCD gluon-mediated processes [84] are expected to be small and were neglected. The generated events were passed through the detailed Geant4 simulation of the ATLAS detector [85,86] and processed with the same software as used to reconstruct the data. Conditions in the ATLAS detector, such as the average number of pp interactions per bunch crossing, changed throughout Run 2. Separate samples were produced with 2015–2016 conditions, 2017 conditions, and 2018 conditions, where each sample is normalised according to the integrated luminosity of the corresponding run period. The effect of multiple interactions in the same or neighbouring bunch crossings (pile-up) was modelled by overlaying each simulated hard-scattering event with inelastic pp events generated with Pythia 8.186 using the NNPDF2.3lo parton distribution functions and the A3 tune [87].

The production rates for the SM Higgs boson with $m_H = 125$ GeV, obtained from the CERN Yellow Reports [37,45], are assumed throughout this analysis. The ggH sample is normalised such that it reproduces the total cross section predicted by a next-to-next-to-next-to-leading-order (N^{3}LO) QCD calculation with NLO electroweak corrections applied [88–91]. The VBF sample is normalised to an approximate next-to-next-to-leading-order (NNLO) QCD cross section with NLO electroweak corrections applied [92–94]. The samples for the associated production of a W or Z boson with a Higgs boson are normalised to cross sections calculated at NNLO in QCD with NLO electroweak corrections [95,96] including the NLO QCD corrections [97] for $gg \to ZH$. The production of $t\bar{t}H$ is normalised to cross sections calculated at NLO in QCD with NLO electroweak corrections [37]. The production cross section used to scale the ggH sample to account for the $b\bar{b}H$ mecha-

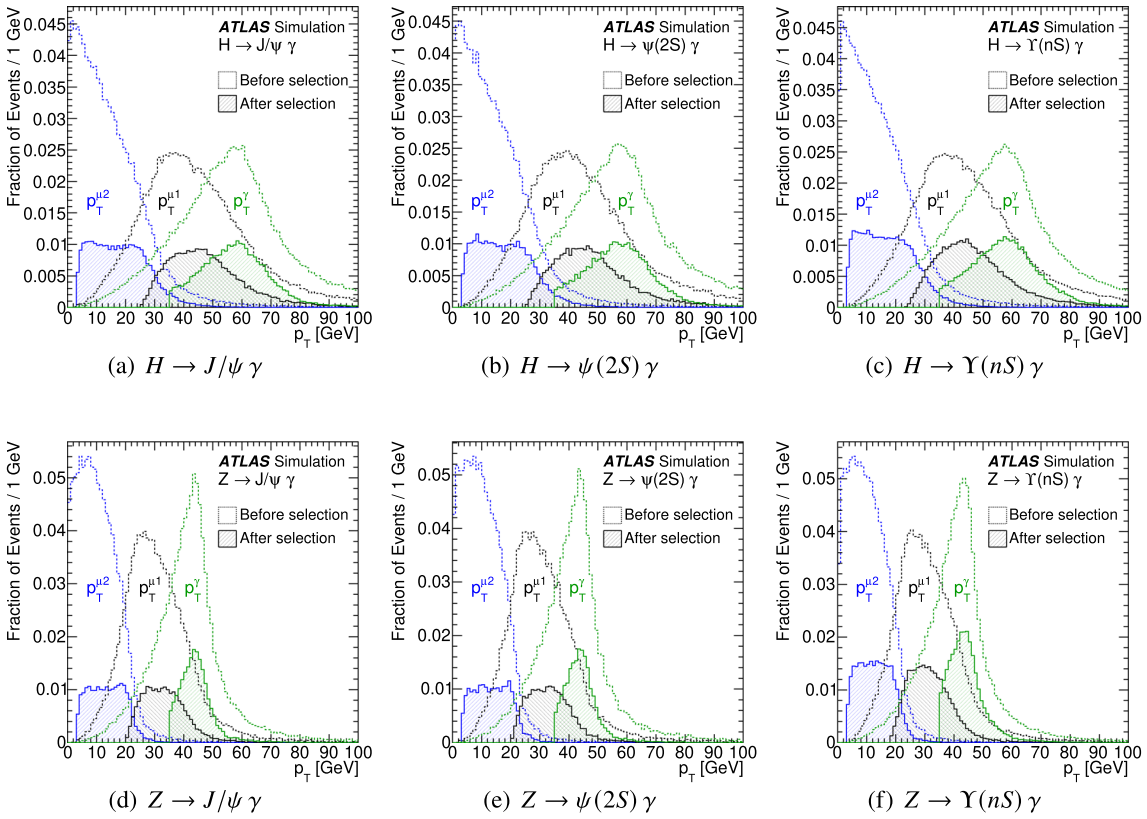

Fig. 2 Generator-level transverse momentum (p_{T}) distributions of the photon and muons for **a** $H \to J/\psi\,\gamma$, **b** $H \to \psi(2S)\,\gamma$, **c** $H \to \Upsilon(nS)\,\gamma$, **d** $Z \to J/\psi\,\gamma$, **e** $Z \to \psi(2S)\,\gamma$ and **f** $Z \to \Upsilon(nS)\,\gamma$ simulated events, respectively. The dashed-line distributions with a clear fill show the events at generator level which fall within the analysis geometric acceptance (both muons are required to have $|\eta^{\mu}| < 2.5$, while the photon is required to have $|\eta^{\gamma}| < 2.37$, excluding the region $1.37 < |\eta^{\gamma}| < 1.52$), and are each normalised to unity. The solid-line distributions with a hatched fill show the fraction of these events which pass the full analysis event selection described in Sect. 3. The relative difference between the two sets of distributions corresponds to the effects of reconstruction, trigger, and event selection efficiencies. The leading muon candidate is denoted by $p_{\mathrm{T}}^{\mu 1}$ (black), the subleading candidate by $p_{\mathrm{T}}^{\mu 2}$ (blue), and the photon candidate is denoted by p_{T}^{γ} (green)

nism was calculated at a mix of NNLO and NLO accuracy in QCD, with no electroweak corrections [37]. The production rate for the Z boson is normalised to the total cross section obtained from a measurement by the ATLAS Collaboration using 81 pb^{-1} of $\sqrt{s} = 13$ TeV data [44]. The branching fractions for the decays $\mathcal{Q} \to \mu^+\mu^-$ used in signal normalisation are taken from the Review of Particle Physics [98], as are the inclusive branching fractions for t-quark decays to hadrons or leptons in the normalisation of the $t\bar{t}H$ samples. The effects of meson polarisation on the dimuon kinematic distributions are accounted for via a reweighting of the simulated events, which are initially simulated without polarisation. The quarkonium states in the decay of the Higgs boson are expected to be transversely polarised; the quarkonium states in the decay of the Z boson are expected to be longitudinally polarised, due to a vanishing contribution from the transversely polarised meson [47]. Accounting for meson polarisation results in a 2–3% decrease in Higgs boson signal efficiency and a 9–10% increase in Z boson signal efficiency.

Figure 2 shows the generator-level photon and muon p_{T} distributions from the simulated $H(Z) \to \mathcal{Q}\gamma$ signal events. For the $J/\psi\,\gamma \to \mu^+\mu^-\,\gamma$ and $\psi(2S)\,\gamma \to \mu^+\mu^-\,\gamma$ final states, the total signal efficiency is 19% for the Higgs boson decays and 10% for the Z boson decays. These values take into account the trigger, reconstruction, identification, and isolation efficiencies, as well as the kinematic acceptance. The corresponding values for the $\Upsilon(1S, 2S, 3S)\,\gamma \to \mu^+\mu^-\,\gamma$ final states are 21% and 13%. The difference in efficiency between the Higgs and Z boson decays arises primarily from the softer photon and muon p_{T} distributions associated with $Z \to \mathcal{Q}\gamma$ production, as seen by comparing Fig. 2a and d for the $J/\psi\,\gamma$ case, Fig. 2b and e for the $\psi(2S)\,\gamma$ case, and Fig. 2c and f for the $\Upsilon(nS)\,\gamma$ case.

The $m_{\mu^+\mu^-\gamma}$ resolution is 1.6–1.8% for both the Higgs and Z boson decays. For each of the final states, a two-dimensional probability density function (PDF) is used to model the signal in $m_{\mu^+\mu^-\gamma}$ and $m_{\mu^+\mu^-}$. The Higgs boson signals are modelled with the sum of two bivariate Gaussian

distributions, which describe the approximately 60% correlations between the two mass variables in each decay channel as well as the effects of detector resolution. For Z boson decays, since the Z boson natural width is comparable to the detector resolution, the correlation between $m_{\mu^+\mu^-\gamma}$ and $m_{\mu^+\mu^-}$ is small, of order 10%, and is neglected, and the two mass distributions are treated as uncorrelated. The $m_{\mu^+\mu^-\gamma}$ distributions of the Z boson signals are modelled with the sum of two Voigtian PDFs corrected with a mass-dependent efficiency factor, which accounts for the changing selection efficiency along the Z lineshape that arises from the kinematic requirements described in Sect. 3. The Voigtian shape is a convolution of a Breit–Wigner distribution, which describes the natural width of the Z boson, and a Gaussian distribution, which describes detector resolution effects. The $m_{\mu^+\mu^-}$ distributions of the Z boson decays are modelled with a sum of two Gaussian PDFs, where the peak value and resolution parameters of the PDFs are fixed to the values obtained in a fit to the simulated event samples.

Systematic uncertainties in the signal yield and inferred branching fraction of the H and Z boson decays are considered. Uncertainties in the Higgs boson production cross sections total 5.8% [37,45]. The uncertainty in the measured Z boson production cross section is 2.9% [44], where the luminosity component of the uncertainty in the Z boson production cross-section measurement is treated as completely uncorrelated with the integrated luminosity uncertainty of data set used in this search. The uncertainty in the integrated luminosity is estimated to be 1.7% [67,68], using primary luminosity measurements from the LUCID-2 detector [66]. The uncertainty in the acceptance of the Higgs boson signal due to the choice of MC generator parameter values, parton distribution functions, set of tuned parameters for the underlying event, and parton showering, is estimated by studying how different choices affect the acceptance at generator level. The total uncertainty in the Higgs boson signal acceptance is estimated to be 1.8%. For the Z boson, the respective signal acceptance uncertainty is determined to be 1.0% by comparing the Z boson kinematic distributions in simulated events with measurements in data [99]. Trigger efficiencies for photons are determined from samples enriched with $Z \to e^+e^-$ events in data [100]. The photon trigger efficiency is estimated to contribute a systematic uncertainty of 0.8% to the expected signal yields [64,65]. Photon identification efficiencies are determined using the enriched $Z \to e^+e^-$ event samples, as well as inclusive photon events and $Z \to \ell^+\ell^-\gamma$ events [101,102]. The photon identification efficiency uncertainties, for both the converted and unconverted photons, are 1.7–1.9% for the Higgs and Z boson signals. The effect of the muon reconstruction and identification efficiency uncertainty is 2.2–2.4% [103]. The photon energy scale uncertainty, determined from $Z \to e^+e^-$ events and validated using $Z \to \ell^+\ell^-\gamma$ events [104,105], is propagated through the simulated samples as a function of η^γ and p_{T}^γ. The uncertainty associated with the photon energy scale and resolution in the simulation has a 0.1–0.2% effect on the Higgs and Z boson signal yields. Similarly, the systematic uncertainty associated with the scale of the muon momentum measurement has a 0.1–0.5% effect on the signal yields [103]. To assess any effect on the expected signal yield from imperfect modelling of pile-up, the average number of pile-up interactions is varied in the simulation; the corresponding uncertainty is 0.7–1.1%. These systematic uncertainties in the expected signal yields are summarised in Table 3. The effect of the energy and momentum scale and resolution uncertainties on the Higgs and Z boson signal shapes is negligible.

5 Background modelling

The background is considered to be composed of two distinct contributions which are modelled separately in this analysis. The first is an exclusive contribution originating from $\mu^+\mu^-\gamma$ events produced via the Drell–Yan process, where a highly energetic photon typically arises from final-state radiation. The second, which is the dominant background, is an inclusive contribution mostly from multi-jet and γ+jet events involving dimuon or $\mathcal{Q}$ production. The exclusive background is modelled with simulation, similarly to the signal model in Sect. 4, whilst the inclusive background is modelled with a data-driven technique, discussed in detail in Ref. [106]. The background is modelled independently for the $\psi(nS)$ dimuon mass region, and the B and EC categories of the $\Upsilon(nS)$ dimuon mass region.

5.1 Exclusive background

The Drell–Yan production of dimuons with a highly energetic photon, typically from final-state radiation, $q\bar{q} \to \gamma^*/Z^* \to \mu^+\mu^-\gamma$, constitutes a significant background contribution, exhibiting a characteristic resonant structure in the $m_{\mu^+\mu^-\gamma}$ distribution. The shapes of this background in $m_{\mu^+\mu^-\gamma}$ and $m_{\mu^+\mu^-}$ are modelled using events simulated with Sherpa 2.2.10 [107] at leading order with the NNPDF3.0 parton distribution function set in the $\psi(nS)$ and $\Upsilon(nS)$ $m_{\mu^+\mu^-}$ regions. The normalisation of this background is determined from a fit to the data in the signal region following the selection described in Sect. 3. The resonant shape in $m_{\mu^+\mu^-\gamma}$ is modelled analytically as the sum of a Voigtian function and a threshold function defined as $f(x) = \sqrt{x - x_0}\, \mathrm{e}^{-A(x-x_0)}$, where A and x_0 are constants, $f(x) = 0$ for $x < x_0$, and x is the three-body mass $m_{\mu^+\mu^-\gamma}$. The Voigtian function describes the on-shell Z production, which dominates in the $\Upsilon(nS)$ channels, whereas the threshold function describes the off-shell γ^*/Z^* production, which

Table 3 Summary of the systematic uncertainties in the expected signal yields. In the case of the H decays, the 'signal acceptance' uncertainty was estimated through parton distribution function variations, scale variations and variations of the underlying-event tune. For the Z decays, the 'signal acceptance' uncertainty was estimated by comparing simulation to data

Source of systematic uncertainty	Signal yield uncertainty			
	$H \to \psi(nS)\,\gamma$ (%)	$H \to \Upsilon(nS)\,\gamma$ (%)	$Z \to \psi(nS)\,\gamma$ (%)	$Z \to \Upsilon(nS)\,\gamma$ (%)
Total cross section	5.8	5.8	2.9	2.9
Integrated luminosity	1.7	1.7	1.7	1.7
Signal acceptance	1.8	1.8	1.0	1.0
Muon reconstruction	2.3	2.2	2.4	2.4
Photon identification	1.7	1.7	1.9	1.9
Pile-up uncertainty	0.8	0.7	1.1	1.1
Trigger efficiency	0.7	0.7	0.8	0.8
Photon energy scale	0.1	0.1	0.2	0.2
Muon momentum scale	0.1	0.1	0.5	0.2
Muon momentum resolution (ID)	<0.01	0.01	0.06	0.02
Muon momentum resolution (MS)	0.02	0.01	0.04	0.01

dominates in the $\psi(nS)$ channels. Different forms of the threshold function were considered, but the function above was found to provide the best description of the background shape. The shape in $m_{\mu^+\mu^-}$ is non-resonant and is modelled with a first-order Chebyshev polynomial. The parameters of the shape functions used to model each mass distribution are obtained from a fit to the simulated samples in each category once the signal region selection described in Sect. 3 is imposed. The statistical uncertainty associated with the parameters of the $m_{\mu^+\mu^-\gamma}$ shape function is accounted for via nuisance parameters in the maximum-likelihood fit to data in Sect. 7, based on the fit to the simulated samples, and is found to have a negligible effect on the final result.

5.2 Inclusive background

The dominant background arises from inclusive multi-jet or γ+jet events that involve the production of $\mathcal{Q}$ states, which subsequently decay into $\mu^+\mu^-$, or the production of non-resonant dimuon pairs such as from the Drell–Yan process or from random combinations of muons; the photon candidate may be genuine or, typically, a misidentified jet. The contribution from dimuon events in the inclusive background is separate from the exclusive $q\bar{q} \to \mu^+\mu^-\gamma$ background discussed in Sect. 5.1, as the latter involves a genuine photon candidate originating from the same hard-scattering process. The complicated mixture of background contributions, which involve QCD processes and misidentification of physics objects, and the highly selective phase-space region of interest makes it challenging to model this inclusive background accurately with simulation. Furthermore, the features of the background shape, which exhibits a broad kinematic peak at the location of a possible $Z \to \mathcal{Q}\gamma$ signal, combined with the relatively low number of events in the signal region make background modelling through direct fits of parametric models to the data unsuitable. For this reason, a generative approach is pursued, where the $m_{\mu^+\mu^-\gamma}$ shape of the inclusive background is obtained with a non-parametric data-driven model, described in Ref. [106] and used in several previous analyses [49,50,53,54], using templates to describe the kinematic distributions. The background normalisation is extracted directly from a fit to the data, and shape variations are incorporated in the background model in the final discriminating variable; these shape variations are also profiled in the fit.

The background model generation uses a sample of approximately 1.8×10^4 $\psi(nS)\,\gamma$ and 8.9×10^3 $\Upsilon(nS)\,\gamma$ candidate events. These events pass all the kinematic selection requirements described in Sect. 3, except that the $\mathcal{Q}$ and γ candidates are not required to satisfy the nominal isolation requirements, and a looser minimum $p_{\mathrm{T}}^{\mu^+\mu^-}$ requirement of 30 GeV is imposed; these events define the background-dominated generation region (GR). The exclusive background contribution is subtracted from the data to prepare for the construction of the inclusive background model. The exclusive background mass shape is obtained from a fit to the simulated events that meet the GR selection criteria. The background model is derived iteratively; in each iteration the exclusive $q\bar{q} \to \mu^+\mu^-\gamma$ contribution and the background model are fitted to the data in the GR to derive the exclusive background normalisation. PDFs are constructed to describe the distributions of the relevant kinematic and isolation variables and their most important correlations. The PDFs of these kinematic and isolation variables are sampled to generate an ensemble of pseudocandidate events, each with complete $\mathcal{Q}$ and γ candidate four-vectors and their associated

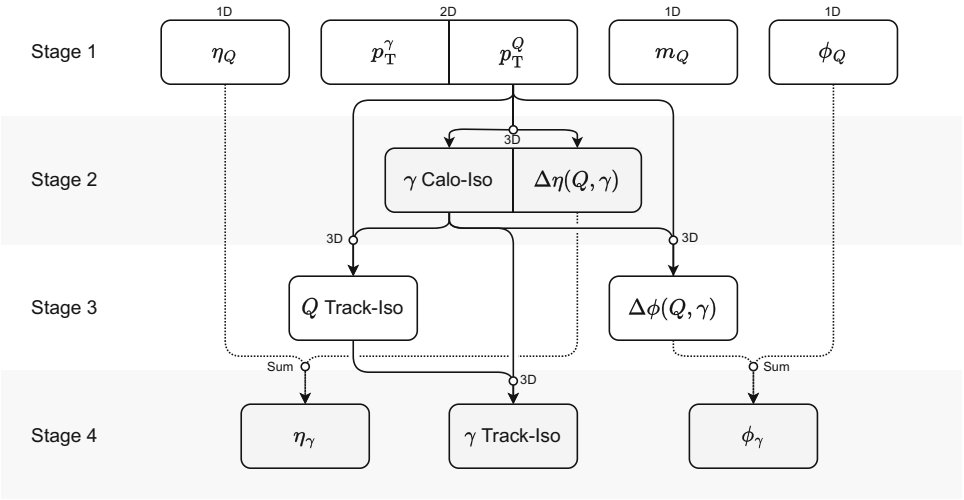

Fig. 3 The data-driven sequential sampling method used to generate pseudocandidate events for the inclusive background model. The labels '1D' and '2D' refer to the dimensionality of the PDFs used in the model generation of the variables underneath. Vertices labelled '3D' signify that the output variable (or variables), indentifed by the arrow leading out of the vertex, is sampled from a three-dimensional PDF described in bins of the input variable (or variables), indentifed by the lines leading into the vertex. If two variables share a border, they are sampled simultaneously from a joint PDF. Vertices labelled 'Sum' signify that the output variable is calculated directly from the sum of the input variables

isolation values. The important correlations among the kinematic and isolation variables of the background events, in particular between the $\mathcal{Q}$ and γ candidate transverse momenta $p_{\mathrm{T}}^{\mathcal{Q}}$ and p_{T}^{γ}, are retained in the generation of the pseudocandidate events through the following sequential sampling scheme, shown diagrammatically in Fig. 3:

1. The $\mathcal{Q}$-candidate pseudorapidity $\eta_{\mathcal{Q}}$, mass $m_{\mathcal{Q}}$, and azimuthal angle $\phi_{\mathcal{Q}}$, are drawn independently from one-dimensional PDFs, and values for $p_{\mathrm{T}}^{\mathcal{Q}}$ and p_{T}^{γ} are drawn simultaneously from a two-dimensional PDF.
2. The pseudorapidity difference between the $\mathcal{Q}$ and γ candidates, $\Delta\eta(\mathcal{Q},\gamma)$, and the γ-candidate calorimeter isolation are drawn simultaneously from a three-dimensional PDF, based on the value previously drawn for $p_{\mathrm{T}}^{\mathcal{Q}}$.
3. The $\mathcal{Q}$-candidate track isolation and the azimuthal angular separation between the $\mathcal{Q}$ and γ candidates, $\Delta\phi(\mathcal{Q},\gamma)$, are drawn separately from two three-dimensional PDFs, given the selected values of the γ-candidate calorimeter isolation and $p_{\mathrm{T}}^{\mathcal{Q}}$.
4. The γ-candidate track isolation is drawn from a three-dimensional PDF using the previously sampled values of the $\mathcal{Q}$-candidate track isolation and γ-candidate calorimeter isolation variables, and the values for η_γ and ϕ_γ are calculated from the values drawn for $\eta_{\mathcal{Q}}$, $\phi_{\mathcal{Q}}$, $\Delta\eta(\mathcal{Q},\gamma)$, and $\Delta\phi(\mathcal{Q},\gamma)$.

The nominal selection requirements are imposed and the surviving pseudocandidates are used to construct templates for the $m_{\mu^+\mu^-\gamma}$ distributions, which are then smoothed using a Gaussian kernel density estimation method [108]. Potential contamination of the GR sample from signal events is expected to be negligible. Signal injection tests were performed where a significant amount of signal, much larger than the signal branching fraction excluded in the presented analysis, was added to the GR to investigate the effect of such a potential signal contamination on the model; it was found that the presence of the signal is largely inconsequential to the shape of the background model and does not lead to any peaking structures in the background templates. The ability to predict data using the background model is studied in several validation regions (VRs), defined by selections looser than the nominal signal requirements and tighter than the generation region requirements. The requirements imposed in each of the selection regions used in the analysis are summarised in Table 4. The application of the $p_{\mathrm{T}}^{\mu^+\mu^-}$ requirement (VR1), the muon isolation requirements (VR2), and the photon isolation requirement (VR3) are each checked with this method, and in all regions the background model is found to describe the data well. This is shown in the comparison of the background model with data in each VR in Fig. 4, which includes the exclusive background contribution. The exclusive background shape in each selection region is obtained from a fit to the simulated events, and the normalisation is extrapolated from the fit to data in the GR.

The shape of the background model in three-body mass, $m_{\mu^+\mu^-\gamma}$, is allowed to vary around the nominal shape, and the parameters controlling these systematic variations are treated as nuisance parameters in the maximum-likelihood fit

Table 4 Summary of the selection regions used in the analysis. The term 'Full' indicates the corresponding requirement applied in the SR, and discussed in Sect. 3. The relaxed photon isolation requires the sum of the p_{T} of all ID tracks originating from the primary vertex and within $\Delta R = 0.2$ of the photon direction, excluding any associated with the reconstructed photon, to be less than 20% of p_{T}^{γ} and the sum of the p_{T} of the calorimeter energy clusters within $\Delta R = 0.4$ of the photon direction, excluding the energy of the reconstructed photon, to be less than $\left(2.45\ \mathrm{GeV} + 0.4 \times p_{\mathrm{T}}^{\gamma}\ [\mathrm{GeV}]\right)$. The relaxed $\mathcal{Q}$ isolation requires the sum of the p_{T} of the ID tracks within $\Delta R = \min\{10\ \mathrm{GeV}/(p_{\mathrm{T}}^{\mu}\ [\mathrm{GeV}]), 0.3\}$ of the leading muon to be less than 40% of $p_{\mathrm{T}}^{\mathcal{Q}}$

Region	$p_{\mathrm{T}}^{\mu\mu}$	Photon isolation	$\mathcal{Q}$ Isolation
Generation region (GR)	> 30 GeV	Relaxed	Relaxed
Validation region 1 (VR1)	Full	Relaxed	Relaxed
Validation region 2 (VR2)	> 30 GeV	Relaxed	Full
Validation region 3 (VR3)	> 30 GeV	Full	Relaxed
Signal region (SR)	Full	Full	Full

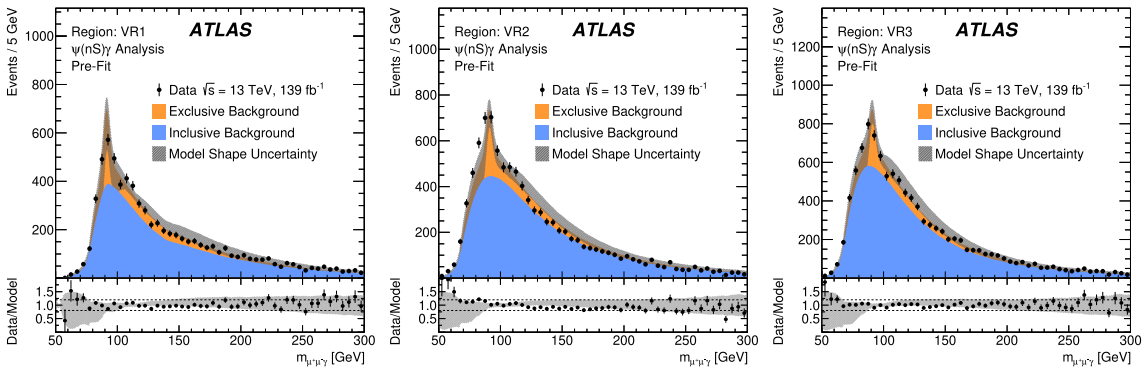

(a) $H(Z) \to \psi(nS)\gamma$ VR1 (b) $H(Z) \to \psi(nS)\gamma$ VR2 (c) $H(Z) \to \psi(nS)\gamma$ VR3

(d) $H(Z) \to \Upsilon(nS)\gamma$ VR1 (e) $H(Z) \to \Upsilon(nS)\gamma$ VR2 (f) $H(Z) \to \Upsilon(nS)\gamma$ VR3

Fig. 4 The distribution of $m_{\mu^+\mu^-\gamma}$ in data compared to the prediction of the background model for **a–c** $H(Z) \to \psi(nS)\,\gamma$ and **d–f** $H(Z) \to \Upsilon(nS)\,\gamma$ in the VR1, VR2 and VR3 validation regions. The total background is normalised to the observed number of events within the region shown, where the ratio of the exclusive and inclusive background components is extrapolated from the generation region. The uncertainty band corresponds to the uncertainty envelope derived from variations in the inclusive background modelling procedure. The dashed lines in the ratio plot in each figure indicate 1.2 and 0.8 on the y-axis. It should be noted that these plots are pre-fit, where the shapes of the inclusive and exclusive background components are fixed to the nominal template. In the maximum-likelihood fit to data in the signal region, the normalisation of each background is free, and their shapes are allowed to morph according to the defined shape variations

described in Sect. 6. Three such shape variations are implemented to allow the background template to adjust to the observed data. The first variation is produced via a scale variation of the p_{T}^{γ} distribution in the model, which allows the peak of the three-body mass distribution to shift to lower or higher masses; the second variation is produced via a linear distortion of the shape of the $\Delta\phi(\mathcal{Q}, \gamma)$ distribution, which allows the width of the three-body mass distribution

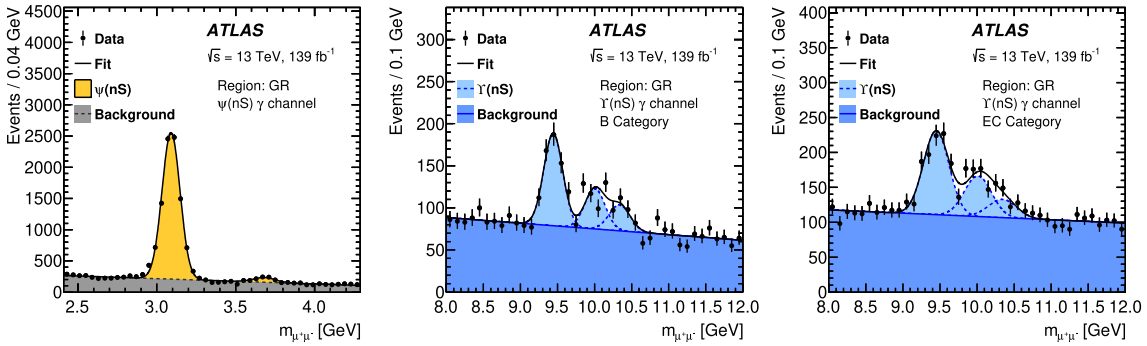

Fig. 5 Distribution of $\mu^+\mu^-$ invariant mass for **a** $\psi(nS)\,\gamma$, **b** $\Upsilon(nS)\,\gamma$ barrel category (B) and **c** $\Upsilon(nS)\,\gamma$ endcap category (EC). Candidates satisfy the requirements of the background generation region (GR) defined in Sect. 5.2. The error bars on the data points denote their statistical uncertainty

to increase or decrease; the third variation is produced via a global tilt of the three-body mass distribution around a pivot point, which allows the background to adapt to slopes with respect to the data. The first two variations are straightforward alterations to the underlying kinematics of the pseudocandidates, which cause corresponding changes in the three-body mass. Their nuisance parameters are loosely constrained by a Gaussian term in the likelihood, which arbitrarily assigns the $\pm 1\sigma$ variations to a relatively large change in the shape, and these are subsequently constrained by the data. The third variation is applied directly to the final three-body mass template and left unconstrained in the final fit.

The $m_{\mu^+\mu^-}$ distribution for $\psi(nS)\,\gamma$ candidates that meet the background model generation criteria is shown in Fig. 5a and exhibits clear peaks at the J/ψ and $\psi(2S)$ masses. In Fig. 5b and c, the corresponding distributions for the selected $\Upsilon(nS)\,\gamma$ candidates are shown respectively for the B and EC categories, where the individual $\Upsilon(1S)$,$\Upsilon(2S)$, and $\Upsilon(3S)$ peaks can be observed. During the $m_{\mu^+\mu^-\gamma}$ background model generation, a value for $m_{\mu^+\mu^-}$ is drawn from the distributions shown in Fig. 5. No significant correlations between $m_{\mu^+\mu^-}$ and $m_{\mu^+\mu^-\gamma}$ are observed. Thus, the $m_{\mu^+\mu^-}$ distribution itself is modelled independently of $m_{\mu^+\mu^-\gamma}$ using analytical PDFs. The $\psi(nS)$ and $\Upsilon(nS)$ peaks are modelled with Gaussian PDFs, while the inclusive background is modelled with a first-order Chebyshev polynomial function; these functions were found to be sufficient to describe the data, given its statistical uncertainty. The parameters of these PDFs are obtained by means of a one-dimensional fit to events selected in the background model generation region, as shown in Fig. 5, and are used to model the $m_{\mu^+\mu^-}$ distribution in the maximum-likelihood fit in Sect. 6. It is noted that the slope of the inclusive background is allowed to adapt to the observed data in the fit to the signal region, and that the relative normalisations of the different contributions to $m_{\mu^+\mu^-}$ are left free.

6 Statistical methods

The data selected by the signal region criteria are compared with background and signal predictions using a two-dimensional (2D) unbinned maximum-likelihood fit in $m_{\mu^+\mu^-\gamma}$ and $m_{\mu^+\mu^-}$, for events with $m_{\mu^+\mu^-\gamma} < 300$ GeV. This allows the $H(Z) \to \mathcal{Q}\gamma$ signals to be distinguished from each other, as well as the from the exclusive and inclusive background contributions. The likelihood function $\mathcal{L}$ for each of the $\psi(nS)$ and $\Upsilon(nS)$ analyses is constructed using the signal and background models described in Sects. 4 and 5. The parameters of interest $\vec{\mu} = \{\mu_i\}$ are the signal strengths, which correspond to the signal rate normalised to the SM expectation, for each of the Higgs and Z boson signals counted by the index i. The likelihood for the $\psi(nS)$ analysis when n events are observed in the signal region is defined as[2]:

$$\begin{aligned}\mathcal{L}(\vec{\mu},\vec{b},\alpha,\theta,\theta') = \mathcal{P}\Bigg(n|\sum_{i=1}^{4}\mu_i\cdot s_i(\vec{\alpha}) \\ +\sum_{j=1}^{4} b_j\Bigg)\times\prod_r \mathcal{G}(\alpha_r|0,1) \\ \times\prod_{k=1}^{n}\Bigg(\sum_{i=1}^{4}\mathcal{F}_i^s\cdot\mathcal{S}_i(m^k_{\mu^+\mu^-\gamma},m^k_{\mu^+\mu^-}|\mu_i) \\ +\sum_{j=1}^{4}\mathcal{F}_j^b\cdot\mathcal{R}_j(m^k_{\mu^+\mu^-\gamma}|\vec{\theta})\mathcal{M}_j(m^k_{\mu^+\mu^-}|\theta')\Bigg) \\ \times\prod_l \mathcal{G}(\theta_l|0,1)\end{aligned}$$

[2] The likelihood for the $\Upsilon(nS)$ analysis is defined similarly, but with the events divided further into two exclusive categories.

In the above equation, $\mathcal{P}$ is the Poisson distribution for n observed events given the total signal and background. The symbol $s_i(\vec{\alpha})$ denotes the expected SM signal yield for signal i as modified by the nuisance parameters $\vec{\alpha}$, which correspond to the signal normalisation systematic uncertainties discussed in Sect. 4. These nuisance parameters are counted by index r and are constrained with standard Gaussian PDF terms, $\mathcal{G}$. The normalisation parameters associated with each independent background contribution are denoted by $\vec{b} = \{b_j\}$. These are not constrained and are determined directly from the fit to the data. In the case of the $\psi(nS)$ analysis, the background components are exclusive $q\bar{q} \to \mu^+\mu^-\gamma$ production, inclusive J/ψ decays, inclusive $\psi(2S)$ decays, and inclusive non-resonant dimuon production.[3] The symbols $\mathcal{F}_i^s$ and $\mathcal{F}_j^b$ denote the signal i and background j as fractions of the total signal and background, respectively. The shape of signal i in $(m_{\mu^+\mu^-\gamma}, m_{\mu^+\mu^-})$ is given by the PDF $\mathcal{S}_i$. Correspondingly, the shape of the background component j is given by the product of PDFs $\mathcal{R}_j(m_{\mu^+\mu^-\gamma})$ and $\mathcal{M}_j(m_{\mu^+\mu^-})$, since no correlations between $m_{\mu^+\mu^-}$ and $m_{\mu^+\mu^-\gamma}$ are observed in background shape. The nuisance parameters $\vec{\theta}$ parameterise the systematic variations of the background shapes discussed in Sect. 5. They are counted by index l and are constrained with standard Gaussian terms. The only exception is the nuisance parameter related to the 'global tilt' systematic shape variation of the inclusive background, which is not constrained. The nuisance parameter θ' corresponds to the slope in $m_{\mu^+\mu^-}$ of the non-resonant component of the inclusive background, which is free in the fit.

Upper limits are set on the branching fractions for the Higgs and Z boson decays into $\mathcal{Q}\gamma$ using the $\mathrm{CL_s}$ modified frequentist formalism [109] with the profile-likelihood-ratio test statistic and the asymptotic approximations derived in Ref. [110]. When setting limits for one of the signals, the other potential signal contributions are treated as nuisance parameters and are profiled in the fit. Only the decays $\mathcal{Q} \to \mu^+\mu^-$ are considered in the limit setting, feed-down from $Q' \to Q + X$ transitions are not included.

The ability of the fit to identify potential signal contributions was verified through signal injection tests. Signals corresponding to a branching fraction of 5×10^{-4} and 5×10^{-7} for the Higgs and Z boson decays, respectively, were injected into an Asimov dataset [110] constructed from a background-only fit in the signal region. The full fit accurately recovered the injected signals.

[3] In the case of the $\Upsilon(nS)$ analysis, the background components are exclusive $q\bar{q} \to \mu^+\mu^-\gamma$ production, inclusive $\Upsilon(1S)$, $\Upsilon(2S)$, and $\Upsilon(3S)$ decays, and inclusive non-resonant dimuon production, and are fit separately in the B and EC categories.

7 Results

In total, 3394 events are observed in the $\psi(nS)\gamma$ signal region and 3577 events are observed in the $\Upsilon(nS)\gamma$ signal region. The results of the background-only fits for the $\psi(nS)\gamma$ and $\Upsilon(nS)\gamma$ analyses are shown in Figs. 6 and 7 respectively, where the signal distributions shown correspond to the extracted 95% confidence-level (CL) branching fraction upper limits. The expected and observed numbers of background events within the $m_{\mu^+\mu^-\gamma}$ ranges relevant to the Higgs and Z boson signals are given in Table 5, where the expected backgrounds are obtained from these background-only fits. The exclusive contribution to the total background in these regions of relevance ranges from approximately 10% for the $H \to J/\psi\gamma$ and 22% for $H \to \psi(2S)\gamma$ to 21% and 41% for the corresponding Z boson decay searches. For the $\Upsilon(nS)\gamma$ analysis the exclusive contribution ranges from 24% to 29% for the ranges of relevance for the Higgs boson searches, while for the ranges of relevance for the Z boson searches it is between 75% and 79%. Table 5 also shows the expected number of signal events for reference branching fractions near the sensitivity of the analysis: 10^{-3} for $H \to \mathcal{Q}\gamma$ and 10^{-6} for $Z \to \mathcal{Q}\gamma$.

From the fit to the observed data, the largest observed local excess is 1.9σ in the search for $Z \to J/\psi\gamma$, followed by a 0.8σ excess in the search for $H \to \psi(2S)\gamma$. The expected and observed 95% CL upper limits on the branching fractions for Higgs and Z boson decays into a quarkonium state and a photon are presented in Table 6, along with the observed upper limits in terms of Higgs and Z boson production cross section times branching fraction to a quarkonium state and a photon. The expected sensitivity improves by a factor of approximately two relative to the previous ATLAS result presented in Ref. [50]; this is in line with what is expected from the increase in integrated luminosity for this search, as this analysis is limited primarily by statistical uncertainties. The systematic uncertainties in the signal normalisation and background shape described respectively in Sects. 4 and 5 result in a 0.8% increase of the expected 95% CL upper limit on the branching fraction of the $H \to J/\psi\gamma$ decay. For the $Z \to J/\psi\gamma$ decay the effect is larger, 4.2%, mostly due to the systematic uncertainty in the background shape. The increase is 0.1% for $H \to \psi(2S)\gamma$, and 0.6% for $Z \to \psi(2S)\gamma$. Similar behaviour is observed in the $\Upsilon(nS)\gamma$ analysis, with systematic uncertainties resulting in a 0.1–0.8% deterioration in the sensitivity to the $H \to \Upsilon(1S, 2S, 3S)\gamma$ decays and a 0.3–0.5% deterioration in the sensitivity to the $Z \to \Upsilon(1S, 2S, 3S)\gamma$ decays.

For the interpretation of these searches in terms of constraints on the charm- and bottom-quark Yukawa couplings the approach presented in Refs. [31,38] is employed: The ratio of signal strength (μ) measurements for the $H \to J/\psi\gamma$ and $H \to \gamma\gamma$ channels corresponds to the

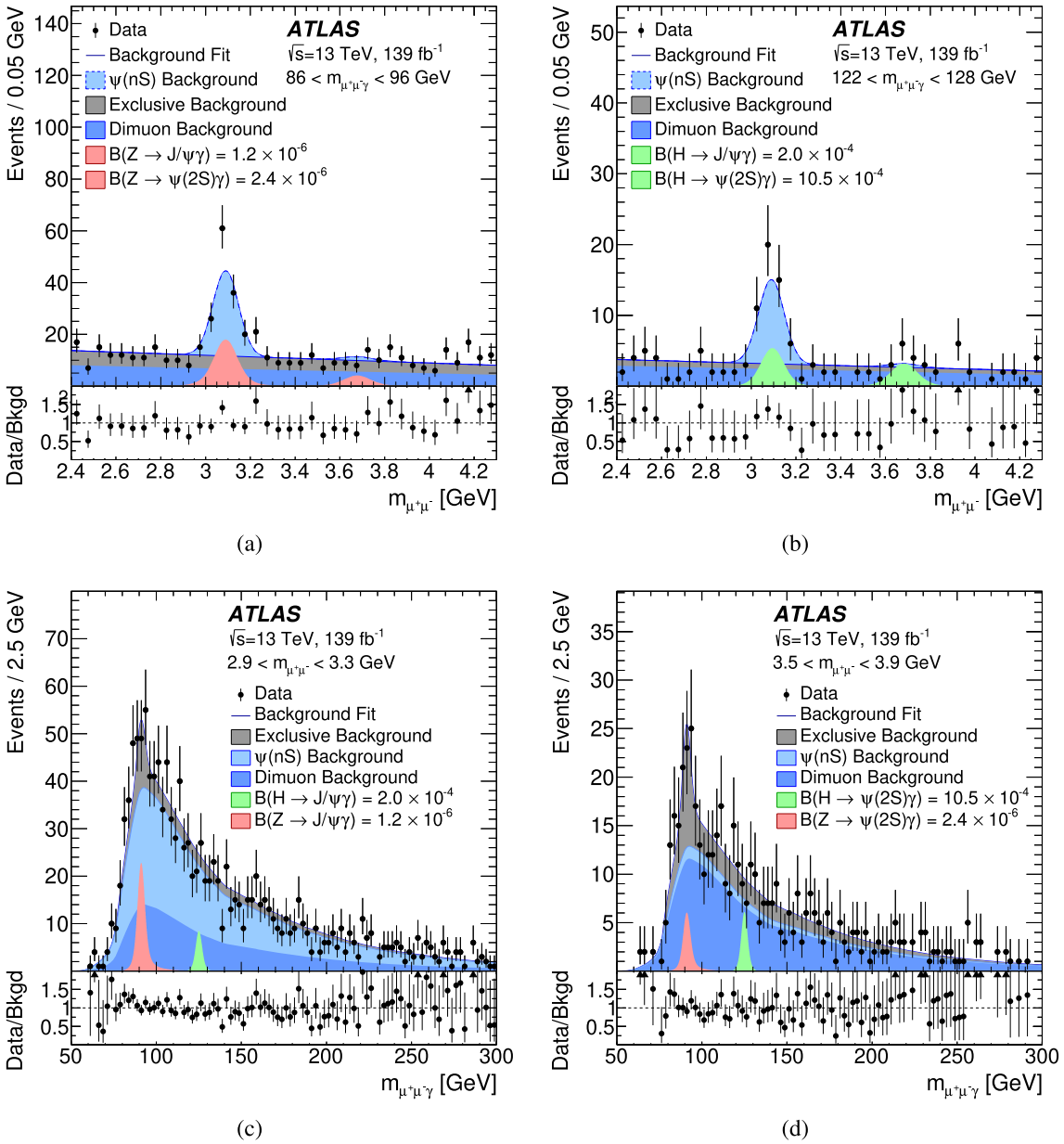

Fig. 6 Projection of the $\psi(nS)$ channel fit in $m_{\mu^+\mu^-}$ for the **a** Z boson and **b** Higgs boson $m_{\mu^+\mu^-\gamma}$ regions, and in $m_{\mu^+\mu^-\gamma}$ for the **c** J/ψ and **d** $\psi(2S)$ $m_{\mu^+\mu^-}$ regions. The dimuon/$\mathcal{Q}(nS)$ backgrounds in the legend refer to the inclusive background contribution which is non-resonant/resonant in $m_{\mu^+\mu^-}$. The branching fraction of each of the signals is set to the observed 95% CL upper limit

ratio of measurements of their production cross section times branching fraction $\sigma \times \mathcal{B}$, normalised to their respective SM expectations. This is, to a good approximation, equal to the ratio of the respective partial decay widths Γ normalised to their SM expectation Γ^{SM}, since the dependence on the production mechanism and Higgs total width cancels out. The ratio κ_c/κ_γ of the coupling modifiers, each of which is the ratio of the coupling to its SM value, for the charm-quark Yukawa coupling and the effective coupling of Higgs boson to photons can be estimated as:

$$\frac{\mu_{H\to J/\psi\,\gamma}}{\mu_{H\to\gamma\gamma}} = \frac{\sigma_H \mathcal{B}_{H\to J/\psi\,\gamma}/\sigma_H^{\mathrm{SM}}\mathcal{B}^{\mathrm{SM}}_{H\to J/\psi\,\gamma}}{\sigma_H \mathcal{B}_{H\to\gamma\gamma}/\sigma_H^{\mathrm{SM}}\mathcal{B}^{\mathrm{SM}}_{H\to\gamma\gamma}}$$
$$\approx \frac{\Gamma_{H\to J/\psi\,\gamma}/\,\Gamma^{\mathrm{SM}}_{H\to J/\psi\,\gamma}}{\Gamma_{H\to\gamma\gamma}/\,\Gamma^{\mathrm{SM}}_{H\to\gamma\gamma}} = \frac{|\mathcal{A}_{\mathrm{ind}} + \mathcal{A}_{\mathrm{dir}}\kappa_c/\kappa_\gamma|^2}{\Gamma^{\mathrm{SM}}_{H\to J/\psi\,\gamma}}$$

The indirect and direct amplitudes $\mathcal{A}$ for $H \to J/\psi\,\gamma$ and $H \to \Upsilon(nS)\,\gamma$ interfere destructively and are obtained from Ref. [36].[4] The signal strength for $H \to \gamma\gamma$ is

[4] The corresponding direct and indirect amplitude values for $H \to \psi(2S)\,\gamma$ could not be obtained from the literature.

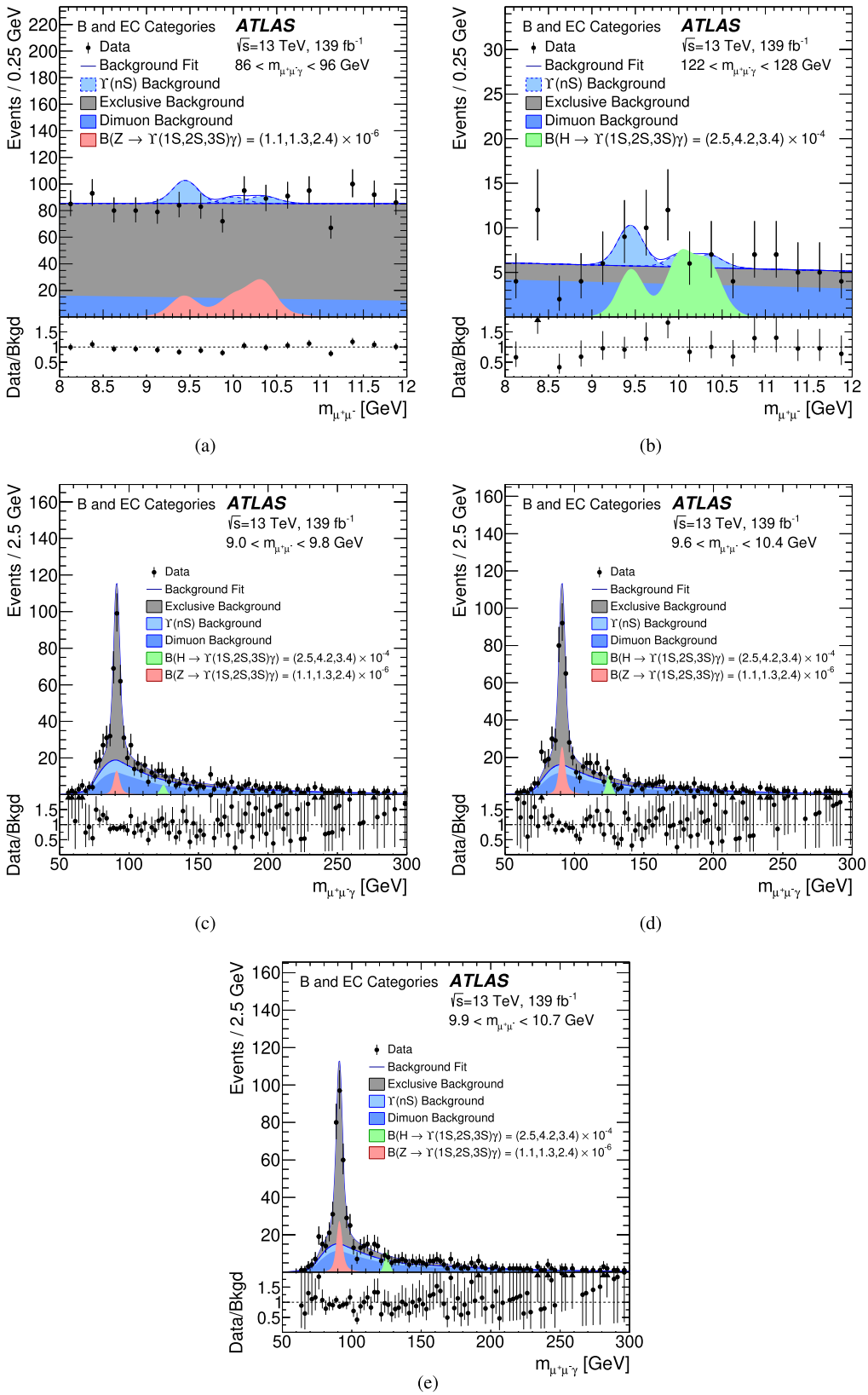

Fig. 7 Projection of the $\Upsilon(nS)$ channel fit in $m_{\mu^+\mu^-}$ for the **a** Z boson and **b** Higgs boson $m_{\mu^+\mu^-\gamma}$ regions, and in $m_{\mu^+\mu^-\gamma}$ for the $\Upsilon(1S, 2S, 3S)$ $m_{\mu^+\mu^-}$ regions in **c**–**e**, respectively. The dimuon/$\mathcal{Q}(nS)$ backgrounds in the legend refer to the inclusive background contribution which is non-resonant/resonant in $m_{\mu^+\mu^-}$. The branching fraction of each of the signals is set to the observed 95% CL upper limit

Table 5 Numbers of observed and expected background events for the $m_{\mu^+\mu^-\gamma}$ ranges of interest. Each expected background and the corresponding uncertainty of its mean is obtained from a background-only fit to the data; the uncertainty does not take into account statistical fluctuations in each mass range. Expected Z and Higgs boson signal contributions, with their corresponding total systematic uncertainty, are shown for reference branching fractions of 10^{-6} and 10^{-3}, respectively. The ranges in $m_{\mu^+\mu^-}$ are centred around each quarkonium resonance, with a width driven by the resolution of the detector; in particular, the ranges for the $\Upsilon(nS)$ resonances are based on the resolution in the endcaps. It is noted that the discrepancy between the observed and expected backgrounds for $m_{\mu^+\mu^-} = 9.0$–9.8 GeV in the endcaps was found to have a small impact on the observed limit for $Z \to \Upsilon(1S)\,\gamma$

Category	$m_{\mu^+\mu^-}$ range (GeV)	Observed (expected) background				Z signal for $\mathcal{B} = 10^{-6}$	H signal for $\mathcal{B} = 10^{-3}$
		$m_{\mu^+\mu^-\gamma}$ range (GeV)					
		86–96		122–128			
Inclusive	2.9–3.3	198	(185.6 ± 5.9)	61	(59.1 ± 1.6)	49.3 ± 2.4	87.8 ± 6.1
Inclusive	3.5–3.9	83	(82.5 ± 4.0)	21	(22.9 ± 0.9)	6.5 ± 0.3	11.8 ± 0.8
Barrel	9.0–9.8	125	(125.3 ± 4.7)	12	(11.6 ± 0.6)	11.4 ± 0.6	20.2 ± 1.4
Barrel	9.6–10.4	118	(121.9 ± 4.6)	14	(10.7 ± 0.6)	8.8 ± 0.4	15.3 ± 1.1
Barrel	9.9–10.7	102	(119.9 ± 4.5)	11	(10.2 ± 0.6)	10.1 ± 0.5	17.4 ± 1.2
Endcap	9.0–9.8	133	(162.9 ± 5.7)	16	(13.6 ± 0.7)	15.5 ± 0.8	20.5 ± 1.4
Endcap	9.6–10.4	150	(157.1 ± 5.6)	11	(11.7 ± 0.5)	11.7 ± 0.6	15.8 ± 1.1
Endcap	9.9–10.7	171	(156.7 ± 5.8)	7	(11.4 ± 0.6)	13.5 ± 0.7	17.6 ± 1.2

Table 6 Expected, with the corresponding $\pm 1\sigma$ intervals, and observed 95% CL branching fraction upper limits for the Higgs and Z boson decays into a quarkonium state and a photon. Standard Model production of the Higgs boson is assumed. The corresponding upper limits on the production cross section times branching fraction $\sigma \times \mathcal{B}$ are also shown

Decay channel	95% CL upper limits					
	Branching fraction				$\sigma \times \mathcal{B}$	
	Higgs boson (10^{-4})		Z boson (10^{-6})		Higgs boson [fb]	Z boson [fb]
	Expected	Observed	Expected	Observed	Observed	Observed
$J/\psi\,\gamma$	$1.8^{+0.8}_{-0.5}$	2.0	$0.7^{+0.3}_{-0.2}$	1.2	11	69
$\psi(2S)\,\gamma$	$8.1^{+3.6}_{-2.3}$	10.5	$3.0^{+1.3}_{-0.8}$	2.4	58	142
$\Upsilon(1S)\,\gamma$	$2.7^{+1.2}_{-0.8}$	2.5	$1.6^{+0.6}_{-0.4}$	1.1	14	62
$\Upsilon(2S)\,\gamma$	$3.4^{+1.5}_{-1.0}$	4.2	$2.1^{+0.8}_{-0.6}$	1.3	24	74
$\Upsilon(3S)\,\gamma$	$3.0^{+1.3}_{-0.8}$	3.4	$1.9^{+0.8}_{-0.5}$	2.4	19	143

obtained from Ref. [111]. An observed 95% CL interval of $(-133, 175)$ is obtained for κ_c/κ_γ, with the expected interval being $(-120, 161)$. The interval is dominated by the statistical uncertainty of the $H \to J/\psi\,\gamma$ search. The correlated components in the uncertainties of the two measurements were removed, but this had negligible impact. The theoretical uncertainties of the amplitudes result in a widening of the obtained interval by approximately 8%, mainly through the uncertainty in the real part of the direct amplitude. Furthermore, the magnitude of the direct amplitude, which is sensitive to the charm-quark coupling to the Higgs boson, is significantly smaller in the most recent theory calculations [34,36] than in earlier ones [29], leading to much weaker constraints. Very large values of κ_c lead to tensions with other ATLAS [112] and CMS [113] measurements of Higgs boson couplings [114]. A similar relation can be written for the ratio κ_b/κ_γ, where κ_b is the coupling modifier for the bottom-quark Yukawa coupling. Combining the three $\Upsilon(nS)\,\gamma$ decays, and accounting for the -21% correlation between $\mu_{H\to\Upsilon(2S)\,\gamma}$ and $\mu_{H\to\Upsilon(3S)\,\gamma}$, a 95% CL interval of $(-37, 40)$ is obtained for κ_b/κ_γ. The corresponding expected 95% CL interval is $(-37, 39)$. The $\Upsilon(1S)\,\gamma$ decay contributes most of the sensitivity to κ_b/κ_γ thanks to its indirect amplitude being the largest amongst the $\Upsilon(nS)\,\gamma$ decays. Similarly to the κ_c/κ_γ case, the statistical uncertainty of the search for exclusive Higgs boson decays into $\Upsilon(nS)\,\gamma$ dominates the interval. The theoretical uncertainties of the amplitudes enlarge the interval by 12%.

8 Summary

Searches for the exclusive decays of Higgs and Z bosons into a vector quarkonium state and a photon have been

performed with a $\sqrt{s} = 13$ TeV pp collision data sample collected with the ATLAS detector at the LHC and corresponding to an integrated luminosity of 139 fb^{-1}. The observed data are compatible with the background expectations. The 95% CL upper limits obtained for the $J/\psi\,\gamma$ final state are $\mathcal{B}(H \to J/\psi\,\gamma) < 2.0 \times 10^{-4}$ and $\mathcal{B}(Z \to J/\psi\,\gamma) < 1.2 \times 10^{-6}$. The corresponding upper limits for the $\psi(2S)\,\gamma$ final state are $\mathcal{B}(H \to \psi(2S)\,\gamma) < 10.5 \times 10^{-4}$ and $\mathcal{B}(Z \to \psi(2S)\,\gamma) < 2.4 \times 10^{-6}$. The 95% CL upper limits $\mathcal{B}(H \to \Upsilon(nS)\,\gamma) < (2.5, 4.2, 3.4) \times 10^{-4}$ and $\mathcal{B}(Z \to \Upsilon(nS)\,\gamma) < (1.1, 1.3, 2.4) \times 10^{-6}$ are set for the $\Upsilon(1S, 2S, 3S)\,\gamma$ final states. These upper limits represent an improvement by a factor of approximately two relative to the previous results from the ATLAS Collaboration using 36.1 fb^{-1} of $\sqrt{s} = 13$ TeV pp collision data. Further, constraints are set on the ratio κ_c/κ_γ and κ_b/κ_γ of the Higgs boson coupling modifiers. An observed 95% CL interval of $(-133, 175)$ is obtained for κ_c/κ_γ, and a 95% CL interval of $(-37, 40)$ is obtained for κ_b/κ_γ.

Acknowledgements We thank CERN for the very successful operation of the LHC, as well as the support staff from our institutions without whom ATLAS could not be operated efficiently. We acknowledge the support of ANPCyT, Argentina; YerPhI, Armenia; ARC, Australia; BMWFW and FWF, Austria; ANAS, Azerbaijan; CNPq and FAPESP, Brazil; NSERC, NRC and CFI, Canada; CERN; ANID, Chile; CAS, MOST and NSFC, China; Minciencias, Colombia; MEYS CR, Czech Republic; DNRF and DNSRC, Denmark; IN2P3-CNRS and CEA-DRF/IRFU, France; SRNSFG, Georgia; BMBF, HGF and MPG, Germany; GSRI, Greece; RGC and Hong Kong SAR, China; ISF and Benoziyo Center, Israel; INFN, Italy; MEXT and JSPS, Japan; CNRST, Morocco; NWO, Netherlands; RCN, Norway; MEiN, Poland; FCT, Portugal; MNE/IFA, Romania; MESTD, Serbia; MSSR, Slovakia; ARRS and MIZŠ, Slovenia; DSI/NRF, South Africa; MICINN, Spain; SRC and Wallenberg Foundation, Sweden; SERI, SNSF and Cantons of Bern and Geneva, Switzerland; MOST, Taiwan; TENMAK, Türkiye; STFC, UK; DOE and NSF, USA. In addition, individual groups and members have received support from BCKDF, CANARIE, Compute Canada and CRC, Canada; PRIMUS 21/SCI/017 and UNCE SCI/013, Czech Republic; COST, ERC, ERDF, Horizon 2020 and Marie Skłodowska-Curie Actions, European Union; Investissements d'Avenir Labex, Investissements d'Avenir Idex and ANR, France; DFG and AvH Foundation, Germany; Herakleitos, Thales and Aristeia programmes co-financed by EU-ESF and the Greek NSRF, Greece; BSF-NSF and MINERVA, Israel; Norwegian Financial Mechanism 2014–2021, Norway; NCN and NAWA, Poland; La Caixa Banking Foundation, CERCA Programme Generalitat de Catalunya and PROMETEO and GenT Programmes Generalitat Valenciana, Spain; Göran Gustafssons Stiftelse, Sweden; The Royal Society and Leverhulme Trust, UK. The crucial computing support from all WLCG partners is acknowledged gratefully, in particular from CERN, the ATLAS Tier-1 facilities at TRIUMF (Canada), NDGF (Denmark, Norway, Sweden), CC-IN2P3 (France), KIT/GridKA (Germany), INFN-CNAF (Italy), NL-T1 (Netherlands), PIC (Spain), ASGC (Taiwan), RAL (UK) and BNL (USA), the Tier-2 facilities worldwide and large non-WLCG resource providers. Major contributors of computing resources are listed in Ref. [115].

Data Availability Statement This manuscript has no associated data or the data will not be deposited. [Authors' comment: All ATLAS scientific output is published in journals, and preliminary results are made available in Conference Notes. All are openly available, without restriction on use by external parties beyond copyright law and the standard conditions agreed by CERN. Data associated with journal publications are also made available: tables and data from plots (e.g. cross section values, likelihood profiles, selection efficiencies, cross section limits, ...) are stored in appropriate repositories such as HEPDATA (http://hepdata.cedar.ac.uk/). ATLAS also strives to make additional material related to the paper available that allows a reinterpretation of the data in the context of new theoretical models. For example, an extended encapsulation of the analysis is often provided for measurements in the framework of RIVET (http://rivet.hepforge.org/)." This information is taken from the ATLAS Data Access Policy, which is a public document that can be downloaded from http://opendata.cern.ch/record/413.]

Funded by SCOAP^3. SCOAP^3 supports the goals of the International Year of Basic Sciences for Sustainable Development.

References

1. ATLAS Collaboration, The ATLAS Experiment at the CERN Large Hadron Collider. JINST **3**, S08003 (2008). https://doi.org/10.1088/1748-0221/3/08/S08003
2. CMS Collaboration, The CMS experiment at the CERN LHC. JINST **3**, S08004 (2008). https://doi.org/10.1088/1748-0221/3/08/S08004
3. ATLAS Collaboration, Observation of a new particle in the search for the Standard Model Higgs boson with the ATLAS detector at the LHC. Phys. Lett. B **716**, 1 (2012). https://doi.org/10.1016/j.physletb.2012.08.020. arXiv:1207.7214 [hep-ex]
4. CMS Collaboration, Observation of a new boson at a mass of 125 GeV with the CMS experiment at the LHC. Phys. Lett. B **716**, 30 (2012). https://doi.org/10.1016/j.physletb.2012.08.021. arXiv:1207.7235 [hep-ex]
5. ATLAS Collaboration, A detailed map of Higgs boson interactions by the ATLAS experiment ten years after the discovery. Nature **607**, 52 (2022). https://doi.org/10.1038/s41586-022-04893-w. arXiv:2207.00092 [hep-ex]
6. CMS Collaboration, A portrait of the Higgs boson by the CMS experiment ten years after the discovery. Nature **607**, 60 (2022). https://doi.org/10.1038/s41586-022-04892-x. arXiv:2207.00043 [hep-ex]
7. F. Englert, R. Brout, Broken symmetry and the mass of gauge vector mesons. Phys. Rev. Lett. **13**, 321 (1964)
8. P.W. Higgs, Broken symmetries, massless particles and gauge fields. Phys. Lett. **12**, 132 (1964)
9. ATLAS Collaboration, Measurements of Higgs boson production cross-sections in the $H \to \tau^+\tau^-$ decay channel in pp collisions at $\sqrt{s} = 13$ TeV with the ATLAS detector. JHEP **08**, 175 (2022). https://doi.org/10.1007/JHEP08(2022)175. arXiv:2201.08269 [hep-ex]

10. CMS Collaboration, Measurements of Higgs boson production in the decay channel with a pair of τ leptons in proton–proton collisions at $\sqrt{s} = 13$ TeV (2022). arXiv:2204.12957 [hep-ex]
11. ATLAS Collaboration, Observation of $H \to b\bar{b}$ decays and VH production with the ATLAS detector. Phys. Lett. B **786**, 59 (2018). https://doi.org/10.1016/j.physletb.2018.09.013. arXiv:1808.08238 [hep-ex]
12. CMS Collaboration, Observation of Higgs Boson Decay to Bottom Quarks. Phys. Rev. Lett. **121**, 121801 (2018). https://doi.org/10.1103/PhysRevLett.121.121801. arXiv:1808.08242 [hep-ex]
13. ATLAS Collaboration, Observation of Higgs boson production in association with a top quark pair at the LHC with the ATLAS detector. Phys. Lett. B **784**, 173 (2018). https://doi.org/10.1016/j.physletb.2018.07.035. arXiv:1806.00425 [hep-ex]
14. CMS Collaboration, Observation of $t\bar{t}H$ Production. Phys. Rev. Lett. **120**, 231801 (2018). https://doi.org/10.1103/PhysRevLett.120.231801. arXiv:1804.02610 [hep-ex]
15. CMS Collaboration, Evidence for Higgs boson decay to a pair of muons. JHEP **01**, 148 (2021). https://doi.org/10.1007/JHEP01(2021)148. arXiv:2009.04363 [hep-ex]
16. ATLAS Collaboration, A search for the dimuon decay of the Standard Model Higgs boson with the ATLAS detector. Phys. Lett. B **812**, 135980 (2021). https://doi.org/10.1016/j.physletb.2020.135980. arXiv:2007.07830 [hep-ex]
17. ATLAS Collaboration, Search for the Decay of the Higgs Boson to Charm Quarks with the ATLAS Experiment. Phys. Rev. Lett. **120**, 211802 (2018). https://doi.org/10.1103/PhysRevLett.120.211802. arXiv:1802.04329 [hep-ex]
18. ATLAS Collaboration, Direct constraint on the Higgs-charm coupling from a search for Higgs boson decays into charm quarks with the ATLAS detector (2022). arXiv:2201.11428 [hep-ex]
19. CMS Collaboration, A search for the standard model Higgs boson decaying to charm quarks. JHEP **03**, 131 (2020). https://doi.org/10.1007/JHEP03(2020)131. arXiv:1912.01662 [hep-ex]
20. CMS Collaboration, Search for Higgs boson decay to a charm quark-antiquark pair in proton-proton collisions at $\sqrt{s} = 13$ TeV (2022). arXiv:2205.05550 [hep-ex]
21. ATLAS Collaboration, Search for the Higgs boson decays $H \to ee$ and $H \to e\mu$ in pp collisions at $\sqrt{s} = 13$ TeV with the ATLAS detector. Phys. Lett. B **801**, 135148 (2020). https://doi.org/10.1016/j.physletb.2019.135148. arXiv:1909.10235 [hep-ex]
22. CMS Collaboration, Search for a standard model-like Higgs boson in the $\mu^+\mu^-$ and e^+e^- decay channels at the LHC. Phys. Lett. B **744**, 184 (2015). https://doi.org/10.1016/j.physletb.2015.03.048. arXiv:1410.6679 [hep-ex]
23. ATLAS Collaboration, Search for top quark decays $t \to qH$, with $H \to \gamma\gamma$, in $\sqrt{s} = 13$ TeV pp collisions using the ATLAS detector. JHEP **10**, 129 (2017). https://doi.org/10.1007/JHEP10(2017)129. arXiv:1707.01404 [hep-ex]
24. ATLAS Collaboration, Search for flavor-changing neutral currents in top quark decays $t \to Hc$ and $t \to Hu$ in multilepton final states in proton–proton collisions at $\sqrt{s} = 13$ TeV with the ATLAS detector. Phys. Rev. D **98**, 032002 (2018). https://doi.org/10.1103/PhysRevD.98.032002. arXiv:1805.03483 [hep-ex]
25. CMS Collaboration, Search for flavor-changing neutral current interactions of the top quark and the Higgs boson decaying to a bottom quark-antiquark pair at $\sqrt{s}$ =13 TeV. JHEP **02**, 169 (2021). https://doi.org/10.1007/JHEP02(2022)169. arXiv:2112.09734 [hep-ex]
26. CMS Collaboration, Search for flavor-changing neutral current interactions of the top quark and Higgs boson in final states with two photons in proton–proton collisions at $\sqrt{s} = 13$ TeV, (2021). arXiv:2111.02219 [hep-ex]
27. ATLAS Collaboration, Searches for lepton-flavour-violating decays of the Higgs boson in $\sqrt{s} = 13$ TeV pp collisions with the ATLAS detector. Phys. Lett. B **800**, 135069 (2020). https://doi.org/10.1016/j.physletb.2019.135069. arXiv:1907.06131 [hep-ex]
28. CMS Collaboration, Search for lepton-flavor violating decays of the Higgs boson in the $\mu\tau$ and eτ final states in proton–proton collisions at $\sqrt{s}$ = 13 TeV. Phys. Rev. D **104**, 032013 (2021). https://doi.org/10.1103/PhysRevD.104.032013. arXiv:2105.03007 [hep-ex]
29. G. Bodwin, F. Petriello, S. Stoynev, M. Velasco, Higgs boson decays to quarkonia and the $H\bar{c}c$ coupling. Phys. Rev. D **88**, 053003 (2013). https://doi.org/10.1103/PhysRevD.88.053003. arXiv:1306.5770 [hep-ph]
30. M. Doroshenko, V. Kartvelishvili, E. Chikovani, S. Esakiya, Vector quarkonium in decays of heavy Higgs particles. Yad. Fiz. **46**, 864 (1987)
31. M. König, M. Neubert, Exclusive radiative Higgs decays as probes of light-quark Yukawa couplings. JHEP **08**, 012 (2015). https://doi.org/10.1007/JHEP08(2015)012. arXiv:1505.03870 [hep-ph]
32. G.T. Bodwin, H.S. Chung, J.-H. Ee, J. Lee, F. Petriello, Relativistic corrections to Higgs-boson decays to quarkonia. Phys. Rev. D **90**, 113010 (2014). https://doi.org/10.1103/PhysRevD.90.113010. arXiv:1407.6695 [hep-ph]
33. G.T. Bodwin, H.S. Chung, J.-H. Ee, J. Lee, New approach to the resummation of logarithms in Higgs-boson decays to a vector quarkonium plus a photon. Phys. Rev. D **95**, 054018 (2017). https://doi.org/10.1103/PhysRevD.95.054018. arXiv:1603.06793 [hep-ph]
34. G.T. Bodwin, H.S. Chung, J.-H. Ee, J. Lee, Addendum: new approach to the resummation of logarithms in Higgs-boson decays to a vector quarkonium plus a photon [Phys. Rev. D 95, 054018 (2017)]. Phys. Rev. D **96**, 116014 (2017). https://doi.org/10.1103/PhysRevD.96.116014. arXiv:1710.09872 [hep-ph]
35. C. Zhou, M. Song, G. Li, Y.-J. Zhou, J.-Y. Guo, Next-to-leading order QCD corrections to Higgs boson decay to quarkonium plus a photon. Chin. Phys. C **40**, 123105 (2016). https://doi.org/10.1088/1674-1137/40/12/123105. arXiv:1607.02704 [hep-ph]
36. N. Brambilla, H.S. Chung, W.K. Lai, V. Shtabovenko, A. Vairo, Order v^4 corrections to Higgs boson decay into $J/\psi + \gamma$. Phys. Rev. D **100**, 054038 (2019). https://doi.org/10.1103/PhysRevD.100.054038. arXiv:1907.06473 [hep-ph]
37. D. de Florian et al., Handbook of LHC Higgs Cross Sections: 4. Deciphering the Nature of the Higgs Sector (2016). https://doi.org/10.23731/CYRM-2017-002. arXiv:1610.07922 [hep-ph]
38. G. Perez, Y. Soreq, E. Stamou, K. Tobioka, Constraining the charm Yukawa and Higgs-quark coupling universality. Phys. Rev. D **92**, 033016 (2015). https://doi.org/10.1103/PhysRevD.92.033016. arXiv:1503.00290 [hep-ph]
39. C.D. Froggatt, H.B. Nielsen, Hierarchy of quark masses, cabibbo angles and CP violation. Nucl. Phys. B **147**, 277 (1979). https://doi.org/10.1016/0550-3213(79)90316-X
40. L. Randall, R. Sundrum, Large mass hierarchy from a small extra dimension. Phys. Rev. Lett. **83**, 3370 (1999). arXiv:9905.22110 [hep-ph]
41. G. D'Ambrosio, G.F. Giudice, G. Isidori, A. Strumia, Minimal flavor violation: an effective field theory approach. Nucl. Phys. B **645**, 155 (2002). arXiv:0207.03610 [hep-ph]
42. G.F. Giudice, O. Lebedev, Higgs-dependent Yukawa couplings. Phys. Lett. B **665**, 79 (2008). https://doi.org/10.1016/j.physletb.2008.05.062. arXiv:0804.1753 [hep-ph]
43. M.J. Dugan, H. Georgi, D.B. Kaplan, Anatomy of a composite Higgs model. Nucl. Phys. B **254**, 299 (1985). https://doi.org/10.1016/0550-3213(85)90221-4
44. ATLAS Collaboration, Measurement of $W^{\pm}$ and Z-boson production cross sections in pp collisions at $\sqrt{s} = 13$ TeV with the ATLAS detector. Phys. Lett. B **759**, 601 (2016). https://doi.org/10.1016/j.physletb.2016.06.023. arXiv:1603.09222 [hep-ex]

45. A. Dainese et al., Report on the Physics at the HL-LHC, and Perspectives for the HE-LHC (2019). https://cds.cern.ch/record/2703572. https://doi.org/10.23731/CYRM-2019-007
46. Y. Grossman, M. König, M. Neubert, Exclusive radiative decays of W and Z bosons in QCD factorization. JHEP **04**, 101 (2015). https://doi.org/10.1007/JHEP04(2015)101. arXiv:1501.06569 [hep-ph]
47. T.-C. Huang, F. Petriello, Rare exclusive decays of the Z boson revisited. Phys. Rev. D **92**, 014007 (2015). https://doi.org/10.1103/PhysRevD.92.014007. arXiv:1411.5924 [hep-ph]
48. G.T. Bodwin, H.S. Chung, J.-H. Ee, J. Lee, Z-boson decays to a vector quarkonium plus a photon. Phys. Rev. D **97**, 016009 (2018). https://doi.org/10.1103/PhysRevD.97.016009. arXiv:1709.09320 [hep-ph]
49. ATLAS Collaboration, Search for Higgs and Z Boson Decays to $J/\psi\gamma$ and $\Upsilon(n\mathrm{S})\gamma$ with the ATLAS Detector. Phys. Rev. Lett. **114**, 121801 (2015). https://doi.org/10.1103/PhysRevLett.114.121801. arXiv:1501.03276 [hep-ex]
50. ATLAS Collaboration, Searches for exclusive Higgs and Z boson decays into $J/\psi\gamma$, $\psi(2\mathrm{S})\gamma$, and $\Upsilon(n\mathrm{S})\gamma$ at $\sqrt{s} = 13$ TeV with the ATLAS detector. Phys. Lett. B **786**, 134 (2018). https://doi.org/10.1016/j.physletb.2018.09.024. arXiv:1807.00802 [hep-ex]
51. CMS Collaboration, Search for a Higgs boson decaying into $\gamma^*\gamma \to \ell\ell\gamma$ with low dilepton mass in pp collisions at $\sqrt{s} = 8$ TeV. Phys. Lett. B **753**, 341 (2016). https://doi.org/10.1016/j.physletb.2015.12.039. arXiv:1507.03031 [hep-ex]
52. CMS Collaboration, Search for rare decays of Z and Higgs bosons to J/ψ and a photon in proton–proton collisions at $\sqrt{s} = 13$ TeV. Eur. Phys. J. C **79**, 94 (2019). https://doi.org/10.1140/epjc/s10052-019-6562-5. arXiv:1810.10056 [hep-ex]
53. ATLAS Collaboration, Search for Higgs and Z Boson Decays to $\phi\gamma$ with the ATLAS Detector. Phys. Rev. Lett. **117**, 111802 (2016). https://doi.org/10.1103/PhysRevLett.117.111802. arXiv:1607.03400 [hep-ex]
54. ATLAS Collaboration, Search for exclusive Higgs and Z boson decays to $\phi\gamma$ and $\rho\gamma$ with the ATLAS detector. JHEP **07**, 127 (2018). https://doi.org/10.1007/JHEP07(2018)127. arXiv:1712.02758 [hep-ex]
55. CMS Collaboration, Search for decays of the 125 GeV Higgs boson into a Z boson and a ρ or ϕ meson. JHEP **11**, 039 (2020). https://doi.org/10.1007/JHEP11(2020)039. arXiv:2007.05122 [hep-ex]
56. CMS Collaboration, Search for Higgs and Z boson decays to J/ψ or Υ pairs in the four-muon final state in proton–proton collisions at $\sqrt{s} = 13$ TeV. Phys. Lett. B **797**, 134811 (2019). https://doi.org/10.1016/j.physletb.2019.134811. arXiv:1905.10408 [hep-ex]
57. LHC Higgs Cross Section Working Group, Handbook of LHC Higgs Cross Sections: 3. Higgs Properties, CERN-2013-004 (CERN, Geneva, 2013). arXiv:1307.1347 [hep-ph]
58. ATLAS Collaboration, ATLAS Insertable B-Layer: Technical Design Report, ATLAS-TDR-19; CERN-LHCC-2010-013, 2010, https://cds.cern.ch/record/1291633, Addendum: ATLAS-TDR-19-ADD-1; CERN-LHCC-2012-009, 2012, https://cds.cern.ch/record/1451888
59. ATLAS IBL Collaboration, Production and integration of the ATLAS Insertable B-layer. JINST **13**, T05008 (2018). https://doi.org/10.1088/1748-0221/13/05/T05008. arXiv:1803.00844 [physics.ins-det]
60. ATLAS Collaboration, Performance of the ATLAS trigger system in 2015, Eur. Phys. J. C 77 (2017) 317, https://doi.org/10.1140/epjc/s10052-017-4852-3. arXiv:1611.09661 [hep-ex]
61. ATLAS Collaboration, The ATLAS Collaboration Software and Firmware, ATL-SOFT-PUB-2021-001 (2021) https://cds.cern.ch/record/2767187
62. ATLAS Collaboration, ATLAS data quality operations and performance for 2015–2018 data-taking, JINST 15 (2020) P04003, https://doi.org/10.1088/1748-0221/15/04/P04003 arXiv:1911.04632 [physics.ins-det]
63. ATLAS Collaboration, Electron and photon performance measurements with the ATLAS detector using the 2015–2017 LHC proton-proton collision data. JINST **14**, P12006 (2019). https://doi.org/10.1088/1748-0221/14/12/P12006. arXiv:1908.00005 [hep-ex]
64. ATLAS Collaboration, Performance of electron and photon triggers in ATLAS during LHC Run 2, Eur. Phys. J. C **80**, 47 (2020). https://doi.org/10.1140/epjc/s10052-019-7500-2. arXiv:1909.00761 [hep-ex]
65. ATLAS Collaboration, Performance of the ATLAS muon triggers in Run 2. JINST **15**, P09015 (2020). https://doi.org/10.1088/1748-0221/15/09/p09015. arXiv:2004.13447 [hep-ex]
66. G. Avoni et al., The new LUCID-2 detector for luminosity measurement and monitoring in ATLAS. JINST **13**, P07017 (2018). https://doi.org/10.1088/1748-0221/13/07/P07017
67. ATLAS Collaboration, Luminosity determination in pp collisions at $\sqrt{s} = 8$ TeV using the ATLAS detector at the LHC. Eur. Phys. J. C **76**, 653 (2016). https://doi.org/10.1140/epjc/s10052-016-4466-1. arXiv:1608.03953 [hep-ex]
68. ATLAS Collaboration, Luminosity determination in pp collisions at $\sqrt{s} = 13$ TeV using the ATLAS detector at the LHC, ATLAS-CONF-2019-021 (2019). https://cds.cern.ch/record/2677054
69. ATLAS Collaboration, Measurement of the muon reconstruction performance of the ATLAS detector using 2011 and 2012 LHC proton–proton collision data. Eur. Phys. J. C **74**, 3130 (2014). https://doi.org/10.1140/epjc/s10052-014-3130-x. arXiv:1407.3935 [hep-ex]
70. V. Kostyukhin, VKalVrt-package for vertex reconstruction in ATLAS., ATL-PHYS-2003-031, CERN (2003). https://cds.cern.ch/record/685551
71. ATLAS Collaboration, Muon reconstruction and identification efficiency in ATLAS using the full Run 2 pp collision data set at $\sqrt{s} = 13$ TeV. Eur. Phys. J. C **81**, 578 (2021). https://doi.org/10.1140/epjc/s10052-021-09233-2. arXiv:2012.00578 [hep-ex]
72. P. Nason, A new method for combining NLO QCD with shower Monte Carlo algorithms. JHEP **11**, 040 (2004). arXiv:0409.14610 [hep-ph]
73. S. Frixione, P. Nason, C. Oleari, Matching NLO QCD computations with parton shower simulations: the POWHEG method. JHEP **11**, 070 (2007). https://doi.org/10.1088/1126-6708/2007/11/070. arXiv:0709.2092 [hep-ph]
74. S. Alioli, P. Nason, C. Oleari, E. Re, A general framework for implementing NLO calculations in shower Monte Carlo programs: the POWHEG BOX. JHEP **06**, 043 (2010). https://doi.org/10.1007/JHEP06(2010)043. arXiv:1002.2581 [hep-ph]
75. S. Alioli, P. Nason, C. Oleari, E. Re, NLO Higgs boson production via gluon fusion matched with shower in POWHEG. JHEP **04**, 002 (2009). https://doi.org/10.1088/1126-6708/2009/04/002. arXiv:0812.0578 [hep-ph]
76. P. Nason, C. Oleari, NLO Higgs boson production via vector-boson fusion matched with shower in POWHEG. JHEP **02**, 037 (2010). https://doi.org/10.1007/JHEP02(2010)037. arXiv:0911.5299 [hep-ph]
77. T. Sjöstrand, S. Mrenna, P. Z. Skands, A brief introduction to PYTHIA 8.1. Comput. Phys. Commun. **178**, 852 (2008). https://doi.org/10.1016/j.cpc.2008.01.036. arXiv:0710.3820 [hep-ph]
78. T. Sjöstrand, S. Mrenna, P. Z. Skands, PYTHIA 6.4 physics and manual. JHEP **05**, 026 (2006). arXiv:0603.17510 [hep-ph]
79. New Generation of Parton Distributions with Uncertainties from Global QCD Analysis. JHEP **07**, 012 (2002). arXiv:0201.19510 [hep-ph]
80. ATLAS Collaboration, Measurement of the Z/γ^* boson transverse momentum distribution in pp collisions at $\sqrt{s} = 7$ TeV

with the ATLAS detector. JHEP **09**, 145 (2014). https://doi.org/10.1007/JHEP09(2014)145. arXiv:1406.3660 [hep-ex]
81. NNPDF Collaboration, Parton distributions with LHC data. Nucl. Phys. B **867**, 244 (2013). https://doi.org/10.1016/j.nuclphysb.2012.10.003. arXiv:1207.1303 [hep-ph]
82. ATLAS Collaboration, ATLAS Pythia8 tunes to 7 TeV data (2014). https://cds.cern.ch/record/1966419
83. J. Alwall et al., The automated computation of tree-level and next-to-leading order differential cross sections, and their matching to parton shower simulations. JHEP **07**, 079 (2014). https://doi.org/10.1007/JHEP07(2014)079. arXiv:1405.0301 [hep-ph]
84. E. Jones, W.J. Murray, Mass biases in exclusive radiative hadronic decays of W bosons at the LHC. New J. Phys. **23**, 113035 (2021). https://doi.org/10.1088/1367-2630/ac3572. arXiv:2009.01073 [hep-ex]
85. S. Agostinelli et al., GEANT4: a simulation toolkit. Nucl. Instrum. Methods A **506**, 250 (2003). https://doi.org/10.1140/epjc/s10052-010-1429-9
86. ATLAS Collaboration, The ATLAS Simulation Infrastructure. Eur. Phys. J. C **70**, 823 (2010). https://doi.org/10.1140/epjc/s10052-010-1429-9. arXiv:1005.4568 [physics.ins-det]
87. ATLAS Collaboration, The Pythia 8 A3 tune description of ATLAS minimum bias and inelastic measurements incorporating the Donnachie-Landshoff diffractive model (2016). https://cds.cern.ch/record/2206965
88. C. Anastasiou, C. Duhr, F. Dulat, F. Herzog, B. Mistlberger, Higgs Boson Gluon–Fusion production in QCD at three loops. Phys. Rev. Lett. **114**, 212001 (2015). https://doi.org/10.1103/PhysRevLett.114.212001. arXiv:1503.06056 [hep-ph]
89. C. Anastasiou et al., High precision determination of the gluon fusion Higgs boson cross-section at the LHC. JHEP **05**, 058 (2016). https://doi.org/10.1007/JHEP05(2016)058. arXiv:1602.00695 [hep-ph]
90. S. Actis, G. Passarino, C. Sturm, S. Uccirati, NLO electroweak corrections to Higgs boson production at hadron colliders. Phys. Lett. B **670**, 12 (2008). https://doi.org/10.1016/j.physletb.2008.10.018. arXiv:0809.1301 [hep-ph]
91. C. Anastasiou, R. Boughezal, F. Petriello, Mixed QCD-electroweak corrections to Higgs boson production in gluon fusion. JHEP **04**, 003 (2009). https://doi.org/10.1088/1126-6708/2009/04/003. arXiv:0811.3458 [hep-ph]
92. M. Ciccolini, A. Denner, S. Dittmaier, Strong and electroweak corrections to the production of a Higgs Boson + 2 jets via weak interactions at the large hadron collider. Phys. Rev. Lett. **99**, 161803 (2007). https://doi.org/10.1103/PhysRevLett.99.161803. arXiv:0707.0381 [hep-ph]
93. M. Ciccolini, A. Denner, S. Dittmaier, Electroweak and QCD corrections to Higgs production via vector-boson fusion at the LHC. Phys. Rev. D **77**, 013002 (2008). https://doi.org/10.1103/PhysRevD.77.013002. arXiv:0710.4749 [hep-ph]
94. P. Bolzoni, F. Maltoni, S.-O. Moch, M. Zaro, Higgs boson production via vector-boson fusion at next-to-next-to-leading order in QCD. Phys. Rev. Lett. **105**, 011801 (2010). https://doi.org/10.1103/PhysRevLett.105.011801. arXiv:1003.4451 [hep-ph]
95. O. Brein, A. Djouadi, R. Harlander, NNLO QCD corrections to the Higgs-strahlung processes at hadron colliders. Phys. Lett. B **579**, 149 (2004). https://doi.org/10.1016/j.physletb.2003.10.112. arXiv:hep-ph/0307206
96. A. Denner, S. Dittmaier, S. Kallweit, A. Mück, Electroweak corrections to Higgs-strahlung off W/Z bosons at the Tevatron and the LHC with HAWK. JHEP **03**, 075 (2012). https://doi.org/10.1007/JHEP03(2012)075. arXiv:1112.5142 [hep-ph]
97. L. Altenkamp, S. Dittmaier, R.V. Harlander, H. Rzehak, T.J.E. Zirke, Gluon-induced Higgs-strahlung at next-to-leading order QCD. JHEP **02**, 078 (2013). https://doi.org/10.1007/JHEP02(2013)078. arXiv:1211.5015 [hep-ph]
98. P. Zyla et al. (Particle Data Group), Review of Particle Physics, PTEP 2020 (2020) 083C01, and 2021 update. https://doi.org/10.1093/ptep/ptaa104
99. ATLAS Collaboration, Measurement of the transverse momentum distribution of Drell–Yan lepton pairs in proton–proton collisions at $\sqrt{s} = 13$ TeV with the ATLAS detector. Eur. Phys. J. C **80**, 616 (2020). https://doi.org/10.1140/epjc/s10052-020-8001-z. arXiv:1912.02844 [hep-ex]
100. ATLAS Collaboration, Performance of the Electron and Photon Trigger in p-p Collisions at $\sqrt{s} = 7$ with the ATLAS Detector at the LHC, ATLAS-CONF-2011-114 (2011). http://cds.cern.ch/record/1375551
101. ATLAS Collaboration, Measurement of the photon identification efficiencies with the ATLAS detector using LHC Run-1 data. Eur. Phys. J. C **76**, 666 (2016). https://doi.org/10.1140/epjc/s10052-016-4507-9. arXiv:1606.01813 [hep-ex]
102. ATLAS Collaboration, Photon identification in 2015 ATLAS data, ATL-PHYS-PUB-2016-014, CERN (2016). https://cds.cern.ch/record/2203125
103. ATLAS Collaboration, Muon reconstruction performance of the ATLAS detector in proton–proton collision data at $\sqrt{s} = 13$ TeV. Eur. Phys. J. C **76**, 292 (2016). https://doi.org/10.1140/epjc/s10052-016-4120-y. arXiv:1603.05598 [hep-ex]
104. ATLAS Collaboration, Electron and photon energy calibration with the ATLAS detector using LHC Run 1 dat. Eur. Phys. J. C **74**, 3071 (2014). https://doi.org/10.1140/epjc/s10052-014-3071-4. arXiv:1407.5063 [hep-ex]
105. ATLAS Collaboration, Electron and photon energy calibration with the ATLAS detector using data collected in 2015 at $\sqrt{s}$ =13 TeV, CERN (2016). https://cds.cern.ch/record/2203514
106. A. Chisholm et al., Non-parametric data-driven background modelling using conditional probabilities (2021). arXiv:2112.00650 [hep-ex]
107. T. Gleisberg et al., Event generation with SHERPA 1.1. JHEP **02**, 007 (2009). https://doi.org/10.1088/1126-6708/2009/02/007. arXiv:0811.4622 [hep-ph]
108. K. Cranmer, Kernel estimation in high-energy physics. Comput. Phys. Commun. **136**, 198 (2001). arXiv:0011.05710 [hep-ex]
109. A.L. Read, Presentation of search results: the CL_s technique. J. Phys. G **28**, 2693 (2002). https://doi.org/10.1088/0954-3899/28/10/313
110. G. Cowan, K. Cranmer, E. Gross, O. Vitells, Asymptotic formulae for likelihood-based tests of new physics. Eur. Phys. J. C **71**, 1554 (2011). https://doi.org/10.1140/epjc/s10052-011-1554-0 (Erratum: Eur. Phys. J. C 73 (2013) 2501). arXiv:1007.1727 [physics.data-an]
111. ATLAS Collaboration, Measurement of the properties of Higgs boson production at $\sqrt{s}$=13 TeV in the $H \to \gamma\gamma$ channel using 139 fb^{-1} of pp collision data with the ATLAS experiment (2020). https://cds.cern.ch/record/2725727
112. ATLAS Collaboration, Combined measurements of Higgs boson production and decay using up to 80 fb^{-1} of proton–proton collision data at $\sqrt{s} = 13$ TeV collected with the ATLAS experiment. Phys. Rev. D **101**, 012002 (2020). https://doi.org/10.1103/PhysRevD.101.012002. arXiv:1909.02845 [hep-ex]
113. CMS Collaboration, Combined measurements of Higgs boson couplings in proton–proton collisions at $\sqrt{s} = 13$ TeV. Eur. Phys. J. C **79**, 421 (2019). https://doi.org/10.1140/epjc/s10052-019-6909-y. arXiv:1809.10733 [hep-ex]
114. N.M. Coyle, C.E.M. Wagner, V. Wei, Bounding the charm Yukawa coupling. Phys. Rev. D **100**, 073013 (2019). https://doi.org/10.1103/PhysRevD.100.073013. arXiv:1905.09360 [hep-ph]
115. ATLAS Collaboration, ATLAS Computing Acknowledgements, ATL-SOFT-PUB-2021-003 (2021). https://cds.cern.ch/record/2776662

ATLAS Collaboration[*]

G. Aad[101], B. Abbott[119], D. C. Abbott[102], K. Abeling[55], S. H. Abidi[29], A. Aboulhorma[35e], H. Abramowicz[150], H. Abreu[149], Y. Abulaiti[116], A. C. Abusleme Hoffman[136a], B. S. Acharya[68a,68b,p], B. Achkar[55], C. Adam Bourdarios[4], L. Adamczyk[84a], L. Adamek[154], S. V. Addepalli[26], J. Adelman[114], A. Adiguzel[21c], S. Adorni[56], T. Adye[133], A. A. Affolder[135], Y. Afik[36], M. N. Agaras[13], J. Agarwala[72a,72b], A. Aggarwal[99], C. Agheorghiesei[27c], J. A. Aguilar-Saavedra[129f], A. Ahmad[36], F. Ahmadov[38,z], W. S. Ahmed[103], S. Ahuja[94], X. Ai[48], G. Aielli[75a,75b], I. Aizenberg[168], M. Akbiyik[99], T. P. A. Åkesson[97], A. V. Akimov[37], K. Al Khoury[41], G. L. Alberghi[23b], J. Albert[164], P. Albicocco[53], M. J. Alconada Verzini[89], S. Alderweireldt[52], M. Aleksa[36], I. N. Aleksandrov[38], C. Alexa[27b], T. Alexopoulos[10], A. Alfonsi[113], F. Alfonsi[23b], M. Alhroob[119], B. Ali[131], S. Ali[147], M. Aliev[37], G. Alimonti[70a], W. Alkakhi[55], C. Allaire[36], B. M. M. Allbrooke[145], P. P. Allport[20], A. Aloisio[71a,71b], F. Alonso[89], C. Alpigiani[137], E. Alunno Camelia[75a,75b], M. Alvarez Estevez[98], M. G. Alviggi[71a,71b], Y. Amaral Coutinho[81b], A. Ambler[103], C. Amelung[36], C. G. Ames[108], D. Amidei[105], S. P. Amor Dos Santos[129a], S. Amoroso[48], K. R. Amos[162], C. S. Amrouche[56], V. Ananiev[124], C. Anastopoulos[138], T. Andeen[11], J. K. Anders[19], S. Y. Andrean[47a,47b], A. Andreazza[70a,70b], S. Angelidakis[9], A. Angerami[41,ac], A. V. Anisenkov[37], A. Annovi[73a], C. Antel[56], M. T. Anthony[138], E. Antipov[120], M. Antonelli[53], D. J. A. Antrim[17a], F. Anulli[74a], M. Aoki[82], T. Aoki[152], J. A. Aparisi Pozo[162], M. A. Aparo[145], L. Aperio Bella[48], C. Appelt[18], N. Aranzabal[36], V. Araujo Ferraz[81a], C. Arcangeletti[53], A. T. H. Arce[51], E. Arena[91], J.-F. Arguin[107], S. Argyropoulos[54], J.-H. Arling[48], A. J. Armbruster[36], O. Arnaez[154], H. Arnold[113], Z. P. Arrubarrena Tame[108], G. Artoni[74a,74b], H. Asada[110], K. Asai[117], S. Asai[152], N. A. Asbah[61], J. Assahsah[35d], K. Assamagan[29], R. Astalos[28a], R. J. Atkin[33a], M. Atkinson[161], N. B. Atlay[18], H. Atmani[62b], P. A. Atmasiddha[105], K. Augsten[131], S. Auricchio[71a,71b], A. D. Auriol[20], V. A. Austrup[170], G. Avner[149], G. Avolio[36], K. Axiotis[56], M. K. Ayoub[14c], G. Azuelos[107,ag], D. Babal[28a], H. Bachacou[134], K. Bachas[151,s], A. Bachiu[34], F. Backman[47a,47b], A. Badea[61], P. Bagnaia[74a,74b], M. Bahmani[18], A. J. Bailey[162], V. R. Bailey[161], J. T. Baines[133], C. Bakalis[10], O. K. Baker[171], P. J. Bakker[113], E. Bakos[15], D. Bakshi Gupta[8], S. Balaji[146], R. Balasubramanian[113], E. M. Baldin[37], P. Balek[132], E. Ballabene[70a,70b], F. Balli[134], L. M. Baltes[63a], W. K. Balunas[32], J. Balz[99], E. Banas[85], M. Bandieramonte[128], A. Bandyopadhyay[24], S. Bansal[24], L. Barak[150], E. L. Barberio[104], D. Barberis[57a,57b], M. Barbero[101], G. Barbour[95], K. N. Barends[33a], T. Barillari[109], M.-S. Barisits[36], T. Barklow[142], R. M. Barnett[17a], P. Baron[121], D. A. Baron Moreno[100], A. Baroncelli[62a], G. Barone[29], A. J. Barr[125], L. Barranco Navarro[47a,47b], F. Barreiro[98], J. Barreiro Guimarães da Costa[14a], U. Barron[150], M. G. Barros Teixeira[129a], S. Barsov[37], F. Bartels[63a], R. Bartoldus[142], A. E. Barton[90], P. Bartos[28a], A. Basalaev[48], A. Basan[99], M. Baselga[49], I. Bashta[76a,76b], A. Bassalat[66,b], M. J. Basso[154], C. R. Basson[100], R. L. Bates[59], S. Batlamous[35e], J. R. Batley[32], B. Batool[140], M. Battaglia[135], D. Battulga[18], M. Bauce[74a,74b], P. Bauer[24], A. Bayirli[21a], J. B. Beacham[51], T. Beau[126], P. H. Beauchemin[157], F. Becherer[54], P. Bechtle[24], H. P. Beck[19,r], K. Becker[166], C. Becot[48], A. J. Beddall[21d], V. A. Bednyakov[38], C. P. Bee[144], L. J. Beemster[15], T. A. Beermann[36], M. Begalli[81d], M. Begel[29], A. Behera[144], J. K. Behr[48], C. Beirao Da Cruz E Silva[36], J. F. Beirer[55,36], F. Beisiegel[24], M. Belfkir[158], G. Bella[150], L. Bellagamba[23b], A. Bellerive[34], P. Bellos[20], K. Beloborodov[37], K. Belotskiy[37], N. L. Belyaev[37], D. Benchekroun[35a], F. Bendebba[35a], Y. Benhammou[150], D. P. Benjamin[29], M. Benoit[29], J. R. Bensinger[26], S. Bentvelsen[113], L. Beresford[36], M. Beretta[53], D. Berge[18], E. Bergeaas Kuutmann[160], N. Berger[4], B. Bergmann[131], J. Beringer[17a], S. Berlendis[7], G. Bernardi[5], C. Bernius[142], F. U. Bernlochner[24], T. Berry[94], P. Berta[132], A. Berthold[50], I. A. Bertram[90], S. Bethke[109], A. Betti[74a,74b], A. J. Bevan[93], M. Bhamjee[33c], S. Bhatta[144], D. S. Bhattacharya[165], P. Bhattarai[26], V. S. Bhopatkar[120], R. Bi[29,aj], R. M. Bianchi[128], O. Biebel[108], R. Bielski[122], M. Biglietti[76a], T. R. V. Billoud[131], M. Bindi[55], A. Bingul[21b], C. Bini[74a,74b], S. Biondi[23a,23b], A. Biondini[91], C. J. Birch-sykes[100], G. A. Bird[20,133], M. Birman[168], T. Bisanz[36], E. Bisceglie[43a,43b], D. Biswas[169,l], A. Bitadze[100], K. Bjørke[124], I. Bloch[48], C. Blocker[26], A. Blue[59], U. Blumenschein[93], J. Blumenthal[99], G. J. Bobbink[113], V. S. Bobrovnikov[37], M. Boehler[54], D. Bogavac[36], A. G. Bogdanchikov[37], C. Bohm[47a], V. Boisvert[94], P. Bokan[48], T. Bold[84a], M. Bomben[5], M. Bona[93], M. Boonekamp[134], C. D. Booth[94], A. G. Borbély[59], H. M. Borecka-Bielska[107], L. S. Borgna[95], G. Borissov[90], D. Bortoletto[125], D. Boscherini[23b], M. Bosman[13], J. D. Bossio Sola[36], K. Bouaouda[35a], J. Boudreau[128], E. V. Bouhova-Thacker[90], D. Boumediene[40], R. Bouquet[5], A. Boveia[118], J. Boyd[36], D. Boye[29], I. R. Boyko[38], J. Bracinik[20], N. Brahimi[62d], G. Brandt[170], O. Brandt[32], F. Braren[48], B. Brau[102],

J. E. Brau[122], K. Brendlinger[48], R. Brener[168], L. Brenner[36], R. Brenner[160], S. Bressler[168], B. Brickwedde[99], D. Britton[59], D. Britzger[109], I. Brock[24], G. Brooijmans[41], W. K. Brooks[136f], E. Brost[29], T. L. Bruckler[125], P. A. Bruckman de Renstrom[85], B. Brüers[48], D. Bruncko[28b,*], A. Bruni[23b], G. Bruni[23b], M. Bruschi[23b], N. Bruscino[74a,74b], L. Bryngemark[142], T. Buanes[16], Q. Buat[137], P. Buchholz[140], A. G. Buckley[59], I. A. Budagov[38,*], M. K. Bugge[124], O. Bulekov[37], B. A. Bullard[61], S. Burdin[91], C. D. Burgard[48], A. M. Burger[40], B. Burghgrave[8], J. T. P. Burr[32], C. D. Burton[11], J. C. Burzynski[141], E. L. Busch[41], V. Büscher[99], P. J. Bussey[59], J. M. Butler[25], C. M. Buttar[59], J. M. Butterworth[95], W. Buttinger[133], C. J. Buxo Vazquez[106], A. R. Buzykaev[37], G. Cabras[23b], S. Cabrera Urbán[162], D. Caforio[58], H. Cai[128], Y. Cai[14a,14d], V. M. M. Cairo[36], O. Cakir[3a], N. Calace[36], P. Calafiura[17a], G. Calderini[126], P. Calfayan[67], G. Callea[59], L. P. Caloba[81b], D. Calvet[40], S. Calvet[40], T. P. Calvet[101], M. Calvetti[73a,73b], R. Camacho Toro[126], S. Camarda[36], D. Camarero Munoz[26], P. Camarri[75a,75b], M. T. Camerlingo[76a,76b], D. Cameron[124], C. Camincher[164], M. Campanelli[95], A. Camplani[42], V. Canale[71a,71b], A. Canesse[103], M. Cano Bret[79], J. Cantero[162], Y. Cao[161], F. Capocasa[26], M. Capua[43a,43b], A. Carbone[70a,70b], R. Cardarelli[75a], J. C. J. Cardenas[8], F. Cardillo[162], T. Carli[36], G. Carlino[71a], J. I. Carlotto[13], B. T. Carlson[128,t], E. M. Carlson[155a,164], L. Carminati[70a,70b], M. Carnesale[74a,74b], S. Caron[112], E. Carquin[136f], S. Carrá[70a,70b], G. Carratta[23a,23b], F. Carrio Argos[33g], J. W. S. Carter[154], T. M. Carter[52], M. P. Casado[13,i], A. F. Casha[154], E. G. Castiglia[171], F. L. Castillo[63a], L. Castillo Garcia[13], V. Castillo Gimenez[162], N. F. Castro[129a,129e], A. Catinaccio[36], J. R. Catmore[124], V. Cavaliere[29], N. Cavalli[23a,23b], V. Cavasinni[73a,73b], E. Celebi[21a], F. Celli[125], M. S. Centonze[69a,69b], K. Cerny[121], A. S. Cerqueira[81a], A. Cerri[145], L. Cerrito[75a,75b], F. Cerutti[17a], A. Cervelli[23b], S. A. Cetin[21d], Z. Chadi[35a], D. Chakraborty[114], M. Chala[129f], J. Chan[169], W. Y. Chan[152], J. D. Chapman[32], B. Chargeishvili[148b], D. G. Charlton[20], T. P. Charman[93], M. Chatterjee[19], S. Chekanov[6], S. V. Chekulaev[155a], G. A. Chelkov[38,a], A. Chen[105], B. Chen[150], B. Chen[164], C. Chen[62a], H. Chen[14c], H. Chen[29], J. Chen[62c], J. Chen[26], S. Chen[152], S. J. Chen[14c], X. Chen[62c], X. Chen[14b,af], Y. Chen[62a], C. L. Cheng[169], H. C. Cheng[64a], A. Cheplakov[38], E. Cheremushkina[48], E. Cherepanova[113], R. Cherkaoui El Moursli[35e], E. Cheu[7], K. Cheung[65], L. Chevalier[134], V. Chiarella[53], G. Chiarelli[73a], N. Chiedde[101], G. Chiodini[69a], A. S. Chisholm[20], A. Chitan[27b], M. Chitishvili[162], Y. H. Chiu[164], M. V. Chizhov[38], K. Choi[11], A. R. Chomont[74a,74b], Y. Chou[102], E. Y. S. Chow[113], T. Chowdhury[33g], L. D. Christopher[33g], K. L. Chu[64a], M. C. Chu[64a], X. Chu[14a,14d], J. Chudoba[130], J. J. Chwastowski[85], D. Cieri[109], K. M. Ciesla[84a], V. Cindro[92], A. Ciocio[17a], F. Cirotto[71a,71b], Z. H. Citron[168,m], M. Citterio[70a], D. A. Ciubotaru[27b], B. M. Ciungu[154], A. Clark[56], P. J. Clark[52], J. M. Clavijo Columbie[48], S. E. Clawson[100], C. Clement[47a,47b], J. Clercx[48], L. Clissa[23a,23b], Y. Coadou[101], M. Cobal[68a,68c], A. Coccaro[57b], R. F. Coelho Barrue[129a], R. Coelho Lopes De Sa[102], S. Coelli[70a], H. Cohen[150], A. E. C. Coimbra[70a,70b], B. Cole[41], J. Collot[60], P. Conde Muiño[129a,129g], M. P. Connell[33c], S. H. Connell[33c], I. A. Connelly[59], E. I. Conroy[125], F. Conventi[71a,ah], H. G. Cooke[20], A. M. Cooper-Sarkar[125], F. Cormier[163], L. D. Corpe[36], M. Corradi[74a,74b], E. E. Corrigan[97], F. Corriveau[103,y], A. Cortes-Gonzalez[18], M. J. Costa[162], F. Costanza[4], D. Costanzo[138], B. M. Cote[118], G. Cowan[94], J. W. Cowley[32], K. Cranmer[116], S. Crépé-Renaudin[60], F. Crescioli[126], M. Cristinziani[140], M. Cristoforetti[77a,77b,d], V. Croft[157], G. Crosetti[43a,43b], A. Cueto[36], T. Cuhadar Donszelmann[159], H. Cui[14a,14d], Z. Cui[7], A. R. Cukierman[142], W. R. Cunningham[59], F. Curcio[43a,43b], P. Czodrowski[36], M. M. Czurylo[63b], M. J. Da Cunha Sargedas De Sousa[62a], J. V. Da Fonseca Pinto[81b], C. Da Via[100], W. Dabrowski[84a], T. Dado[49], S. Dahbi[33g], T. Dai[105], C. Dallapiccola[102], M. Dam[42], G. D'amen[29], V. D'Amico[108], J. Damp[99], J. R. Dandoy[127], M. F. Daneri[30], M. Danninger[141], V. Dao[36], G. Darbo[57b], S. Darmora[6], S. J. Das[29,aj], S. D'Auria[70a,70b], C. David[155b], T. Davidek[132], D. R. Davis[51], B. Davis-Purcell[34], I. Dawson[93], K. De[8], R. De Asmundis[71a], M. De Beurs[113], N. De Biase[48], S. De Castro[23a,23b], N. De Groot[112], P. de Jong[113], H. De la Torre[106], A. De Maria[14c], A. De Salvo[74a], U. De Sanctis[75a,75b], A. De Santo[145], J. B. De Vivie De Regie[60], D. V. Dedovich[38], J. Degens[113], A. M. Deiana[44], F. Del Corso[23a,23b], J. Del Peso[98], F. Del Rio[63a], F. Deliot[134], C. M. Delitzsch[49], M. Della Pietra[71a,71b], D. Della Volpe[56], A. Dell'Acqua[36], L. Dell'Asta[70a,70b], M. Delmastro[4], P. A. Delsart[60], S. Demers[171], M. Demichev[38], S. P. Denisov[37], L. D'Eramo[114], D. Derendarz[85], F. Derue[126], P. Dervan[91], K. Desch[24], K. Dette[154], C. Deutsch[24], P. O. Deviveiros[36], F. A. Di Bello[74a,74b], A. Di Ciaccio[75a,75b], L. Di Ciaccio[4], A. Di Domenico[74a,74b], C. Di Donato[71a,71b], A. Di Girolamo[36], G. Di Gregorio[73a,73b], A. Di Luca[77a,77b], B. Di Micco[76a,76b], R. Di Nardo[76a,76b], C. Diaconu[101], F. A. Dias[113], T. Dias Do Vale[141], M. A. Diaz[136a,136b], F. G. Diaz Capriles[24], M. Didenko[162], E. B. Diehl[105], L. Diehl[54], S. Díez Cornell[48], C. Diez Pardos[140], C. Dimitriadi[24,160], A. Dimitrievska[17a],

W. Ding[14b], J. Dingfelder[24], I.-M. Dinu[27b], S. J. Dittmeier[63b], F. Dittus[36], F. Djama[101], T. Djobava[148b], J. I. Djuvsland[16], C. Doglioni[97,100], J. Dolejsi[132], Z. Dolezal[132], M. Donadelli[81c], B. Dong[62c], J. Donini[40], A. D'Onofrio[14c], M. D'Onofrio[91], J. Dopke[133], A. Doria[71a], M. T. Dova[89], A. T. Doyle[59], M. A. Draguet[125], E. Drechsler[141], E. Dreyer[168], I. Drivas-koulouris[10], A. S. Drobac[157], M. Drozdova[56], D. Du[62a], T. A. du Pree[113], F. Dubinin[37], M. Dubovsky[28a], E. Duchovni[168], G. Duckeck[108], O. A. Ducu[27b], D. Duda[109], A. Dudarev[36], M. D'uffizi[100], L. Duflot[66], M. Dührssen[36], C. Dülsen[170], A. E. Dumitriu[27b], M. Dunford[63a], S. Dungs[49], K. Dunne[47a,47b], A. Duperrin[101], H. Duran Yildiz[3a], M. Düren[58], A. Durglishvili[148b], B. L. Dwyer[114], G. I. Dyckes[17a], M. Dyndal[84a], S. Dysch[100], B. S. Dziedzic[85], Z. O. Earnshaw[145], B. Eckerova[28a], M. G. Eggleston[51], E. Egidio Purcino De Souza[81b], L. F. Ehrke[56], G. Eigen[16], K. Einsweiler[17a], T. Ekelof[160], P. A. Ekman[97], Y. El Ghazali[35b], H. El Jarrari[35e,147], A. El Moussaouy[35a], V. Ellajosyula[160], M. Ellert[160], F. Ellinghaus[170], A. A. Elliot[93], N. Ellis[36], J. Elmsheuser[29], M. Elsing[36], D. Emeliyanov[133], A. Emerman[41], Y. Enari[152], I. Ene[17a], S. Epari[13], J. Erdmann[49], A. Ereditato[19], P. A. Erland[85], M. Errenst[170], M. Escalier[66], C. Escobar[162], E. Etzion[150], G. Evans[129a], H. Evans[67], M. O. Evans[145], A. Ezhilov[37], S. Ezzarqtouni[35a], F. Fabbri[59], L. Fabbri[23a,23b], G. Facini[95], V. Fadeyev[135], R. M. Fakhrutdinov[37], S. Falciano[74a], P. J. Falke[24], S. Falke[36], J. Faltova[132], Y. Fan[14a], Y. Fang[14a,14d], G. Fanourakis[46], M. Fanti[70a,70b], M. Faraj[68a,68b], A. Farbin[8], A. Farilla[76a], T. Farooque[106], S. M. Farrington[52], F. Fassi[35e], D. Fassouliotis[9], M. Faucci Giannelli[75a,75b], W. J. Fawcett[32], L. Fayard[66], P. Federicova[130], O. L. Fedin[37,a], G. Fedotov[37], M. Feickert[161], L. Feligioni[101], A. Fell[138], D. E. Fellers[122], C. Feng[62b], M. Feng[14b], Z. Feng[113], M. J. Fenton[159], A. B. Fenyuk[37], L. Ferencz[48], S. W. Ferguson[45], J. Ferrando[48], A. Ferrari[160], P. Ferrari[113], R. Ferrari[72a], D. Ferrere[56], C. Ferretti[105], F. Fiedler[99], A. Filipčič[92], E. K. Filmer[1], F. Filthaut[112], M. C. N. Fiolhais[129a,129c,c], L. Fiorini[162], F. Fischer[140], W. C. Fisher[106], T. Fitschen[20], I. Fleck[140], P. Fleischmann[105], T. Flick[170], L. Flores[127], M. Flores[33d,ad], L. R. Flores Castillo[64a], F. M. Follega[77a,77b], N. Fomin[16], J. H. Foo[154], B. C. Forland[67], A. Formica[134], A. C. Forti[100], E. Fortin[101], A. W. Fortman[61], M. G. Foti[17a], L. Fountas[9,j], D. Fournier[66], H. Fox[90], P. Francavilla[73a,73b], S. Francescato[61], M. Franchini[23a,23b], S. Franchino[63a], D. Francis[36], L. Franco[112], L. Franconi[19], M. Franklin[61], G. Frattari[26], A. C. Freegard[93], P. M. Freeman[20], W. S. Freund[81b], N. Fritzsche[50], A. Froch[54], D. Froidevaux[36], J. A. Frost[125], Y. Fu[62a], M. Fujimoto[117], E. Fullana Torregrosa[162,*], J. Fuster[162], A. Gabrielli[23a,23b], A. Gabrielli[154], P. Gadow[48], G. Gagliardi[57a,57b], L. G. Gagnon[17a], G. E. Gallardo[125], E. J. Gallas[125], B. J. Gallop[133], R. Gamboa Goni[93], K. K. Gan[118], S. Ganguly[152], J. Gao[62a], Y. Gao[52], F. M. Garay Walls[136a,136b], B. Garcia[29,aj], C. García[162], J. E. García Navarro[162], J. A. García Pascual[14a], M. Garcia-Sciveres[17a], R. W. Gardner[39], D. Garg[79], R. B. Garg[142,q], S. Gargiulo[54], C. A. Garner[154], V. Garonne[29], S. J. Gasiorowski[137], P. Gaspar[81b], G. Gaudio[72a], V. Gautam[13], P. Gauzzi[74a,74b], I. L. Gavrilenko[37], A. Gavrilyuk[37], C. Gay[163], G. Gaycken[48], E. N. Gazis[10], A. A. Geanta[27b,27e], C. M. Gee[135], J. Geisen[97], M. Geisen[99], C. Gemme[57b], M. H. Genest[60], S. Gentile[74a,74b], S. George[94], W. F. George[20], T. Geralis[46], L. O. Gerlach[55], P. Gessinger-Befurt[36], M. Ghasemi Bostanabad[164], M. Ghneimat[140], A. Ghosal[140], A. Ghosh[159], A. Ghosh[7], B. Giacobbe[23b], S. Giagu[74a,74b], N. Giangiacomi[154], P. Giannetti[73a], A. Giannini[62a], S. M. Gibson[94], M. Gignac[135], D. T. Gil[84b], A. K. Gilbert[84a], B. J. Gilbert[41], D. Gillberg[34], G. Gilles[113], N. E. K. Gillwald[48], L. Ginabat[126], D. M. Gingrich[2,ag], M. P. Giordani[68a,68c], P. F. Giraud[134], G. Giugliarelli[68a,68c], D. Giugni[70a], F. Giuli[36], I. Gkialas[9,j], L. K. Gladilin[37], C. Glasman[98], G. R. Gledhill[122], M. Glisic[122], I. Gnesi[43b,f], Y. Go[29,aj], M. Goblirsch-Kolb[26], D. Godin[107], S. Goldfarb[104], T. Golling[56], M. G. D. Gololo[33g], D. Golubkov[37], J. P. Gombas[106], A. Gomes[129a,129b], G. Gomes Da Silva[140], A. J. Gomez Delegido[162], R. Goncalves Gama[55], R. Gonçalo[129a,129c], G. Gonella[122], L. Gonella[20], A. Gongadze[38], F. Gonnella[20], J. L. Gonski[41], R. Y. González Andana[52], S. González de la Hoz[162], S. Gonzalez Fernandez[13], R. Gonzalez Lopez[91], C. Gonzalez Renteria[17a], R. Gonzalez Suarez[160], S. Gonzalez-Sevilla[56], G. R. Gonzalvo Rodriguez[162], L. Goossens[36], N. A. Gorasia[20], P. A. Gorbounov[37], B. Gorini[36], E. Gorini[69a,69b], A. Gorišek[92], A. T. Goshaw[51], M. I. Gostkin[38], C. A. Gottardo[36], M. Gouighri[35b], V. Goumarre[48], A. G. Goussiou[137], N. Govender[33c], C. Goy[4], I. Grabowska-Bold[84a], K. Graham[34], E. Gramstad[124], S. Grancagnolo[18], M. Grandi[145], V. Gratchev[37,*], P. M. Gravila[27f], F. G. Gravili[69a,69b], H. M. Gray[17a], M. Greco[69a,69b], C. Grefe[24], I. M. Gregor[48], P. Grenier[142], C. Grieco[13], A. A. Grillo[135], K. Grimm[31,n], S. Grinstein[13,v], J.-F. Grivaz[66], E. Gross[168], J. Grosse-Knetter[55], C. Grud[105], A. Grummer[111], J. C. Grundy[125], L. Guan[105], W. Guan[169], C. Gubbels[163], J. G. R. Guerrero Rojas[162], G. Guerrieri[68a,68b], F. Guescini[109], R. Gugel[99], J. A. M. Guhit[105], A. Guida[48], T. Guillemin[4], E. Guilloton[133,166], S. Guindon[36], F. Guo[14a,14d],

J. Guo[62c], L. Guo[66], Y. Guo[105], R. Gupta[48], S. Gurbuz[24], S. S. Gurdasani[54], G. Gustavino[36], M. Guth[56], P. Gutierrez[119], L. F. Gutierrez Zagazeta[127], C. Gutschow[95], C. Guyot[134], C. Gwenlan[125], C. B. Gwilliam[91], E. S. Haaland[124], A. Haas[116], M. Habedank[48], C. Haber[17a], H. K. Hadavand[8], A. Hadef[99], S. Hadzic[109], M. Haleem[165], J. Haley[120], J. J. Hall[138], G. D. Hallewell[101], L. Halser[19], K. Hamano[164], H. Hamdaoui[35e], M. Hamer[24], G. N. Hamity[52], J. Han[62b], K. Han[62a], L. Han[14c], L. Han[62a], S. Han[17a], Y. F. Han[154], K. Hanagaki[82], M. Hance[135], D. A. Hangal[41,ac], H. Hanif[141], M. D. Hank[39], R. Hankache[100], J. B. Hansen[42], J. D. Hansen[42], P. H. Hansen[42], K. Hara[156], D. Harada[56], T. Harenberg[170], S. Harkusha[37], Y. T. Harris[125], N. M. Harrison[118], P. F. Harrison[166], N. M. Hartman[142], N. M. Hartmann[108], Y. Hasegawa[139], A. Hasib[52], S. Haug[19], R. Hauser[106], M. Havranek[131], C. M. Hawkes[20], R. J. Hawkings[36], S. Hayashida[110], D. Hayden[106], C. Hayes[105], R. L. Hayes[163], C. P. Hays[125], J. M. Hays[93], H. S. Hayward[91], F. He[62a], Y. He[153], Y. He[126], M. P. Heath[52], V. Hedberg[97], A. L. Heggelund[124], N. D. Hehir[93], C. Heidegger[54], K. K. Heidegger[54], W. D. Heidorn[80], J. Heilman[34], S. Heim[48], T. Heim[17a], J. G. Heinlein[127], J. J. Heinrich[122], L. Heinrich[109,ae], J. Hejbal[130], L. Helary[48], A. Held[169], S. Hellesund[124], C. M. Helling[163], S. Hellman[47a,47b], C. Helsens[36], R. C. W. Henderson[90], L. Henkelmann[32], A. M. Henriques Correia[36], H. Herde[142], Y. Hernández Jiménez[144], M. G. Herrmann[108], T. Herrmann[50], G. Herten[54], R. Hertenberger[108], L. Hervas[36], N. P. Hessey[155a], H. Hibi[83], E. Higón-Rodriguez[162], S. J. Hillier[20], I. Hinchliffe[17a], F. Hinterkeuser[24], M. Hirose[123], S. Hirose[156], D. Hirschbuehl[170], T. G. Hitchings[100], B. Hiti[92], J. Hobbs[144], R. Hobincu[27e], N. Hod[168], M. C. Hodgkinson[138], B. H. Hodkinson[32], A. Hoecker[36], J. Hofer[48], D. Hohn[54], T. Holm[24], M. Holzbock[109], L. B. A. H. Hommels[32], B. P. Honan[100], J. Hong[62c], T. M. Hong[128], Y. Hong[55], J. C. Honig[54], A. Hönle[109], B. H. Hooberman[161], W. H. Hopkins[6], Y. Horii[110], S. Hou[147], A. S. Howard[92], J. Howarth[59], J. Hoya[6], M. Hrabovsky[121], A. Hrynevich[37], T. Hryn'ova[4], P. J. Hsu[65], S.-C. Hsu[137], Q. Hu[41,ac], Y. F. Hu[14a,14d,ai], D. P. Huang[95], S. Huang[64b], X. Huang[14c], Y. Huang[62a], Y. Huang[14a], Z. Huang[100], Z. Hubacek[131], M. Huebner[24], F. Huegging[24], T. B. Huffman[125], M. Huhtinen[36], S. K. Huiberts[16], R. Hulsken[103], N. Huseynov[12,a], J. Huston[106], J. Huth[61], R. Hyneman[142], S. Hyrych[28a], G. Iacobucci[56], G. Iakovidis[29], I. Ibragimov[140], L. Iconomidou-Fayard[66], P. Iengo[71a,71b], R. Iguchi[152], T. Iizawa[56], Y. Ikegami[82], A. Ilg[19], N. Ilic[154], H. Imam[35a], T. Ingebretsen Carlson[47a,47b], G. Introzzi[72a,72b], M. Iodice[76a], V. Ippolito[74a,74b], M. Ishino[152], W. Islam[169], C. Issever[18,48], S. Istin[21a,al], H. Ito[167], J. M. Iturbe Ponce[64a], R. Iuppa[77a,77b], A. Ivina[168], J. M. Izen[45], V. Izzo[71a], P. Jacka[130,131], P. Jackson[1], R. M. Jacobs[48], B. P. Jaeger[141], C. S. Jagfeld[108], G. Jäkel[170], K. Jakobs[54], T. Jakoubek[168], J. Jamieson[59], K. W. Janas[84a], G. Jarlskog[97], A. E. Jaspan[91], M. Javurkova[102], F. Jeanneau[134], L. Jeanty[122], J. Jejelava[148a,aa], P. Jenni[54,g], C. E. Jessiman[34], S. Jézéquel[4], J. Jia[144], X. Jia[61], X. Jia[14a,14d], Z. Jia[14c], Y. Jiang[62a], S. Jiggins[52], J. Jimenez Pena[109], S. Jin[14c], A. Jinaru[27b], O. Jinnouchi[153], P. Johansson[138], K. A. Johns[7], D. M. Jones[32], E. Jones[166], P. Jones[32], R. W. L. Jones[90], T. J. Jones[91], R. Joshi[118], J. Jovicevic[15], X. Ju[17a], J. J. Junggeburth[36], A. Juste Rozas[13,v], S. Kabana[136e], A. Kaczmarska[85], M. Kado[74a,74b], H. Kagan[118], M. Kagan[142], A. Kahn[41], A. Kahn[127], C. Kahra[99], T. Kaji[167], E. Kajomovitz[149], N. Kakati[168], C. W. Kalderon[29], A. Kamenshchikov[154], S. Kanayama[153], N. J. Kang[135], Y. Kano[110], D. Kar[33g], K. Karava[125], M. J. Kareem[155b], E. Karentzos[54], I. Karkanias[151], S. N. Karpov[38], Z. M. Karpova[38], V. Kartvelishvili[90], A. N. Karyukhin[37], E. Kasimi[151], C. Kato[62d], J. Katzy[48], S. Kaur[34], K. Kawade[139], K. Kawagoe[88], T. Kawamoto[134], G. Kawamura[55], E. F. Kay[164], F. I. Kaya[157], S. Kazakos[13], V. F. Kazanin[37], Y. Ke[144], J. M. Keaveney[33a], R. Keeler[164], G. V. Kehris[61], J. S. Keller[34], A. S. Kelly[95], D. Kelsey[145], J. J. Kempster[20], K. E. Kennedy[41], O. Kepka[130], B. P. Kerridge[166], S. Kersten[170], B. P. Kerševan[92], S. Keshri[66], L. Keszeghova[28a], S. Ketabchi Haghighat[154], M. Khandoga[126], A. Khanov[120], A. G. Kharlamov[37], T. Kharlamova[37], E. E. Khoda[137], T. J. Khoo[18], G. Khoriauli[165], J. Khubua[148b], Y. A. R. Khwaira[66], M. Kiehn[36], A. Kilgallon[122], D. W. Kim[47a,47b], E. Kim[153], Y. K. Kim[39], N. Kimura[95], A. Kirchhoff[55], D. Kirchmeier[50], C. Kirfel[24], J. Kirk[133], A. E. Kiryunin[109], T. Kishimoto[152], D. P. Kisliuk[154], C. Kitsaki[10], O. Kivernyk[24], M. Klassen[63a], C. Klein[34], L. Klein[165], M. H. Klein[105], M. Klein[91], S. B. Klein[56], U. Klein[91], P. Klimek[36], A. Klimentov[29], F. Klimpel[109], T. Klingl[24], T. Klioutchnikova[36], F. F. Klitzner[108], P. Kluit[113], S. Kluth[109], E. Kneringer[78], T. M. Knight[154], A. Knue[54], D. Kobayashi[88], R. Kobayashi[86], M. Kocian[142], P. Kodyš[132], D. M. Koeck[145], P. T. Koenig[24], T. Koffas[34], N. M. Köhler[36], M. Kolb[134], I. Koletsou[4], T. Komarek[121], K. Köneke[54], A. X. Y. Kong[1], T. Kono[117], N. Konstantinidis[95], B. Konya[97], R. Kopeliansky[67], S. Koperny[84a], K. Korcyl[85], K. Kordas[151], G. Koren[150], A. Korn[95], S. Korn[55], I. Korolkov[13], N. Korotkova[37], B. Kortman[113], O. Kortner[109], S. Kortner[109], W. H. Kostecka[114], V. V. Kostyukhin[140], A. Kotsokechagia[134], A. Kotwal[51], A. Koulouris[36], A. Kourkoumeli-Charalampidi[72a,72b],

C. Kourkoumelis[9], E. Kourlitis[6], O. Kovanda[145], R. Kowalewski[164], W. Kozanecki[134], A. S. Kozhin[37], V. A. Kramarenko[37], G. Kramberger[92], P. Kramer[99], M. W. Krasny[126], A. Krasznahorkay[36], J. A. Kremer[99], T. Kresse[50], J. Kretzschmar[91], K. Kreul[18], P. Krieger[154], F. Krieter[108], S. Krishnamurthy[102], A. Krishnan[63b], M. Krivos[132], K. Krizka[17a], K. Kroeninger[49], H. Kroha[109], J. Kroll[130], J. Kroll[127], K. S. Krowpman[106], U. Kruchonak[38], H. Krüger[24], N. Krumnack[80], M. C. Kruse[51], J. A. Krzysiak[85], A. Kubota[153], O. Kuchinskaia[37], S. Kuday[3a], D. Kuechler[48], J. T. Kuechler[48], S. Kuehn[36], T. Kuhl[48], V. Kukhtin[38], Y. Kulchitsky[37,a], S. Kuleshov[136d,136b], M. Kumar[33g], N. Kumari[101], M. Kuna[60], A. Kupco[130], T. Kupfer[49], A. Kupich[37], O. Kuprash[54], H. Kurashige[83], L. L. Kurchaninov[155a], Y. A. Kurochkin[37], A. Kurova[37], E. S. Kuwertz[36], M. Kuze[153], A. K. Kvam[102], J. Kvita[121], T. Kwan[103], K. W. Kwok[64a], N. G. Kyriacou[105], L. A. O. Laatu[101], C. Lacasta[162], F. Lacava[74a,74b], H. Lacker[18], D. Lacour[126], N. N. Lad[95], E. Ladygin[38], B. Laforge[126], T. Lagouri[136e], S. Lai[55], I. K. Lakomiec[84a], N. Lalloue[60], J. E. Lambert[119], S. Lammers[67], W. Lampl[7], C. Lampoudis[151], A. N. Lancaster[114], E. Lançon[29], U. Landgraf[54], M. P. J. Landon[93], V. S. Lang[54], R. J. Langenberg[102], A. J. Lankford[159], F. Lanni[36], K. Lantzsch[24], A. Lanza[72a], A. Lapertosa[57a,57b], J. F. Laporte[134], T. Lari[70a], F. Lasagni Manghi[23b], M. Lassnig[36], V. Latonova[130], T. S. Lau[64a], A. Laudrain[99], A. Laurier[34], S. D. Lawlor[94], Z. Lawrence[100], M. Lazzaroni[70a,70b], B. Le[100], B. Leban[92], A. Lebedev[80], M. LeBlanc[36], T. LeCompte[6], F. Ledroit-Guillon[60], A. C. A. Lee[95], G. R. Lee[16], L. Lee[61], S. C. Lee[147], S. Lee[47a,47b], T. F. Lee[91], L. L. Leeuw[33c], H. P. Lefebvre[94], M. Lefebvre[164], C. Leggett[17a], K. Lehmann[141], G. Lehmann Miotto[36], M. Leigh[56], W. A. Leight[102], A. Leisos[151,u], M. A. L. Leite[81c], C. E. Leitgeb[48], R. Leitner[132], K. J. C. Leney[44], T. Lenz[24], S. Leone[73a], C. Leonidopoulos[52], A. Leopold[143], C. Leroy[107], R. Les[106], C. G. Lester[32], M. Levchenko[37], J. Levêque[4], D. Levin[105], L. J. Levinson[168], M. P. Lewicki[85], D. J. Lewis[20], B. Li[14b], B. Li[62b], C. Li[62a], C.-Q. Li[62c], H. Li[62a], H. Li[62b], H. Li[14c], H. Li[62b], J. Li[62c], K. Li[137], L. Li[62c], M. Li[14a,14d], Q. Y. Li[62a], S. Li[62c,62d,e], T. Li[62b], X. Li[103], Z. Li[62b], Z. Li[125], Z. Li[103], Z. Li[91], Z. Li[14a,14d], Z. Liang[14a], M. Liberatore[48], B. Liberti[75a], K. Lie[64c], J. Lieber Marin[81b], K. Lin[106], R. A. Linck[67], R. E. Lindley[7], J. H. Lindon[2], A. Linss[48], E. Lipeles[127], A. Lipniacka[16], A. Lister[163], J. D. Little[4], B. Liu[14a], B. X. Liu[141], D. Liu[62c,62d], J. B. Liu[62a], J. K. K. Liu[32], K. Liu[62c,62d], M. Liu[62a], M. Y. Liu[62a], P. Liu[14a], Q. Liu[62c,62d,137], X. Liu[62a], Y. Liu[48], Y. Liu[14c,14d], Y. L. Liu[105], Y. W. Liu[62a], M. Livan[72a,72b], J. Llorente Merino[141], S. L. Lloyd[93], E. M. Lobodzinska[48], P. Loch[7], S. Loffredo[75a,75b], T. Lohse[18], K. Lohwasser[138], M. Lokajicek[130,*], J. D. Long[161], I. Longarini[74a,74b], L. Longo[69a,69b], R. Longo[161], I. Lopez Paz[36], A. Lopez Solis[48], J. Lorenz[108], N. Lorenzo Martinez[4], A. M. Lory[108], A. Lösle[54], X. Lou[47a,47b], X. Lou[14a,14d], A. Lounis[66], J. Love[6], P. A. Love[90], J. J. Lozano Bahilo[162], G. Lu[14a,14d], M. Lu[79], S. Lu[127], Y. J. Lu[65], H. J. Lubatti[137], C. Luci[74a,74b], F. L. Lucio Alves[14c], A. Lucotte[60], F. Luehring[67], I. Luise[144], O. Lukianchuk[66], O. Lundberg[143], B. Lund-Jensen[143], N. A. Luongo[122], M. S. Lutz[150], D. Lynn[29], H. Lyons[91], R. Lysak[130], E. Lytken[97], F. Lyu[14a], V. Lyubushkin[38], T. Lyubushkina[38], H. Ma[29], L. L. Ma[62b], Y. Ma[95], D. M. Mac Donell[164], G. Maccarrone[53], J. C. MacDonald[138], R. Madar[40], W. F. Mader[50], J. Maeda[83], T. Maeno[29], M. Maerker[50], V. Magerl[54], J. Magro[68a,68c], H. Maguire[138], D. J. Mahon[41], C. Maidantchik[81b], A. Maio[129a,129b,129d], K. Maj[84a], O. Majersky[28a], S. Majewski[122], N. Makovec[66], V. Maksimovic[15], B. Malaescu[126], Pa. Malecki[85], V. P. Maleev[37], F. Malek[60], D. Malito[43a,43b], U. Mallik[79], C. Malone[32], S. Maltezos[10], S. Malyukov[38], J. Mamuzic[13], G. Mancini[53], G. Manco[72a,72b], J. P. Mandalia[93], I. Mandić[92], L. Manhaes de Andrade Filho[81a], I. M. Maniatis[151], M. Manisha[134], J. Manjarres Ramos[50], D. C. Mankad[168], A. Mann[108], B. Mansoulie[134], S. Manzoni[36], A. Marantis[151,u], G. Marchiori[5], M. Marcisovsky[130], L. Marcoccia[75a,75b], C. Marcon[70a,70b], M. Marinescu[20], M. Marjanovic[119], Z. Marshall[17a], S. Marti-Garcia[162], T. A. Martin[166], V. J. Martin[52], B. Martin dit Latour[16], L. Martinelli[74a,74b], M. Martinez[13,v], P. Martinez Agullo[162], V. I. Martinez Outschoorn[102], P. Martinez Suarez[13], S. Martin-Haugh[133], V. S. Martoiu[27b], A. C. Martyniuk[95], A. Marzin[36], S. R. Maschek[109], L. Masetti[99], T. Mashimo[152], J. Masik[100], A. L. Maslennikov[37], L. Massa[23b], P. Massarotti[71a,71b], P. Mastrandrea[73a,73b], A. Mastroberardino[43a,43b], T. Masubuchi[152], T. Mathisen[160], N. Matsuzawa[152], J. Maurer[27b], B. Maček[92], D. A. Maximov[37], R. Mazini[147], I. Maznas[151], M. Mazza[106], S. M. Mazza[135], C. Mc Ginn[29], J. P. Mc Gowan[103], S. P. Mc Kee[105], T. G. McCarthy[109], W. P. McCormack[17a], E. F. McDonald[104], A. E. McDougall[113], J. A. Mcfayden[145], G. Mchedlidze[148b], R. P. Mckenzie[33g], T. C. Mclachlan[48], D. J. Mclaughlin[95], K. D. McLean[164], S. J. McMahon[133], P. C. McNamara[104], C. M. Mcpartland[91], R. A. McPherson[164,y], T. Megy[40], S. Mehlhase[108], A. Mehta[91], B. Meirose[45], D. Melini[149], B. R. Mellado Garcia[33g], A. H. Melo[55],

F. Meloni[48], E. D. Mendes Gouveia[129a], A. M. Mendes Jacques Da Costa[20], H. Y. Meng[154], L. Meng[90], S. Menke[109], M. Mentink[36], E. Meoni[43a,43b], C. Merlassino[125], L. Merola[71a,71b], C. Meroni[70a], G. Merz[105], O. Meshkov[37], J. K. R. Meshreki[140], J. Metcalfe[6], A. S. Mete[6], C. Meyer[67], J.-P. Meyer[134], M. Michetti[18], R. P. Middleton[133], L. Mijović[52], G. Mikenberg[168], M. Mikestikova[130], M. Mikuž[92], H. Mildner[138], A. Milic[154], C. D. Milke[44], D. W. Miller[39], L. S. Miller[34], A. Milov[168], D. A. Milstead[47a,47b], T. Min[14c], A. A. Minaenko[37], I. A. Minashvili[148b], L. Mince[59], A. I. Mincer[116], B. Mindur[84a], M. Mineev[38], Y. Mino[86], L. M. Mir[13], M. Miralles Lopez[162], M. Mironova[125], T. Mitani[167], A. Mitra[166], V. A. Mitsou[162], O. Miu[154], P. S. Miyagawa[93], Y. Miyazaki[88], A. Mizukami[82], J. U. Mjörnmark[97], T. Mkrtchyan[63a], T. Mlinarevic[95], M. Mlynarikova[36], T. Moa[47a,47b], S. Mobius[55], K. Mochizuki[107], P. Moder[48], P. Mogg[108], A. F. Mohammed[14a,14d], S. Mohapatra[41], G. Mokgatitswane[33g], B. Mondal[140], S. Mondal[131], K. Mönig[48], E. Monnier[101], L. Monsonis Romero[162], J. Montejo Berlingen[36], M. Montella[118], F. Monticelli[89], N. Morange[66], A. L. Moreira De Carvalho[129a], M. Moreno Llácer[162], C. Moreno Martinez[13], P. Morettini[57b], S. Morgenstern[166], M. Morii[61], M. Morinaga[152], V. Morisbak[124], A. K. Morley[36], F. Morodei[74a,74b], L. Morvaj[36], P. Moschovakos[36], B. Moser[36], M. Mosidze[148b], T. Moskalets[54], P. Moskvitina[112], J. Moss[31,o], E. J. W. Moyse[102], S. Muanza[101], J. Mueller[128], D. Muenstermann[90], R. Müller[19], G. A. Mullier[97], J. J. Mullin[127], D. P. Mungo[70a,70b], J. L. Munoz Martinez[13], D. Munoz Perez[162], F. J. Munoz Sanchez[100], M. Murin[100], W. J. Murray[133,166], A. Murrone[70a,70b], J. M. Muse[119], M. Muškinja[17a], C. Mwewa[29], A. G. Myagkov[37,a], A. J. Myers[8], A. A. Myers[128], G. Myers[67], M. Myska[131], B. P. Nachman[17a], O. Nackenhorst[49], A. Nag[50], K. Nagai[125], K. Nagano[82], J. L. Nagle[29,aj], E. Nagy[101], A. M. Nairz[36], Y. Nakahama[82], K. Nakamura[82], H. Nanjo[123], R. Narayan[44], E. A. Narayanan[111], I. Naryshkin[37], M. Naseri[34], C. Nass[24], G. Navarro[22a], J. Navarro-Gonzalez[162], R. Nayak[150], A. Nayaz[18], P. Y. Nechaeva[37], F. Nechansky[48], L. Nedic[125], T. J. Neep[20], A. Negri[72a,72b], M. Negrini[23b], C. Nellist[112], C. Nelson[103], K. Nelson[105], S. Nemecek[130], M. Nessi[36,h], M. S. Neubauer[161], F. Neuhaus[99], J. Neundorf[48], R. Newhouse[163], P. R. Newman[20], C. W. Ng[128], Y. S. Ng[18], Y. W. Y. Ng[159], B. Ngair[35e], H. D. N. Nguyen[107], R. B. Nickerson[125], R. Nicolaidou[134], J. Nielsen[135], M. Niemeyer[55], N. Nikiforou[36], V. Nikolaenko[37,a], I. Nikolic-Audit[126], K. Nikolopoulos[20], P. Nilsson[29], H. R. Nindhito[56], A. Nisati[74a], N. Nishu[2], R. Nisius[109], J.-E. Nitschke[50], E. K. Nkadimeng[33g], S. J. Noacco Rosende[89], T. Nobe[152], D. L. Noel[32], Y. Noguchi[86], T. Nommensen[146], M. A. Nomura[29], M. B. Norfolk[138], R. R. B. Norisam[95], B. J. Norman[34], J. Novak[92], T. Novak[48], O. Novgorodova[50], L. Novotny[131], R. Novotny[111], L. Nozka[121], K. Ntekas[159], E. Nurse[95], F. G. Oakham[34,ag], J. Ocariz[126], A. Ochi[83], I. Ochoa[129a], S. Oerdek[160], A. Ogrodnik[84a], A. Oh[100], C. C. Ohm[143], H. Oide[153], R. Oishi[152], M. L. Ojeda[48], Y. Okazaki[86], M. W. O'Keefe[91], Y. Okumura[152], A. Olariu[27b], L. F. Oleiro Seabra[129a], S. A. Olivares Pino[136e], D. Oliveira Damazio[29], D. Oliveira Goncalves[81a], J. L. Oliver[159], M. J. R. Olsson[159], A. Olszewski[85], J. Olszowska[85,*], Ö. O. Öncel[54], D. C. O'Neil[141], A. P. O'Neill[19], A. Onofre[129a,129e], P. U. E. Onyisi[11], M. J. Oreglia[39], G. E. Orellana[89], D. Orestano[76a,76b], N. Orlando[13], R. S. Orr[154], V. O'Shea[59], R. Ospanov[62a], G. Otero y Garzon[30], H. Otono[88], P. S. Ott[63a], G. J. Ottino[17a], M. Ouchrif[35d], J. Ouellette[29,aj], F. Ould-Saada[124], M. Owen[59], R. E. Owen[133], K. Y. Oyulmaz[21a], V. E. Ozcan[21a], N. Ozturk[8], S. Ozturk[21d], J. Pacalt[121], H. A. Pacey[32], K. Pachal[51], A. Pacheco Pages[13], C. Padilla Aranda[13], G. Padovano[74a,74b], S. Pagan Griso[17a], G. Palacino[67], A. Palazzo[69a,69b], S. Palazzo[52], S. Palestini[36], M. Palka[84b], J. Pan[171], T. Pan[64a], D. K. Panchal[11], C. E. Pandini[113], J. G. Panduro Vazquez[94], H. Pang[14b], P. Pani[48], G. Panizzo[68a,68c], L. Paolozzi[56], C. Papadatos[107], S. Parajuli[44], A. Paramonov[6], C. Paraskevopoulos[10], D. Paredes Hernandez[64b], T. H. Park[154], M. A. Parker[32], F. Parodi[57a,57b], E. W. Parrish[114], V. A. Parrish[52], J. A. Parsons[41], U. Parzefall[54], B. Pascual Dias[107], L. Pascual Dominguez[150], V. R. Pascuzzi[17a], F. Pasquali[113], E. Pasqualucci[74a], S. Passaggio[57b], F. Pastore[94], P. Pasuwan[47a,47b], P. Patel[85], J. R. Pater[100], J. Patton[91], T. Pauly[36], J. Pearkes[142], M. Pedersen[124], R. Pedro[129a], S. V. Peleganchuk[37], O. Penc[36], E. A. Pender[52], C. Peng[64b], H. Peng[62a], K. E. Penski[108], M. Penzin[37], B. S. Peralva[81d], A. P. Pereira Peixoto[60], L. Pereira Sanchez[47a,47b], D. V. Perepelitsa[29,aj], E. Perez Codina[155a], M. Perganti[10], L. Perini[70a,70b,*], H. Pernegger[36], S. Perrella[36], A. Perrevoort[112], O. Perrin[40], K. Peters[48], R. F. Y. Peters[100], B. A. Petersen[36], T. C. Petersen[42], E. Petit[101], V. Petousis[131], C. Petridou[151], A. Petrukhin[140], M. Pettee[17a], N. E. Pettersson[36], A. Petukhov[37], K. Petukhova[132], A. Peyaud[134], R. Pezoa[136f], L. Pezzotti[36], G. Pezzullo[171], T. M. Pham[169], T. Pham[104], P. W. Phillips[133], M. W. Phipps[161], G. Piacquadio[144], E. Pianori[17a], F. Piazza[70a,70b], R. Piegaia[30], D. Pietreanu[27b], A. D. Pilkington[100], M. Pinamonti[68a,68c], J. L. Pinfold[2], B. C. Pinheiro Pereira[129a], C. Pitman Donaldson[95], D. A. Pizzi[34], L. Pizzimento[75a,75b],

A. Pizzini[113], M.-A. Pleier[29], V. Plesanovs[54], V. Pleskot[132], E. Plotnikova[38], G. Poddar[4], R. Poettgen[97], L. Poggioli[126], I. Pogrebnyak[106], D. Pohl[24], I. Pokharel[55], S. Polacek[132], G. Polesello[72a], A. Poley[141,155a], R. Polifka[131], A. Polini[23b], C. S. Pollard[125], Z. B. Pollock[118], V. Polychronakos[29], E. Pompa Pacchi[74a,74b], D. Ponomarenko[37], L. Pontecorvo[36], S. Popa[27a], G. A. Popeneciu[27d], D. M. Portillo Quintero[155a], S. Pospisil[131], P. Postolache[27c], K. Potamianos[125], I. N. Potrap[38], C. J. Potter[32], H. Potti[1], T. Poulsen[48], J. Poveda[162], M. E. Pozo Astigarraga[36], A. Prades Ibanez[162], M. M. Prapa[46], S. Prell[80], J. Pretel[54], D. Price[100], M. Primavera[69a], M. A. Principe Martin[98], M. L. Proffitt[137], N. Proklova[127], K. Prokofiev[64c], G. Proto[75a,75b], S. Protopopescu[29], J. Proudfoot[6], M. Przybycien[84a], J. E. Puddefoot[138], D. Pudzha[37], P. Puzo[66], D. Pyatiizbyantseva[37], J. Qian[105], D. Qichen[100], Y. Qin[100], T. Qiu[93], A. Quadt[55], M. Queitsch-Maitland[100], G. Quetant[56], G. Rabanal Bolanos[61], D. Rafanoharana[54], F. Ragusa[70a,70b], J. L. Rainbolt[39], J. A. Raine[56], S. Rajagopalan[29], E. Ramakoti[37], K. Ran[14d,48], N. P. Rapheeha[33g], V. Raskina[126], D. F. Rassloff[63a], S. Rave[99], B. Ravina[55], I. Ravinovich[168], M. Raymond[36], A. L. Read[124], N. P. Readioff[138], D. M. Rebuzzi[72a,72b], G. Redlinger[29], K. Reeves[45], J. A. Reidelsturz[170], D. Reikher[150], A. Reiss[99], A. Rej[140], C. Rembser[36], A. Renardi[48], M. Renda[27b], M. B. Rendel[109], A. G. Rennie[59], S. Resconi[70a], M. Ressegotti[57a,57b], E. D. Resseguie[17a], S. Rettie[95], B. Reynolds[118], E. Reynolds[17a], M. Rezaei Estabragh[170], O. L. Rezanova[37], P. Reznicek[132], E. Ricci[77a,77b], R. Richter[109], S. Richter[47a,47b], E. Richter-Was[84b], M. Ridel[126], P. Rieck[116], P. Riedler[36], M. Rijssenbeek[144], A. Rimoldi[72a,72b], M. Rimoldi[48], L. Rinaldi[23a,23b], T. T. Rinn[29], M. P. Rinnagel[108], G. Ripellino[143], I. Riu[13], P. Rivadeneira[48], J. C. Rivera Vergara[164], F. Rizatdinova[120], E. Rizvi[93], C. Rizzi[56], B. A. Roberts[166], B. R. Roberts[17a], S. H. Robertson[103,y], M. Robin[48], D. Robinson[32], C. M. Robles Gajardo[136f], M. Robles Manzano[99], A. Robson[59], A. Rocchi[75a,75b], C. Roda[73a,73b], S. Rodriguez Bosca[63a], Y. Rodriguez Garcia[22a], A. Rodriguez Rodriguez[54], A. M. Rodríguez Vera[155b], S. Roe[36], J. T. Roemer[159], A. R. Roepe-Gier[119], J. Roggel[170], O. Røhne[124], R. A. Rojas[164], B. Roland[54], C. P. A. Roland[67], J. Roloff[29], A. Romaniouk[37], E. Romano[72a,72b], M. Romano[23b], A. C. Romero Hernandez[161], N. Rompotis[91], L. Roos[126], S. Rosati[74a], B. J. Rosser[39], E. Rossi[4], E. Rossi[71a,71b], L. P. Rossi[57b], L. Rossini[48], R. Rosten[118], M. Rotaru[27b], B. Rottler[54], D. Rousseau[66], D. Rousso[32], G. Rovelli[72a,72b], A. Roy[161], A. Rozanov[101], Y. Rozen[149], X. Ruan[33g], A. Rubio Jimenez[162], A. J. Ruby[91], V. H. Ruelas Rivera[18], T. A. Ruggeri[1], F. Rühr[54], A. Ruiz-Martinez[162], A. Rummler[36], Z. Rurikova[54], N. A. Rusakovich[38], H. L. Russell[164], J. P. Rutherfoord[7], K. Rybacki[90], M. Rybar[132], E. B. Rye[124], A. Ryzhov[37], J. A. Sabater Iglesias[56], P. Sabatini[162], L. Sabetta[74a,74b], H. F.-W. Sadrozinski[135], F. Safai Tehrani[74a], B. Safarzadeh Samani[145], M. Safdari[142], S. Saha[103], M. Sahinsoy[109], M. Saimpert[134], M. Saito[152], T. Saito[152], D. Salamani[36], G. Salamanna[76a,76b], A. Salnikov[142], J. Salt[162], A. Salvador Salas[13], D. Salvatore[43a,43b], F. Salvatore[145], A. Salzburger[36], D. Sammel[54], D. Sampsonidis[151], D. Sampsonidou[62c,62d], J. Sánchez[162], A. Sanchez Pineda[4], V. Sanchez Sebastian[162], H. Sandaker[124], C. O. Sander[48], J. A. Sandesara[102], M. Sandhoff[170], C. Sandoval[22b], D. P. C. Sankey[133], A. Sansoni[53], L. Santi[74a,74b], C. Santoni[40], H. Santos[129a,129b], S. N. Santpur[17a], A. Santra[168], K. A. Saoucha[138], J. G. Saraiva[129a,129d], J. Sardain[7], O. Sasaki[82], K. Sato[156], C. Sauer[63b], F. Sauerburger[54], E. Sauvan[4], P. Savard[154,ag], R. Sawada[152], C. Sawyer[133], L. Sawyer[96], I. Sayago Galvan[162], C. Sbarra[23b], A. Sbrizzi[23a,23b], T. Scanlon[95], J. Schaarschmidt[137], P. Schacht[109], D. Schaefer[39], U. Schäfer[99], A. C. Schaffer[66], D. Schaile[108], R. D. Schamberger[144], E. Schanet[108], C. Scharf[18], M. M. Schefer[19], V. A. Schegelsky[37], D. Scheirich[132], F. Schenck[18], M. Schernau[159], C. Scheulen[55], C. Schiavi[57a,57b], Z. M. Schillaci[26], E. J. Schioppa[69a,69b], M. Schioppa[43a,43b], B. Schlag[99], K. E. Schleicher[54], S. Schlenker[36], K. Schmieden[99], C. Schmitt[99], S. Schmitt[48], L. Schoeffel[134], A. Schoening[63b], P. G. Scholer[54], E. Schopf[125], M. Schott[99], J. Schovancova[36], S. Schramm[56], F. Schroeder[170], H.-C. Schultz-Coulon[63a], M. Schumacher[54], B. A. Schumm[135], Ph. Schune[134], A. Schwartzman[142], T. A. Schwarz[105], Ph. Schwemling[134], R. Schwienhorst[106], A. Sciandra[135], G. Sciolla[26], F. Scuri[73a], F. Scutti[104], C. D. Sebastiani[91], K. Sedlaczek[49], P. Seema[18], S. C. Seidel[111], A. Seiden[135], B. D. Seidlitz[41], T. Seiss[39], C. Seitz[48], J. M. Seixas[81b], G. Sekhniaidze[71a], S. J. Sekula[44], L. Selem[4], N. Semprini-Cesari[23a,23b], S. Sen[51], D. Sengupta[56], V. Senthilkumar[162], L. Serin[66], L. Serkin[68a,68b], M. Sessa[76a,76b], H. Severini[119], S. Sevova[142], F. Sforza[57a,57b], A. Sfyrla[56], E. Shabalina[55], R. Shaheen[143], J. D. Shahinian[127], N. W. Shaikh[47a,47b], D. Shaked Renous[168], L. Y. Shan[14a], M. Shapiro[17a], A. Sharma[36], A. S. Sharma[163], P. Sharma[79], S. Sharma[48], P. B. Shatalov[37], K. Shaw[145], S. M. Shaw[100], Q. Shen[62c,5], P. Sherwood[95], L. Shi[95], C. O. Shimmin[171], Y. Shimogama[167], J. D. Shinner[94], I. P. J. Shipsey[125], S. Shirabe[60], M. Shiyakova[38,x], J. Shlomi[168], M. J. Shochet[39], J. Shojaii[104], D. R. Shope[124],

S. Shrestha[118,ak], E. M. Shrif[33g], M. J. Shroff[164], P. Sicho[130], A. M. Sickles[161], E. Sideras Haddad[33g], A. Sidoti[23b], F. Siegert[50], Dj. Sijacki[15], R. Sikora[84a], F. Sili[89], J. M. Silva[20], M. V. Silva Oliveira[36], S. B. Silverstein[47a], S. Simion[66], R. Simoniello[36], E. L. Simpson[59], N. D. Simpson[97], S. Simsek[21d], S. Sindhu[55], P. Sinervo[154], V. Sinetckii[37], S. Singh[141], S. Singh[154], S. Sinha[48], S. Sinha[33g], M. Sioli[23a,23b], I. Siral[122], S.Yu. Sivoklokov[37,*], J. Sjölin[47a,47b], A. Skaf[55], E. Skorda[97], P. Skubic[119], M. Slawinska[85], V. Smakhtin[168], B. H. Smart[133], J. Smiesko[36], S. Yu. Smirnov[37], Y. Smirnov[37], L. N. Smirnova[37,a], O. Smirnova[97], A. C. Smith[41], E. A. Smith[39], H. A. Smith[125], J. L. Smith[91], R. Smith[142], M. Smizanska[90], K. Smolek[131], A. Smykiewicz[85], A. A. Snesarev[37], H. L. Snoek[113], S. Snyder[29], R. Sobie[164,y], A. Soffer[150], C. A. Solans Sanchez[36], E. Yu. Soldatov[37], U. Soldevila[162], A. A. Solodkov[37], S. Solomon[54], A. Soloshenko[38], K. Solovieva[54], O. V. Solovyanov[37], V. Solovyev[37], P. Sommer[36], A. Sonay[13], W. Y. Song[155b], A. Sopczak[131], A. L. Sopio[95], F. Sopkova[28b], V. Sothilingam[63a], S. Sottocornola[72a,72b], R. Soualah[115b], Z. Soumaimi[35e], D. South[48], S. Spagnolo[69a,69b], M. Spalla[109], F. Spanò[94], D. Sperlich[54], G. Spigo[36], M. Spina[145], S. Spinali[90], D. P. Spiteri[59], M. Spousta[132], E. J. Staats[34], A. Stabile[70a,70b], R. Stamen[63a], M. Stamenkovic[113], A. Stampekis[20], M. Standke[24], E. Stanecka[85], M. V. Stange[50], B. Stanislaus[17a], M. M. Stanitzki[48], M. Stankaityte[125], B. Stapf[48], E. A. Starchenko[37], G. H. Stark[135], J. Stark[101,ab], D. M. Starko[155b], P. Staroba[130], P. Starovoitov[63a], S. Stärz[103], R. Staszewski[85], G. Stavropoulos[46], J. Steentoft[160], P. Steinberg[29], A. L. Steinhebel[122], B. Stelzer[141,155a], H. J. Stelzer[128], O. Stelzer-Chilton[155a], H. Stenzel[58], T. J. Stevenson[145], G. A. Stewart[36], M. C. Stockton[36], G. Stoicea[27b], M. Stolarski[129a], S. Stonjek[109], A. Straessner[50], J. Strandberg[143], S. Strandberg[47a,47b], M. Strauss[119], T. Strebler[101], P. Strizenec[28b], R. Ströhmer[165], D. M. Strom[122], L. R. Strom[48], R. Stroynowski[44], A. Strubig[47a,47b], S. A. Stucci[29], B. Stugu[16], J. Stupak[119], N. A. Styles[48], D. Su[142], S. Su[62a], W. Su[62c,62d,137], X. Su[62a,66], K. Sugizaki[152], V. V. Sulin[37], M. J. Sullivan[91], D. M. S. Sultan[77a,77b], L. Sultanaliyeva[37], S. Sultansoy[3b], T. Sumida[86], S. Sun[105], S. Sun[169], O. Sunneborn Gudnadottir[160], M. R. Sutton[145], M. Svatos[130], M. Swiatlowski[155a], T. Swirski[165], I. Sykora[28a], M. Sykora[132], T. Sykora[132], D. Ta[99], K. Tackmann[48,w], A. Taffard[159], R. Tafirout[155a], J. S. Tafoya Vargas[66], R. H. M. Taibah[126], R. Takashima[87], K. Takeda[83], E. P. Takeva[52], Y. Takubo[82], M. Talby[101], A. A. Talyshev[37], K. C. Tam[64b], N. M. Tamir[150], A. Tanaka[152], J. Tanaka[152], R. Tanaka[66], M. Tanasini[57a,57b], J. Tang[62c], Z. Tao[163], S. Tapia Araya[80], S. Tapprogge[99], A. Tarek Abouelfadl Mohamed[106], S. Tarem[149], K. Tariq[62b], G. Tarna[27b], G. F. Tartarelli[70a], P. Tas[132], M. Tasevsky[130], E. Tassi[43a,43b], A. C. Tate[161], G. Tateno[152], Y. Tayalati[35e], G. N. Taylor[104], W. Taylor[155b], H. Teagle[91], A. S. Tee[169], R. Teixeira De Lima[142], P. Teixeira-Dias[94], J. J. Teoh[154], K. Terashi[152], J. Terron[98], S. Terzo[13], M. Testa[53], R. J. Teuscher[154,y], A. Thaler[78], O. Theiner[56], N. Themistokleous[52], T. Theveneaux-Pelzer[18], O. Thielmann[170], D. W. Thomas[94], J. P. Thomas[20], E. A. Thompson[48], P. D. Thompson[20], E. Thomson[127], E. J. Thorpe[93], Y. Tian[55], V. Tikhomirov[37,a], Yu.A. Tikhonov[37], S. Timoshenko[37], E. X. L. Ting[1], P. Tipton[171], S. Tisserant[101], S. H. Tlou[33g], A. Tnourji[40], K. Todome[23a,23b], S. Todorova-Nova[132], S. Todt[50], M. Togawa[82], J. Tojo[88], S. Tokár[28a], K. Tokushuku[82], R. Tombs[32], M. Tomoto[82,110], L. Tompkins[142,q], K. W. Topolnicki[84b], P. Tornambe[102], E. Torrence[122], H. Torres[50], E. Torró Pastor[162], M. Toscani[30], C. Tosciri[39], D. R. Tovey[138], A. Traeet[16], I. S. Trandafir[27b], T. Trefzger[165], A. Tricoli[29], I. M. Trigger[155a], S. Trincaz-Duvoid[126], D. A. Trischuk[26], B. Trocmé[60], A. Trofymov[66], C. Troncon[70a], L. Truong[33c], M. Trzebinski[85], A. Trzupek[85], F. Tsai[144], M. Tsai[105], A. Tsiamis[151], P. V. Tsiareshka[37], S. Tsigaridas[155a], A. Tsirigotis[151,u], V. Tsiskaridze[144], E. G. Tskhadadze[148a], M. Tsopoulou[151], Y. Tsujikawa[86], I. I. Tsukerman[37], V. Tsulaia[17a], S. Tsuno[82], O. Tsur[149], D. Tsybychev[144], Y. Tu[64b], A. Tudorache[27b], V. Tudorache[27b], A. N. Tuna[36], S. Turchikhin[38], I. Turk Cakir[3a], R. Turra[70a], T. Turtuvshin[38], P. M. Tuts[41], S. Tzamarias[151], P. Tzanis[10], E. Tzovara[99], K. Uchida[152], F. Ukegawa[156], P. A. Ulloa Poblete[136c], G. Unal[36], M. Unal[11], A. Undrus[29], G. Unel[159], J. Urban[28b], P. Urquijo[104], G. Usai[8], R. Ushioda[153], M. Usman[107], Z. Uysal[21b], V. Vacek[131], B. Vachon[103], K. O. H. Vadla[124], T. Vafeiadis[36], C. Valderanis[108], E. Valdes Santurio[47a,47b], M. Valente[155a], S. Valentinetti[23a,23b], A. Valero[162], A. Vallier[101,ab], J. A. Valls Ferrer[162], T. R. Van Daalen[137], P. Van Gemmeren[6], M. Van Rijnbach[124,36], S. Van Stroud[95], I. Van Vulpen[113], M. Vanadia[75a,75b], W. Vandelli[36], M. Vandenbroucke[134], E. R. Vandewall[120], D. Vannicola[150], L. Vannoli[57a,57b], R. Vari[74a], E. W. Varnes[7], C. Varni[17a], T. Varol[147], D. Varouchas[66], L. Varriale[162], K. E. Varvell[146], M. E. Vasile[27b], L. Vaslin[40], G. A. Vasquez[164], F. Vazeille[40], T. Vazquez Schroeder[36], J. Veatch[31], V. Vecchio[100], M. J. Veen[102], I. Veliscek[125], L. M. Veloce[154], F. Veloso[129a,129c], S. Veneziano[74a], A. Ventura[69a,69b], A. Verbytskyi[109], M. Verducci[73a,73b], C. Vergis[24], M. Verissimo De Araujo[81b],

W. Verkerke[113], J. C. Vermeulen[113], C. Vernieri[142], P. J. Verschuuren[94], M. Vessella[102], M. C. Vetterli[141,ag], A. Vgenopoulos[151], N. Viaux Maira[136f], T. Vickey[138], O. E. Vickey Boeriu[138], G. H. A. Viehhauser[125], L. Vigani[63b], M. Villa[23a,23b], M. Villaplana Perez[162], E. M. Villhauer[52], E. Vilucchi[53], M. G. Vincter[34], G. S. Virdee[20], A. Vishwakarma[52], C. Vittori[23a,23b], I. Vivarelli[145], V. Vladimirov[166], E. Voevodina[109], F. Vogel[108], P. Vokac[131], J. Von Ahnen[48], E. Von Toerne[24], B. Vormwald[36], V. Vorobel[132], K. Vorobev[37], M. Vos[162], J. H. Vossebeld[91], M. Vozak[113], L. Vozdecky[93], N. Vranjes[15], M. Vranjes Milosavljevic[15], M. Vreeswijk[113], R. Vuillermet[36], O. Vujinovic[99], I. Vukotic[39], S. Wada[156], C. Wagner[102], W. Wagner[170], S. Wahdan[170], H. Wahlberg[89], R. Wakasa[156], M. Wakida[110], V. M. Walbrecht[109], J. Walder[133], R. Walker[108], W. Walkowiak[140], A. M. Wang[61], A. Z. Wang[169], C. Wang[62a], C. Wang[62c], H. Wang[17a], J. Wang[64a], P. Wang[44], R.-J. Wang[99], R. Wang[61], R. Wang[6], S. M. Wang[147], S. Wang[62b], T. Wang[62a], W. T. Wang[79], W. X. Wang[62a], X. Wang[14c], X. Wang[161], X. Wang[62c], Y. Wang[62d], Y. Wang[14c], Z. Wang[105], Z. Wang[51,62c,62d], Z. Wang[105], A. Warburton[103], R. J. Ward[20], N. Warrack[59], A. T. Watson[20], M. F. Watson[20], G. Watts[137], B. M. Waugh[95], A. F. Webb[11], C. Weber[29], M. S. Weber[19], S. M. Weber[63a], C. Wei[62a], Y. Wei[125], A. R. Weidberg[125], J. Weingarten[49], M. Weirich[99], C. Weiser[54], C. J. Wells[48], T. Wenaus[29], B. Wendland[49], T. Wengler[36], N. S. Wenke[109], N. Wermes[24], M. Wessels[63a], K. Whalen[122], A. M. Wharton[90], A. S. White[61], A. White[8], M. J. White[1], D. Whiteson[159], L. Wickremasinghe[123], W. Wiedenmann[169], C. Wiel[50], M. Wielers[133], N. Wieseotte[99], C. Wiglesworth[42], L. A. M. Wiik-Fuchs[54], D. J. Wilbern[119], H. G. Wilkens[36], D. M. Williams[41], H. H. Williams[127], S. Williams[32], S. Willocq[102], P. J. Windischhofer[125], F. Winklmeier[122], B. T. Winter[54], M. Wittgen[142], M. Wobisch[96], R. Wölker[125], J. Wollrath[159], M. W. Wolter[85], H. Wolters[129a,129c], V. W. S. Wong[163], A. F. Wongel[48], S. D. Worm[48], B. K. Wosiek[85], K. W. Woźniak[85], K. Wraight[59], J. Wu[14a,14d], M. Wu[64a], M. Wu[112], S. L. Wu[169], X. Wu[56], Y. Wu[62a], Z. Wu[62a,134], J. Wuerzinger[125], T. R. Wyatt[100], B. M. Wynne[52], S. Xella[42], L. Xia[14c], M. Xia[14b], J. Xiang[64c], X. Xiao[105], M. Xie[62a], X. Xie[62a], J. Xiong[17a], I. Xiotidis[145], D. Xu[14a], H. Xu[62a], H. Xu[62a], L. Xu[62a], R. Xu[127], T. Xu[105], W. Xu[105], Y. Xu[14b], Z. Xu[62b], Z. Xu[142], B. Yabsley[146], S. Yacoob[33a], N. Yamaguchi[88], Y. Yamaguchi[153], H. Yamauchi[156], T. Yamazaki[17a], Y. Yamazaki[83], J. Yan[62c], S. Yan[125], Z. Yan[25], H. J. Yang[62c,62d], H. T. Yang[17a], S. Yang[62a], T. Yang[64c], X. Yang[62a], X. Yang[14a], Y. Yang[44], Z. Yang[62a,105], W.-M. Yao[17a], Y. C. Yap[48], H. Ye[14c], J. Ye[44], S. Ye[29], X. Ye[62a], Y. Yeh[95], I. Yeletskikh[38], M. R. Yexley[90], P. Yin[41], K. Yorita[167], C. J. S. Young[54], C. Young[142], M. Yuan[105], R. Yuan[62b,k], L. Yue[95], X. Yue[63a], M. Zaazoua[35e], B. Zabinski[85], E. Zaid[52], T. Zakareishvili[148b], N. Zakharchuk[34], S. Zambito[56], J. A. Zamora Saa[136d], J. Zang[152], D. Zanzi[54], O. Zaplatilek[131], S. V. Zeißner[49], C. Zeitnitz[170], J. C. Zeng[161], D. T. Zenger Jr[26], O. Zenin[37], T. Ženiš[28a], S. Zenz[93], S. Zerradi[35a], D. Zerwas[66], B. Zhang[14c], D. F. Zhang[138], G. Zhang[14b], J. Zhang[62b], J. Zhang[6], K. Zhang[14a,14d], L. Zhang[14c], P. Zhang[14a,14d], R. Zhang[169], S. Zhang[105], T. Zhang[152], X. Zhang[62c], X. Zhang[62b], Z. Zhang[17a], Z. Zhang[66], H. Zhao[137], P. Zhao[51], T. Zhao[62b], Y. Zhao[135], Z. Zhao[62a], A. Zhemchugov[38], X. Zheng[62a], Z. Zheng[142], D. Zhong[161], B. Zhou[105], C. Zhou[169], H. Zhou[7], N. Zhou[62c], Y. Zhou[7], C. G. Zhu[62b], C. Zhu[14a,14d], H. L. Zhu[62a], H. Zhu[14a], J. Zhu[105], Y. Zhu[62c], Y. Zhu[62a], X. Zhuang[14a], K. Zhukov[37], V. Zhulanov[37], N. I. Zimine[38], J. Zinsser[63b], M. Ziolkowski[140], L. Živković[15], A. Zoccoli[23a,23b], K. Zoch[56], T. G. Zorbas[138], O. Zormpa[46], W. Zou[41], L. Zwalinski[36]

[1] Department of Physics, University of Adelaide, Adelaide, Australia
[2] Department of Physics, University of Alberta, Edmonton, AB, Canada
[3] [(a)]Department of Physics, Ankara University, Ankara, Türkiye; [(b)]Division of Physics, TOBB University of Economics and Technology, Ankara, Türkiye
[4] LAPP, Université Savoie Mont Blanc, CNRS/IN2P3, Annecy, France
[5] APC, Université Paris Cité, CNRS/IN2P3, Paris, France
[6] High Energy Physics Division, Argonne National Laboratory, Argonne, IL, USA
[7] Department of Physics, University of Arizona, Tucson, AZ, USA
[8] Department of Physics, University of Texas at Arlington, Arlington, TX, USA
[9] Physics Department, National and Kapodistrian University of Athens, Athens, Greece
[10] Physics Department, National Technical University of Athens, Zografou, Greece
[11] Department of Physics, University of Texas at Austin, Austin, TX, USA
[12] Institute of Physics, Azerbaijan Academy of Sciences, Baku, Azerbaijan
[13] Institut de Física d'Altes Energies (IFAE), Barcelona Institute of Science and Technology, Barcelona, Spain

[14] [(a)]Institute of High Energy Physics, Chinese Academy of Sciences, Beijing, China; [(b)]Physics Department, Tsinghua University, Beijing, China; [(c)]Department of Physics, Nanjing University, Nanjing, China; [(d)]University of Chinese Academy of Science (UCAS), Beijing, China
[15] Institute of Physics, University of Belgrade, Belgrade, Serbia
[16] Department for Physics and Technology, University of Bergen, Bergen, Norway
[17] [(a)]Physics Division, Lawrence Berkeley National Laboratory, Berkeley, CA, USA; [(b)]University of California, Berkeley, CA, USA
[18] Institut für Physik, Humboldt Universität zu Berlin, Berlin, Germany
[19] Albert Einstein Center for Fundamental Physics and Laboratory for High Energy Physics, University of Bern, Bern, Switzerland
[20] School of Physics and Astronomy, University of Birmingham, Birmingham, UK
[21] [(a)]Department of Physics, Bogazici University, Istanbul, Türkiye; [(b)]Department of Physics Engineering, Gaziantep University, Gaziantep, Türkiye; [(c)]Department of Physics, Istanbul University, Istanbul, Türkiye; [(d)]Istinye University, Sariyer, Istanbul, Türkiye
[22] [(a)]Facultad de Ciencias y Centro de Investigaciónes, Universidad Antonio Nariño, Bogotá, Colombia; [(b)]Departamento de Física, Universidad Nacional de Colombia, Bogotá, Colombia
[23] [(a)]Dipartimento di Fisica e Astronomia A. Righi, Università di Bologna, Bologna, Italy; [(b)]INFN Sezione di Bologna, Bologna, Italy
[24] Physikalisches Institut, Universität Bonn, Bonn, Germany
[25] Department of Physics, Boston University, Boston, MA, USA
[26] Department of Physics, Brandeis University, Waltham, MA, USA
[27] [(a)]Transilvania University of Brasov, Brasov, Romania; [(b)]Horia Hulubei National Institute of Physics and Nuclear Engineering, Bucharest, Romania; [(c)]Department of Physics, Alexandru Ioan Cuza University of Iasi, Iasi, Italy; [(d)]Physics Department, National Institute for Research and Development of Isotopic and Molecular Technologies, Cluj-Napoca, Romania; [(e)]University Politehnica Bucharest, Bucharest, Romania; [(f)]West University in Timisoara, Timisoara, Romania; [(g)]Faculty of Physics, University of Bucharest, Bucharest, Romania
[28] [(a)]Faculty of Mathematics, Physics and Informatics, Comenius University, Bratislava, Slovakia; [(b)]Department of Subnuclear Physics, Institute of Experimental Physics of the Slovak Academy of Sciences, Kosice, Slovak Republic
[29] Physics Department, Brookhaven National Laboratory, Upton, NY, USA
[30] Universidad de Buenos Aires, Facultad de Ciencias Exactas y Naturales, Departamento de Física, y CONICET, Instituto de Fàsica de Buenos Aires (IFIBA), Buenos Aires, Argentina
[31] California State University, Long Beach, CA, USA
[32] Cavendish Laboratory, University of Cambridge, Cambridge, UK
[33] [(a)]Department of Physics, University of Cape Town, Cape Town, South Africa; [(b)]iThemba Labs, Johannesburg, Western Cape, South Africa; [(c)]Department of Mechanical Engineering Science, University of Johannesburg, Johannesburg, South Africa; [(d)]National Institute of Physics, University of the Philippines Diliman (Philippines), Quezon City, Philippines; [(e)]Department of Physics, University of South Africa, Pretoria, South Africa; [(f)]University of Zululand, Kwadlangezwa, South Africa; [(g)]School of Physics, University of the Witwatersrand, Johannesburg, South Africa
[34] Department of Physics, Carleton University, Ottawa, ON, Canada
[35] [(a)]Faculté des Sciences Ain Chock, Réseau Universitaire de Physique des Hautes Energies - Université Hassan II, Casablanca, Morocco; [(b)]Faculté des Sciences, Université Ibn-Tofail, Kenitra, Morocco; [(c)]Faculté des Sciences Semlalia, Université Cadi Ayyad, LPHEA-Marrakech, Marrakesh, Morocco; [(d)]LPMR, Faculté des Sciences, Université Mohamed Premier, Oujda, Morocco; [(e)]Faculté des sciences, Université Mohammed V, Rabat, Morocco; [(f)]Institute of Applied Physics, Mohammed VI Polytechnic University, Ben Guerir, Morocco
[36] CERN, Geneva, Switzerland
[37] Affiliated with an institute covered by a cooperation agreement with CERN, Geneva, Switzerland
[38] Affiliated with an international laboratory covered by a cooperation agreement with CERN, Geneva, Switzerland
[39] Enrico Fermi Institute, University of Chicago, Chicago, IL, USA
[40] LPC, Université Clermont Auvergne, CNRS/IN2P3, Clermont-Ferrand, France
[41] Nevis Laboratory, Columbia University, Irvington, NY, USA
[42] Niels Bohr Institute, University of Copenhagen, Copenhagen, Denmark
[43] [(a)]Dipartimento di Fisica, Università della Calabria, Rende, Italy; [(b)]INFN Gruppo Collegato di Cosenza, Laboratori Nazionali di Frascati, Frascati, Italy

[44] Physics Department, Southern Methodist University, Dallas, TX, USA
[45] Physics Department, University of Texas at Dallas, Richardson, TX, USA
[46] National Centre for Scientific Research "Demokritos", Agia Paraskevi, Greece
[47] [(a)]Department of Physics, Stockholm University, Stockholm, Sweden; [(b)]Oskar Klein Centre, Stockholm, Sweden
[48] Deutsches Elektronen-Synchrotron DESY, Hamburg and Zeuthen, Germany
[49] Fakultät Physik , Technische Universität Dortmund, Dortmund, Germany
[50] Institut für Kern- und Teilchenphysik, Technische Universität Dresden, Dresden, Germany
[51] Department of Physics, Duke University, Durham, NC, USA
[52] SUPA-School of Physics and Astronomy, University of Edinburgh, Edinburgh, UK
[53] INFN e Laboratori Nazionali di Frascati, Frascati, Italy
[54] Physikalisches Institut, Albert-Ludwigs-Universität Freiburg, Freiburg, Germany
[55] II. Physikalisches Institut, Georg-August-Universität Göttingen, Göttingen, Germany
[56] Département de Physique Nucléaire et Corpusculaire, Université de Genève, Geneve, Switzerland
[57] [(a)]Dipartimento di Fisica, Università di Genova, Genoa, Italy; [(b)]INFN Sezione di Genova, Genoa, Italy
[58] II. Physikalisches Institut, Justus-Liebig-Universität Giessen, Giessen, Germany
[59] SUPA-School of Physics and Astronomy, University of Glasgow, Glasgow, UK
[60] LPSC, Université Grenoble Alpes, CNRS/IN2P3, Grenoble INP, Grenoble, France
[61] Laboratory for Particle Physics and Cosmology, Harvard University, Cambridge, MA, USA
[62] [(a)]Department of Modern Physics and State Key Laboratory of Particle Detection and Electronics, University of Science and Technology of China, Hefei, China; [(b)]Institute of Frontier and Interdisciplinary Science and Key Laboratory of Particle Physics and Particle Irradiation (MOE), Shandong University, Qingdao, China; [(c)]School of Physics and Astronomy, Shanghai Jiao Tong University, Key Laboratory for Particle Astrophysics and Cosmology (MOE), SKLPPC, Shanghai, China; [(d)]Tsung-Dao Lee Institute, Shanghai, China
[63] [(a)]Kirchhoff-Institut für Physik, Ruprecht-Karls-Universität Heidelberg, Heidelberg, Germany; [(b)]Physikalisches Institut, Ruprecht-Karls-Universität Heidelberg, Heidelberg, Germany
[64] [(a)]Department of Physics, Chinese University of Hong Kong, Shatin N.T., Hong Kong, China; [(b)]Department of Physics, University of Hong Kong, Hong Kong, China; [(c)]Department of Physics and Institute for Advanced Study, Hong Kong University of Science and Technology, Clear Water Bay, Kowloon, Hong Kong, China
[65] Department of Physics, National Tsing Hua University, Hsinchu, Taiwan
[66] IJCLab, Université Paris-Saclay, CNRS/IN2P3, 91405 Orsay, France
[67] Department of Physics, Indiana University, Bloomington, IN, USA
[68] [(a)]INFN Gruppo Collegato di Udine, Sezione di Trieste, Udine, Italy; [(b)]ICTP, Trieste, Italy; [(c)]Dipartimento Politecnico di Ingegneria e Architettura, Università di Udine, Udine, Italy
[69] [(a)]INFN Sezione di Lecce, Lecce, Italy; [(b)]Dipartimento di Matematica e Fisica, Università del Salento, Lecce, Italy
[70] [(a)]INFN Sezione di Milano, Milan, Italy; [(b)]Dipartimento di Fisica, Università di Milano, Milan, Italy
[71] [(a)]INFN Sezione di Napoli, Naples, Italy; [(b)]Dipartimento di Fisica, Università di Napoli, Naples, Italy
[72] [(a)]INFN Sezione di Pavia, Pavia, Italy; [(b)]Dipartimento di Fisica, Università di Pavia, Pavia, Italy
[73] [(a)]INFN Sezione di Pisa, Pisa, Italy; [(b)]Dipartimento di Fisica E. Fermi, Università di Pisa, Pisa, Italy
[74] [(a)]INFN Sezione di Roma, Rome, Italy; [(b)]Dipartimento di Fisica, Sapienza Università di Roma, Rome, Italy
[75] [(a)]INFN Sezione di Roma Tor Vergata, Rome, Italy; [(b)]Dipartimento di Fisica, Università di Roma Tor Vergata, Rome, Italy
[76] [(a)]INFN Sezione di Roma Tre, Rome, Italy; [(b)]Dipartimento di Matematica e Fisica, Università Roma Tre, Rome, Italy
[77] [(a)]INFN-TIFPA, Trento, Italy; [(b)]Università degli Studi di Trento, Trento, Italy
[78] Department of Astro and Particle Physics, Universität Innsbruck, Innsbruck, Austria
[79] University of Iowa, Iowa City, IA, USA
[80] Department of Physics and Astronomy, Iowa State University, Ames, IA, USA
[81] [(a)]Departamento de Engenharia Elétrica, Universidade Federal de Juiz de Fora (UFJF), Juiz de Fora, Brazil; [(b)]Universidade Federal do Rio De Janeiro COPPE/EE/IF, Rio de Janeiro, Brazil; [(c)]Instituto de Física, Universidade de São Paulo, São Paulo, Brazil; [(d)]Rio de Janeiro State University, Rio de Janeiro, Brazil
[82] KEK, High Energy Accelerator Research Organization, Tsukuba, Japan
[83] Graduate School of Science, Kobe University, Kobe, Japan
[84] [(a)]AGH University of Science and Technology, Faculty of Physics and Applied Computer Science, Kraków, Poland; [(b)]Marian Smoluchowski Institute of Physics, Jagiellonian University, Kraków, Poland

[85] Institute of Nuclear Physics Polish Academy of Sciences, Kraków, Poland
[86] Faculty of Science, Kyoto University, Kyoto, Japan
[87] Kyoto University of Education, Kyoto, Japan
[88] Research Center for Advanced Particle Physics and Department of Physics, Kyushu University, Fukuoka, Japan
[89] Instituto de Física La Plata, Universidad Nacional de La Plata and CONICET, La Plata, Argentina
[90] Physics Department, Lancaster University, Lancaster, UK
[91] Oliver Lodge Laboratory, University of Liverpool, Liverpool, UK
[92] Department of Experimental Particle Physics, Jožef Stefan Institute and Department of Physics, University of Ljubljana, Ljubljana, Slovenia
[93] School of Physics and Astronomy, Queen Mary University of London, London, UK
[94] Department of Physics, Royal Holloway University of London, Egham, UK
[95] Department of Physics and Astronomy, University College London, London, UK
[96] Louisiana Tech University, Ruston, LA, USA
[97] Fysiska institutionen, Lunds universitet, Lund, Sweden
[98] Departamento de Física Teorica C-15 and CIAFF, Universidad Autónoma de Madrid, Madrid, Spain
[99] Institut für Physik, Universität Mainz, Mainz, Germany
[100] School of Physics and Astronomy, University of Manchester, Manchester, UK
[101] CPPM, Aix-Marseille Université, CNRS/IN2P3, Marseille, France
[102] Department of Physics, University of Massachusetts, Amherst, MA, USA
[103] Department of Physics, McGill University, Montreal, QC, Canada
[104] School of Physics, University of Melbourne, Melbourne, VIC, Australia
[105] Department of Physics, University of Michigan, Ann Arbor, MI, USA
[106] Department of Physics and Astronomy, Michigan State University, East Lansing, MI, USA
[107] Group of Particle Physics, University of Montreal, Montreal, QC, Canada
[108] Fakultät für Physik, Ludwig-Maximilians-Universität München, Munich, Germany
[109] Max-Planck-Institut für Physik (Werner-Heisenberg-Institut), Munich, Germany
[110] Graduate School of Science and Kobayashi-Maskawa Institute, Nagoya University, Nagoya, Japan
[111] Department of Physics and Astronomy, University of New Mexico, Albuquerque, NM, USA
[112] Institute for Mathematics, Astrophysics and Particle Physics, Radboud University/Nikhef, Nijmegen, The Netherlands
[113] Nikhef National Institute for Subatomic Physics and University of Amsterdam, Amsterdam, The Netherlands
[114] Department of Physics, Northern Illinois University, DeKalb, IL, USA
[115] [(a)]New York University Abu Dhabi, Abu Dhabi, United Arab Emirates; [(b)]University of Sharjah, Sharjah, United Arab Emirates
[116] Department of Physics, New York University, New York, NY, USA
[117] Ochanomizu University, Otsuka, Bunkyo-ku, Tokyo, Japan
[118] Ohio State University, Columbus, OH, USA
[119] Homer L. Dodge Department of Physics and Astronomy, University of Oklahoma, Norman, OK, USA
[120] Department of Physics, Oklahoma State University, Stillwater, OK, USA
[121] Palacký University, Joint Laboratory of Optics, Olomouc, Czech Republic
[122] Institute for Fundamental Science, University of Oregon, Eugene, OR, USA
[123] Graduate School of Science, Osaka University, Osaka, Japan
[124] Department of Physics, University of Oslo, Oslo, Norway
[125] Department of Physics, Oxford University, Oxford, UK
[126] LPNHE, Sorbonne Université, Université Paris Cité, CNRS/IN2P3, Paris, France
[127] Department of Physics, University of Pennsylvania, Philadelphia, PA, USA
[128] Department of Physics and Astronomy, University of Pittsburgh, Pittsburgh, PA, USA
[129] [(a)]Laboratório de Instrumentação e Física Experimental de Partículas-LIP, Lisbon, Portugal; [(b)]Departamento de Física, Faculdade de Ciências, Universidade de Lisboa, Lisbon, Portugal; [(c)]Departamento de Física, Universidade de Coimbra, Coimbra, Portugal; [(d)]Centro de Física Nuclear da Universidade de Lisboa, Lisbon, Portugal; [(e)]Departamento de Física, Universidade do Minho, Braga, Portugal; [(f)]Departamento de Física Teórica y del Cosmos, Universidad de Granada, Granada, Spain; [(g)]Departamento de Física, Instituto Superior Técnico, Universidade de Lisboa, Lisbon, Portugal
[130] Institute of Physics of the Czech Academy of Sciences, Prague, Czech Republic

[131] Czech Technical University in Prague, Prague, Czech Republic
[132] Charles University, Faculty of Mathematics and Physics, Prague, Czech Republic
[133] Particle Physics Department, Rutherford Appleton Laboratory, Didcot, UK
[134] IRFU, CEA, Université Paris-Saclay, Gif-sur-Yvette, France
[135] Santa Cruz Institute for Particle Physics, University of California Santa Cruz, Santa Cruz, CA, USA
[136] [(a)]Departamento de Física, Pontificia Universidad Católica de Chile, Santiago, Chile; [(b)]Millennium Institute for Subatomic physics at high energy frontier (SAPHIR), Santiago, Chile; [(c)]Instituto de Investigación Multidisciplinario en Ciencia y Tecnología y Departamento de Física, Universidad de La Serena, Frascati, Italy; [(d)]Department of Physics, Universidad Andres Bello, Santiago, Chile; [(e)]Instituto de Alta Investigación, Universidad de Tarapacá, Arica, Chile ; [(f)]Departamento de Física, Universidad Técnica Federico Santa María, Valparaiso, Chile
[137] Department of Physics, University of Washington, Seattle, WA, USA
[138] Department of Physics and Astronomy, University of Sheffield, Sheffield, UK
[139] Department of Physics, Shinshu University, Nagano, Japan
[140] Department Physik, Universität Siegen, Siegen, Germany
[141] Department of Physics, Simon Fraser University, Burnaby, BC, Canada
[142] SLAC National Accelerator Laboratory, Stanford, CA, USA
[143] Department of Physics, Royal Institute of Technology, Stockholm, Sweden
[144] Departments of Physics and Astronomy, Stony Brook University, Stony Brook, NY, USA
[145] Department of Physics and Astronomy, University of Sussex, Brighton, UK
[146] School of Physics, University of Sydney, Sydney, Australia
[147] Institute of Physics, Academia Sinica, Taipei, Taiwan
[148] [(a)]E. Andronikashvili Institute of Physics, Iv. Javakhishvili Tbilisi State University, Tbilisi, Georgia; [(b)]High Energy Physics Institute, Tbilisi State University, Tbilisi, Georgia; [(c)]University of Georgia, Tbilisi, Georgia
[149] Department of Physics, Technion, Israel Institute of Technology, Haifa, Israel
[150] Raymond and Beverly Sackler School of Physics and Astronomy, Tel Aviv University, Tel Aviv, Israel
[151] Department of Physics, Aristotle University of Thessaloniki, Thessaloniki, Greece
[152] International Center for Elementary Particle Physics and Department of Physics, University of Tokyo, Tokyo, Japan
[153] Department of Physics, Tokyo Institute of Technology, Tokyo, Japan
[154] Department of Physics, University of Toronto, Toronto, ON, Canada
[155] [(a)]TRIUMF, Vancouver, BC, Canada; [(b)]Department of Physics and Astronomy, York University, Toronto, ON, Canada
[156] Division of Physics and Tomonaga Center for the History of the Universe, Faculty of Pure and Applied Sciences, University of Tsukuba, Tsukuba, Japan
[157] Department of Physics and Astronomy, Tufts University, Medford, MA, USA
[158] United Arab Emirates University, Al Ain, United Arab Emirates
[159] Department of Physics and Astronomy, University of California Irvine, Irvine, CA, USA
[160] Department of Physics and Astronomy, University of Uppsala, Uppsala, Sweden
[161] Department of Physics, University of Illinois, Urbana, IL, USA
[162] Instituto de Física Corpuscular (IFIC), Centro Mixto Universidad de Valencia - CSIC, Valencia, Spain
[163] Department of Physics, University of British Columbia, Vancouver, BC, Canada
[164] Department of Physics and Astronomy, University of Victoria, Victoria, BC, Canada
[165] Fakultät für Physik und Astronomie, Julius-Maximilians-Universität Würzburg, Würzburg, Germany
[166] Department of Physics, University of Warwick, Coventry, UK
[167] Waseda University, Tokyo, Japan
[168] Department of Particle Physics and Astrophysics, Weizmann Institute of Science, Rehovot, Israel
[169] Department of Physics, University of Wisconsin, Madison, WI, USA
[170] Fakultät für Mathematik und Naturwissenschaften, Fachgruppe Physik, Bergische Universität Wuppertal, Wuppertal, Germany
[171] Department of Physics, Yale University, New Haven, CT, USA

[a] Also Affiliated with an institute covered by a cooperation agreement with CERN, Geneva, Switzerland
[b] Also at An-Najah National University, Nablus, Palestine
[c] Also at Borough of Manhattan Community College, City University of New York, New York, NY, USA

[d] Also at Bruno Kessler Foundation, Trento, Italy
[e] Also at Center for High Energy Physics, Peking University, China
[f] Also at Centro Studi e Ricerche Enrico Fermi, Rome, Italy
[g] Also at CERN, Geneva, Switzerland
[h] Also at Département de Physique Nucléaire et Corpusculaire, Université de Genève, Geneve, Switzerland
[i] Also at Departament de Fisica de la Universitat Autonoma de Barcelona, Barcelona, Spain
[j] Also at Department of Financial and Management Engineering, University of the Aegean, Chios, Greece
[k] Also at Department of Physics and Astronomy, Michigan State University, East Lansing, MI, USA
[l] Also at Department of Physics and Astronomy, University of Louisville, Louisville, KY, USA
[m] Also at Department of Physics, Ben Gurion University of the Negev, Beer Sheva, Israel
[n] Also at Department of Physics, California State University, East Bay, USA
[o] Also at Department of Physics, California State University, Sacramento, USA
[p] Also at Department of Physics, King's College London, London, UK
[q] Also at Department of Physics, Stanford University, Stanford, CA, USA
[r] Also at Department of Physics, University of Fribourg, Fribourg, Switzerland
[s] Also at Department of Physics, University of Thessaly, Volos, Greece
[t] Also at Department of Physics, Westmont College, Santa Barbara, USA
[u] Also at Hellenic Open University, Patras, Greece
[v] Also at Institucio Catalana de Recerca i Estudis Avancats, ICREA, Barcelona, Spain
[w] Also at Institut für Experimentalphysik, Universität Hamburg, Hamburg, Germany
[x] Also at Institute for Nuclear Research and Nuclear Energy (INRNE) of the Bulgarian Academy of Sciences, Sofia, Bulgaria
[y] Also at Institute of Particle Physics (IPP), Montreal, Canada
[z] Also at Institute of Physics, Azerbaijan Academy of Sciences, Baku, Azerbaijan
[aa] Also at Institute of Theoretical Physics, Ilia State University, Tbilisi, Georgia
[ab] Also at L2IT, Université de Toulouse, CNRS/IN2P3, UPS, Toulouse, France
[ac] Also at Lawrence Livermore National Laboratory, Livermore, USA
[ad] Also at National Institute of Physics, University of the Philippines Diliman (Philippines), Quezon City, Philippines
[ae] Also at Technical University of Munich, Munich, Germany
[af] Also at The Collaborative Innovation Center of Quantum Matter (CICQM), Beijing, China
[ag] Also at TRIUMF, Vancouver, BC, Canada
[ah] Also at Università di Napoli Parthenope, Naples, Italy
[ai] Also at University of Chinese Academy of Sciences (UCAS), Beijing, China
[aj] Also at Department of Physics, University of Colorado Boulder, Colorado, USA
[ak] Also at Washington College, Maryland, USA
[al] Also at Yeditepe University, Physics Department, Istanbul, Türkiye
* Deceased